



Durham E-Theses

Barkhausen noise in steels

Birkett, Ailsa Jacqueline

How to cite:

Birkett, Ailsa Jacqueline (1988) *Barkhausen noise in steels*, Durham theses, Durham University.
Available at Durham E-Theses Online: <http://etheses.dur.ac.uk/6455/>

Use policy

The full-text may be used and/or reproduced, and given to third parties in any format or medium, without prior permission or charge, for personal research or study, educational, or not-for-profit purposes provided that:

- a full bibliographic reference is made to the original source
- a [link](#) is made to the metadata record in Durham E-Theses
- the full-text is not changed in any way

The full-text must not be sold in any format or medium without the formal permission of the copyright holders.

Please consult the [full Durham E-Theses policy](#) for further details.

BARKHAUSEN NOISE IN STEELS

AILSJA JACQUELINE BIRKETT

The copyright of this thesis rests with the author.
No quotation from it should be published without
his prior written consent and information derived
from it should be acknowledged.

Submitted for the Degree of PhD

University of Durham

November 1988



4 OCT 1989

ABSTRACT

A survey of the methods of observing Barkhausen noise was made and a suitable system of measurement identified for laboratory measurements to be carried out on steel samples.

A coil system to measure the Barkhausen noise from samples was constructed. The noise was sampled and recorded to microcomputer by means of a transient recorder. The experimental parameters were selected to optimise the data.

A Fast Fourier Transform was performed on the noise data by means of a library routine on a mainframe computer and the results plotted as the power spectra of the data. The recorded voltage profile of the noise was also plotted.

The system was verified by use of grain oriented silicon iron samples. The power spectra and voltage profiles were plotted and, when compared with the results of other workers, were found to be favourable. Tests were performed on constructional steel samples.

The power spectra and voltage profiles from the constructional steels were considered with the coercivity and remanence of the steels and a relationship sought. No simple general relationship was identified although empirical relationships were suggested for some of the data. A knowledge of the microstructure of the steel is required to explain some of the results.

The power spectra and voltage profiles were assessed in terms of the hysteresis loop shape and influence of microstructure on the value of coercivity. It was found that these were the influencing factors in the Barkhausen noise. The effect of plastic deformation on power spectra was investigated.

Results of an industrial investigation were reported.

ACKNOWLEDGEMENTS

I should like to record my thanks to Professors Bransden and Wolfendale for use of the facilities in the Department of Physics, and to British Gas plc. for providing a grant and equipment.

My gratitude is extended to the following:

Dr. W.D. Corner, who has most ably and efficiently guided me through my time at Durham University.

The members of staff of British Gas plc., Dr. L.L. Morgan, Dr. D.M. Paige, Mr. A. Raine, Mr. S. Brown, and others, who have been most helpful in their discussions and prompt actions.

Dr. C.D.H. Williams, for the loan of a low noise amplifier.

Dr. S. Willcock and Dr. M. Hawton, who assisted with the microcomputer programs.

Miss S.M. Thompson who procured the specimen preparation, and performed plastic deformation and coercivity measurements used in Chapter 7 and who also provided some of the photographs.

Miss K. Gittins, for the preparation of a number of the diagrams in this work.

Mr. J. Gallagher for typing the manuscript.

Ailsa J. Birkett, Durham University, November 1988.

CONTENTS

<u>CHAPTER 1 - INTRODUCTION</u>	<u>PAGE</u>
1.1 MAGNETISM	1
1.2 CLASSES OF MAGNETIC BEHAVIOUR	2
1.3 FERROMAGNETISM	3
1.4 MAGNETIC DOMAINS	4
1.5 MAGNETISATION CURVES	7
<u>CHAPTER 2 - THE BARKHAUSEN EFFECT</u>	
2.1 OBSERVATIONS OF BARKHAUSEN NOISE	11
2.2 MAGNETISING COIL	12
2.3 PICK-UP COIL	12
2.4 RECORDING BARKHAUSEN NOISE	14
2.5 FACTORS INFLUENCING BARKHAUSEN NOISE MEASUREMENTS	14
2.6 THE CORRELATION DOMAIN	18
2.7 BARKHAUSEN NOISE IN NDT	19
2.8 GRAIN SIZE MEASUREMENTS	20
2.9 OBSERVATION OF DEFORMATION	21
2.10 OTHER USES IN NDT	22
2.11 RELATIONSHIP WITH BULK MAGNETIC PROPERTIES	22
2.12 MAGNETO-ACOUSTIC EMISSION	23
2.13 THE BARKHAUSEN EFFECT IN SILICON IRON	24
<u>CHAPTER 3 - EQUIPMENT AND EXPERIMENTAL PARAMETERS</u>	
3.1 COIL GEOMETRY	26
3.2 GENERAL LAYOUT OF APPARATUS	27
3.3 SIGNAL AMPLIFICATION	27
3.4 ENVIRONMENTAL SHIELDING	29
3.5 DATA HANDLING	31
3.6 COIL SYSTEM	31
a) Magnetising Coil	31
b) Pick-up Coil	34
3.7 EXPERIMENTAL PARAMETERS	34
a) Constructional Steels	34
b) Silicon Iron	36
3.8 SAMPLES	37
a) Constructional Steels	37
b) Silicon Iron	38
<u>CHAPTER 4 - SILICON IRON</u>	
4.1 RESULTS	39
4.2 DISCUSSION	40
4.3 CONCLUSION	42

CHAPTER 5 - DATA HANDLING - CONSTRUCTIONAL STEELS

5.1	DATA HANDLING	43
	a) Power Spectra	43
	b) Voltage Plots	45
5.2	GRAPHICAL PRESENTATION OF DATA	46
	a) Appearance of Power Spectra	46
	b) Appearance of Voltage Plots	47
5.3	ERROR HANDLING	52

CHAPTER 6 - CONSTRUCTIONAL STEELS - RESULTS

6.1	RELATIONSHIP BETWEEN POWER SPECTRA AND MAGNETIC PROPERTIES	54
6.2	FURTHER POWER SPECTRA WORK	56
6.3	COERCIVITY RANGE	60
6.4	PLASTIC DEFORMATION OF SAMPLE	61
6.5	STRESS RELIEF OF SAMPLE	62
6.6	VOLTAGE PLOT RESULTS	63

CHAPTER 7 - PLASTIC DEFORMATION OF STEEL TYPE 2401

7.1	SAMPLES	66
7.2	EXPERIMENTAL PARAMETERS	66
7.3	RESULTS	67

CHAPTER 8 - INDUSTRIAL APPLICATION OF BARKHAUSEN NOISE

8.1	EQUIPMENT AND SAMPLES	70
8.2	RESULTS	73

CHAPTER 9 - DISCUSSION

9.1	POWER SPECTRA CONSTRUCTIONAL STEELS	77
9.2	PLASTIC DEFORMATION OF SAMPLE 40	81
9.3	BARKHAUSEN NOISE VOLTAGE PLOTS OF CONSTRUCTIONAL STEELS	83
	a) Peak X	85
	b) Plastic Deformation of Sample 40	86
	c) Surface Removal	87
9.4	PLASTIC DEFORMATION OF STEEL TYPE 2401	87
9.5	INDUSTRIAL APPLICATION OF BARKHAUSEN NOISE	90

CHAPTER 10 - CONCLUSIONS AND SUGGESTIONS

<u>APPENDIX A</u>	94
-------------------	----

REFERENCES

CHAPTER 1.	99
CHAPTER 2.	100
CHAPTER 3.	103
CHAPTER 4.	104
CHAPTER 5.	105
CHAPTER 6.	106
CHAPTER 7.	107
CHAPTER 9.	108
CHAPTER 10.	109

CHAPTER 1 - INTRODUCTION

1.1 MAGNETISM

The magnetic properties of some materials have been known for many centuries. The ability to attract and repel other magnets was observed and the concept of poles and fields developed. A summary of some of the basic magnetic parameters is given in this chapter.

A magnetic field in free space with intensity, H , gives rise to a magnetic induction or flux density, B , where;

$$B = \mu_0 H$$

The factor μ_0 is called the permeability of free space. If the same magnetic field acts on a substance there will be an additional component to B due to the material, M . B can now be expressed as;

$$B = \mu_0 (H+M)$$

The relative permeability of the material is given by;

$$\mu_r = \frac{B}{\mu_0 H}$$

Therefore;

$$\frac{B}{\mu_0 H} = 1 + \frac{M}{H}$$



This can be expressed as;

$$\mu_r = 1 + k$$

where k is the susceptibility of the material.

1.2 CLASSES OF MAGNETIC BEHAVIOUR

The response of materials to an applied magnetic field, whether from a permanent magnet or an electric current, has given rise to three general classes of magnetic behaviour; ferromagnetism, diamagnetism and paramagnetism.

Materials showing ferromagnetic behaviour are so named because they display similar responses to iron. The relative permeability $\mu_r \gg 1$ and magnetic saturation can be achieved at relatively small applied fields. In the transition metals there is an interaction between the electron spins resulting in an ordered magnetic system which can only be broken down by high temperatures.

Materials which behave as diamagnets are made up of atoms or ions having no magnetic moment. They do, however, show a response to an applied magnetic field. The individual orbiting electrons behave in such a way as to produce a precessional motion, giving rise to a component of magnetic moment in the opposite direction to the applied field. The susceptibility of these materials is negative.

Materials classed as paramagnets show a small positive susceptibility which increases as temperature is lowered. In a classical paramagnet the susceptibility tends to very large values as absolute zero is approached. In many paramagnets, however, there are interactions between the moments which give rise to magnetic ordering at low temperatures. For these the susceptibility rises to a very large value at some finite temperature; the paramagnetic Curie temperature.

In addition to these three main classes, there are two associated types of magnetic behaviour; antiferromagnetism and ferrimagnetism. An antiferromagnetic material is one in which the magnetic moments are aligned antiparallel to each other giving a net moment of zero; a ferrimagnetic material is similar, but the moments in each direction are unequal giving a net magnetisation.

1.3 FERROMAGNETISM

Steels are in the class of ferromagnets and that class will be discussed in more detail. A ferromagnetic material is one in which very large changes in magnetisation may be measured for small changes in applied field. The magnetisation does not only depend on the applied field but on the previous history of the sample. Permanent magnets can be made

from certain ferromagnetic materials which retain their magnetisation in the absence of an externally applied field. The same material can, however, exist in a state showing little or no permanent magnetisation. The source of magnetic moments in transition metal based ferromagnetic materials is the moment of the electron spin. The interaction between spins causes a situation with parallel alignment of spins to correspond to a state of minimum energy. There is an exchange coupling between the spins of all the atoms which gives a strong enough interaction to explain the observed properties of ferromagnets. The model, however, would suggest that a ferromagnetic material would be unlikely to display a non-magnetised state.

1.4 MAGNETIC DOMAINS

It was therefore postulated by Weiss [1] that the material is divided into magnetic domains, each with a different direction of magnetisation and bounded by a domain wall. The domain model allowed for the total magnetisation to be zero. The domain structure for a material is a minimum energy condition, the energy stored in the magnetic field being balanced by the energy held in the domain walls.

There are various factors which influence the domain pattern in a ferromagnetic material. A magnetic field, H , applied to a domain with magnetic intensity,

M , will give rise to a couple ($HM\sin\theta$) per unit volume, tending to change the direction of M towards the direction of H . θ is the angle between H and M .

The magnitude of H will depend on the demagnetising factors involved and will not necessarily be the value of the applied external field.

The energy involved in determining the domain structure will depend on the magnetocrystalline anisotropy of the material. In a magnetic material there are directions along which it is easier to magnetise the material. If the magnetisation is not along one of the easy directions there will be a contribution to the total energy of the system from the anisotropy. The minimisation of this energy contribution does not necessarily give a minimum energy condition as there may be free poles on the surface of the material giving rise to a magnetostatic energy component. The magnetostatic energy is determined by an internal demagnetising field. There can also be a contribution to the energy of a system from the stress anisotropy of a material. A change in the dimensions of a material is found to accompany changes in magnetisation. This is known as magnetostriction. The work done against the stress of magnetostriction gives a contribution to the domain energy in the form of magnetoelastic energy.

An example of domain patterns in iron is given in Brailsford [2]. It shows how the energy of a system may be minimised (figure 1.1).

- (A) shows that the magnetocrystalline anisotropy component of magnetisation is a minimum if the magnetisation direction is along one of the easy directions. The magnetostatic energy in this case is large.
- (B) shows that the introduction of more domains can reduce the magnetostatic energy without affecting the magnetic anisotropy component.
- (C) shows no free pole energy but there would be a significant contribution to the energy from magnetoelastic energy.
- (D) shows that the energy can be a minimum for anisotropy energy, zero for magnetostatic energy and the magnetoelastic energy can be restricted to small regions at the ends of the block.

The small triangular domains are called closure domains, the domain walls forming these closure domains are called 90° boundaries and those separating the other domains shown are 180° walls. The angle refers to the change in magnetisation direction across the boundary. The total magnetoelastic energy could be reduced by increasing the number of domains. The walls, however, have a finite thickness and an energy

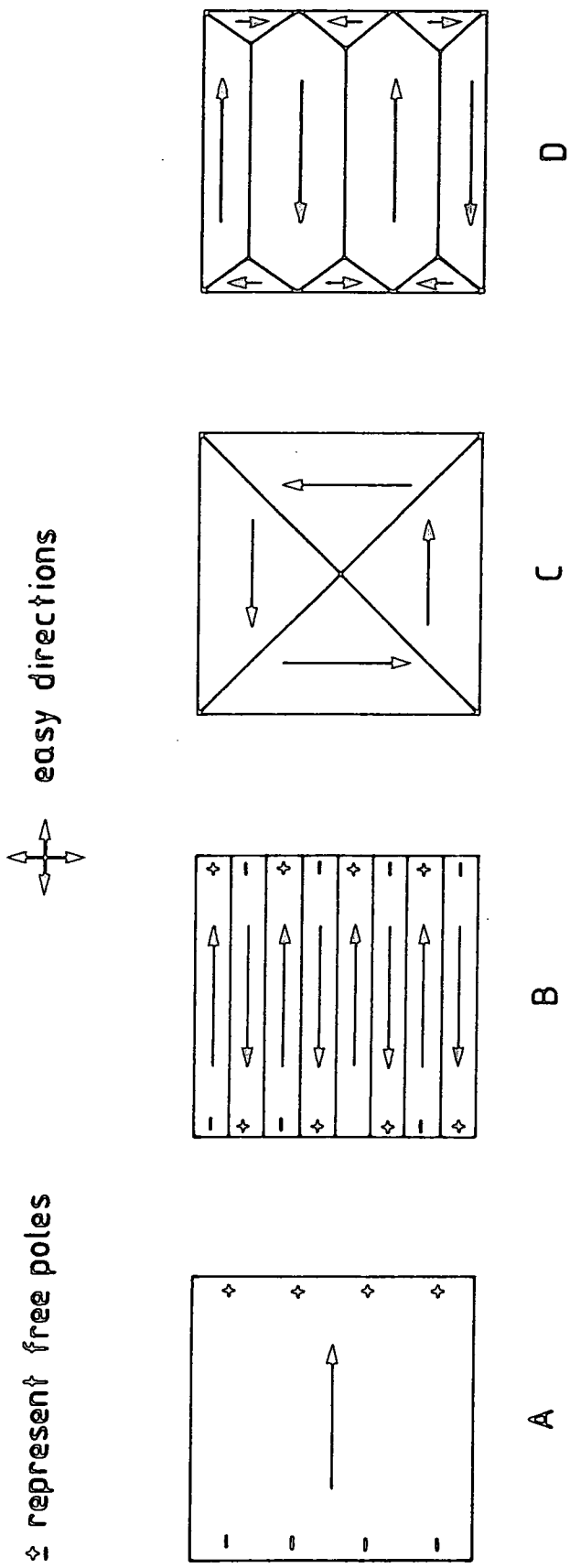


Figure 1.1 Possible Simple Domain Structure (after Brallsford)

associated with them. The minimum energy condition in figure 1.1D must therefore be a balance between the magnetoelastic energy and the boundary wall energy.

1.5 MAGNETISATION CURVES

The existence of domains can be used to explain the shape of the magnetisation curves displayed by ferromagnetic materials. Figure 1.2 shows a typical magnetisation curve. As an external magnetic field, H , is applied to a ferromagnet the domain pattern changes. The direction of magnetisation of a domain may rotate towards the direction of the external field or the domain may change size (volume) by moving its boundary. As the applied field increases, the total magnetisation, M , changes until a further increase in external field causes no change in measured magnetisation. The material is said to be saturated, M_s . If the external field is then reduced the magnetisation will not return to zero along the same path. The domain wall movement is inhibited and there is a lag of the wall movement behind the applied field. At an applied field of zero there is still some magnetisation, called the remanence, while the magnetisation of the material is only reduced to zero at a point called the coercive field. The coercive field, or force, H_c , is the reverse field necessary to demagnetise the sample. The change in applied field

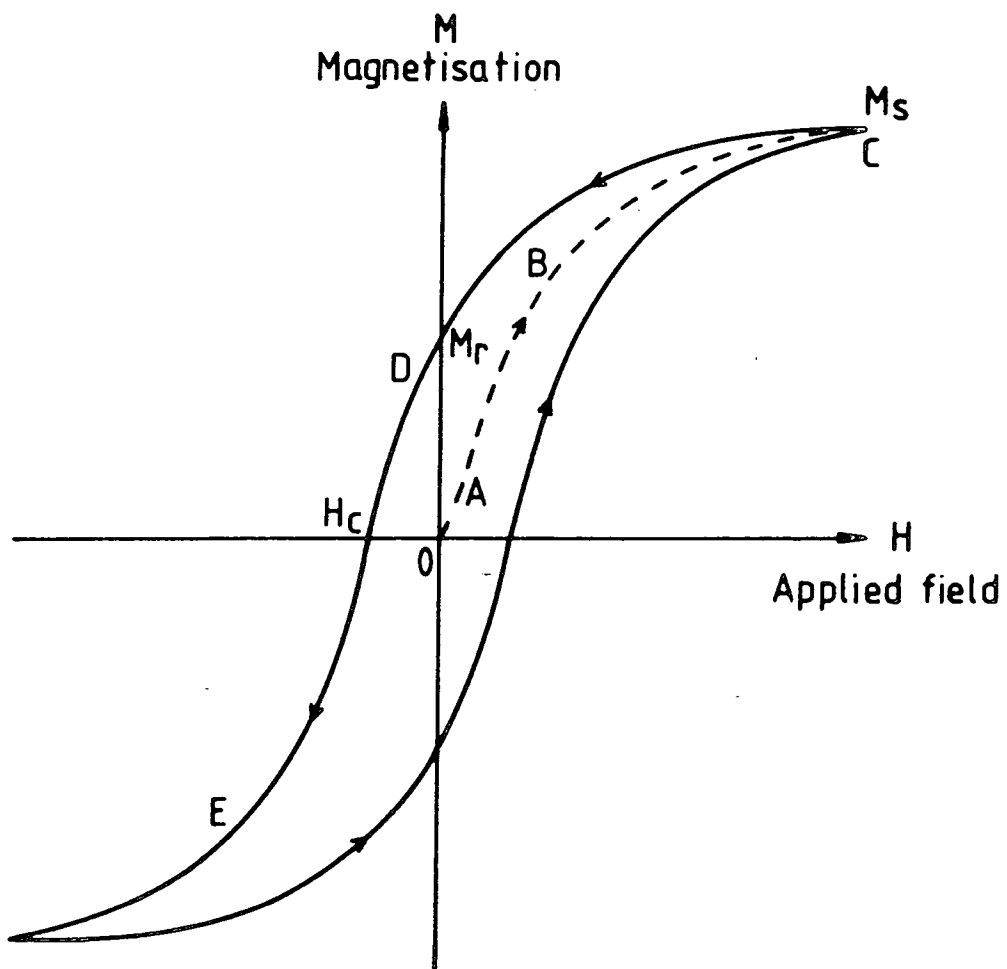


Figure 1.2

A Typical Magnetisation Curve

can continue past the coercive point until saturation is reached in the reverse direction, when it can be increased to forward saturation again giving a closed loop, the hysteresis loop. The work done on the material in changing the domain pattern is proportional to the area enclosed by the loop. Closer inspection of the hysteresis loop reveals that there are distinct regions to it. Figure 1.2 shows these regions. There is a small region, starting from a demagnetised state, (O), for which the change in magnetisation in response to an external field is completely reversible. This is called the Rayleigh region, OA on figure 1.2. Domain walls move but they return to their original position when the field is removed. Beyond the initial region the changes in magnetisation are irreversible, AB on figure 1.2. There is a certain amount of rotation of domain magnetisations, but the majority of the change is due to the irreversible movement of domain walls from one stable position to another. The movement of walls ceases after a certain point on the magnetisation curve and the changes in magnetisation are again reversible, BC on figure 1.2. Most of the changes in this region are due to rotation of the magnetisation. The region CD on figure 1.2 is mostly reversible rotation.

The region of irreversible magnetisation is that which is of interest for the present investigation, as this is where the Barkhausen noise occurs. The

majority of the noise is found in the section DE on figure 1.2. Figure 1.3 shows a two dimensional diagrammatic representation of possible domain wall energy variation. The application of an external field, H, is equivalent to applying a pressure to the domain wall. If the wall travels in a material where the wall energy varies, as shown in figure 1.3, the wall will be displaced from its minimum energy position at s_0 by the applied pressure. If it is displaced, there will be a restoring force on the wall given by the gradient of the wall energy / position curve;

$$\frac{dE_w}{ds} = 2M_s H \cos\theta$$

where M_s is the magnetisation of the domain, H the applied field and θ the angle between M_s and H. The gradient reaches a maximum at the point of inflexion, s_1 . The wall energy / position curve is not a simple curve, as the wall energy will vary as the wall is impeded by impurities or imperfections in the crystal structure. These impediments may be in the form of inclusions, precipitates, grain boundaries or dislocations.

If H is increased further, the wall will make an irreversible move to s_2 where the restoring force is greater and can balance the pressure. The irreversible jumps will occur until the wall reaches the position of maximum wall energy gradient. The irreversible jumps

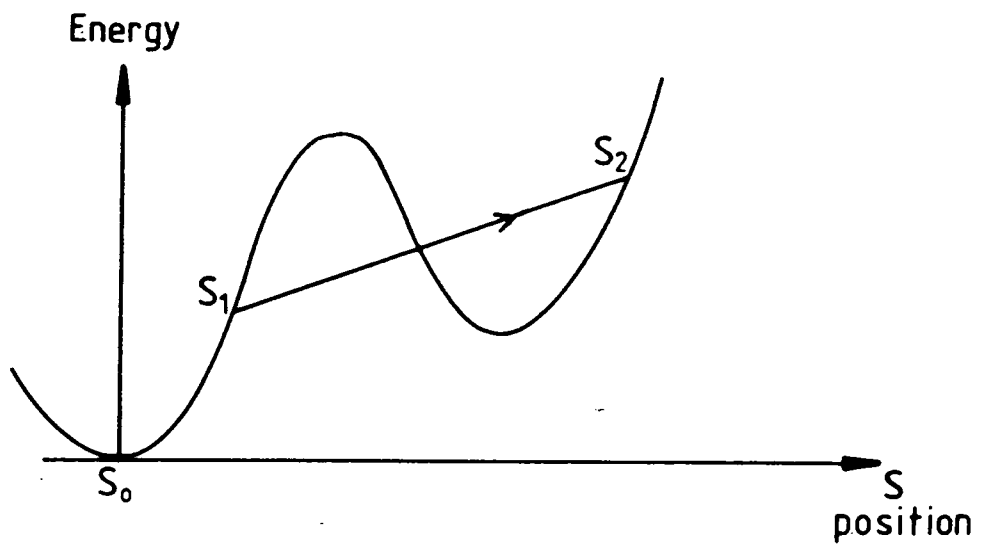


Figure 1.3

Possible Domain Wall Energy / Position Curve

are Barkhausen jumps, each jump representing the small discontinuous movement of a domain wall in the material.

CHAPTER 2 - THE BARKHAUSEN EFFECT

2.1 OBSERVATIONS OF BARKHAUSEN NOISE

The Barkhausen effect was named after its discoverer in 1919 [1]. The effect was first noticed by listening to the sound in headphones connected to a coil surrounding a ferromagnet as the latter was gradually magnetised. The noise was attributed to the sudden changes in magnetisation associated with the motion of domain walls.

The effect has since been studied in different ways. The two major methods are those involving the counting of single jumps and those relating to the power spectra of the jumps. It is possible to observe Barkhausen noise by optical means; the jumps of domain walls may be seen clearly on a suitably prepared surface under a microscope. The study of Barkhausen noise has contributed to the knowledge of materials and their magnetic domain structure and more recently has been assessed as a non-destructive testing (NDT) tool. The range of materials studied is varied; nickel, iron, silicon iron and polycrystalline materials, all have their own Barkhausen characteristics.

2.2 MAGNETISING COIL

The two major methods of observing Barkhausen noise both require a means to provide a magnetic field for the material to be exposed to and a device to "listen" to the Barkhausen noise. The magnetic field has mostly been provided by a coil with a current flowing in it. The coil has either taken the form of an enclosing coil, such as that of Rulka [2], inside which the material to be tested lies, or of a coil wound on a core, such as a C core, which can be surface mounted on a sample [3]. The current flowing in the magnetising coil has mostly been a triangular waveform ramping the field up and down; this gives a constant rate of change of applied field [4]. Some workers have attempted to create a constant rate of change of magnetisation in the sample by means of a feedback system [5].

2.3 PICK-UP COIL

The method of "listening" to the noise has not changed much since early measurements. The usual method is to use a coil to detect the jumps, the measurement being made by the magnitude of the induced voltage in the coil. The pick-up coils used have taken different shapes and sizes. Biorci and Pescatti [6] for example used two coils wound in opposition, each

consisting of 4000 turns, length 1.3cm their axes being aligned with the direction of magnetisation. Tiitto et al. [2] used only one coil of 2000 turns, length 12mm, but it was placed at right angles to the magnetisation direction. Gründl et al. [7] created a three dimensional measuring system for Barkhausen noise and found that there was more Barkhausen noise picked up at 90° to the magnetisation direction than in the magnetisation direction.

The geometry and properties of pick-up coils have been investigated by Tebble et al. [8] and Heiden and Storm [9]. It is clear that the pick-up coil geometry is important as it causes distortion of the appearance of the Barkhausen jumps. One important factor is the length of the coil, as shown by McClure and Schröder [10]. The shape of an individual Barkhausen event is assumed to be a rectangle. The pulse shape is distorted according to a factor αl where l is the coil length and α a function of the permeability of the sample and the distance of a Barkhausen event from the coil. Tebble et al. [8] considered the coil and the Barkhausen jump to be coupled inductors each with a characteristic time constant. If the time constant of the coil is shorter than the time constant of the Barkhausen jump, then the coil will have little effect on the induced pulse shape.

2.4 RECORDING BARKHAUSEN NOISE

Different methods have been employed to record the Barkhausen noise detected. The methods of recording all involve some measurement of the voltage induced on the pick-up coil and variations in the voltage are recorded. Pulse height analyzers [11] have been used to count the size of groups of individual Barkhausen events. The jump amplitude is determined by the induced voltage on the pick-up coil as the external field is slowly varied. This information is passed to a system of electronic gates which record a count in a particular voltage range. This type of measurement in the amplitude domain has been used in the assessment of grain size. [12].

The power spectra of Barkhausen noise are found by the analysis of the Barkhausen signal in the frequency domain. The output of the pick-up coil is continuously monitored and the analysis has been carried out in the past by a thermocouple device connected to a fluxmeter [13] and more recently by on-line spectrum analyzers [2].

2.5 FACTORS INFLUENCING BARKHAUSEN NOISE MEASUREMENTS

The influence of the rate of change of the magnetising field has been studied, as it was apparent that this would affect the Barkhausen noise. The

Barkhausen jumps occur at different points throughout a material as the field level changes. If the field is changing very slowly, single Barkhausen events will be more easily distinguished than if the rate of change of field is fast. There have been various proposals made as to how the magnetising rate affects the distribution of Barkhausen jumps. If the Barkhausen jumps could be completely separated, that is the field was changing infinitely slowly, the jumps would follow a Poisson distribution. However, it has been shown [14] that the single jumps are not independent of each other when a field is applied at a realistic rate of change. The Barkhausen events tend to occur in clusters; this fact was allowed for in a theory by Celasco et al. [14] which considers a train of overlapping pulses of random shape and amplitude. The time distribution suggested was;

$$P(t) = K_1 \exp -\mu_1 t + K_2 \exp -\mu_2 t$$

where the parameters K_1 , K_2 , μ_1 , μ_2 are all determined from physical quantities, e.g. the average duration of a cluster. The power spectrum of such a train of pulses taking into account the correlation between single jumps and the correlation between groups of jumps would be given by;

$$\Phi(\omega) = \varphi(\omega) \left(1 + \frac{2\rho(1-v\tau_0)^2}{1+\omega^2\rho^2\tau_0^2(1-v\tau_0)^2} \right)$$

where $\varphi(\omega)$ is the power spectrum in the absence of any correlation,

ρ is the number of pulses in a cluster

v is the number of pulses per unit time

and τ_0 is the time between pulses.

The above equation was found to be valid for magnetising frequencies in the range 0.001Hz to 1Hz.

The importance of the magnetising frequency was also investigated by Tiitto and Säynäjäkangas [15]. They observed the change in Barkhausen spectrum with increasing sample thickness and magnetising frequency. They concluded that for magnetising frequencies in the range 10^{-2} Hz to 10Hz for all thicknesses of sample there was a clustered portion to the spectrum at low frequency <20kHz. Above this frequency there was a random "white" noise portion with an amplitude dependent on the homogeneity of the sample microstructure. The clustered portion of the spectrum also depends on the amount of noise damping in the material by eddy currents and the surface to volume ratio. The damping was investigated by Tiitto and Säynäjäkangas [15] and a theoretical expression obtained for how noise damping may affect the power spectrum of the Barkhausen noise. For a spectrum

containing components between f_1 and f_2 the damping function may be given as;

$$D(x) = \frac{\int_{f_1}^{f_2} g(f) \exp(-Ax f) df}{\int_{f_1}^{f_2} g(f) df}$$

where A is a constant

x is the depth of measurement

and $g(f)$ is the noise function

($g(f) = 1$ for white noise).

The expression was also used to investigate the effect of the thickness of the sample on power spectra. The power spectrum profile was shown to be constant only for infinitely thin samples, so it was concluded that sample thickness plays a part in determining Barkhausen noise characteristics. However, the choice of magnetising frequency is still more important. The surface to volume ratio was found to affect the spectra when the sample was <0.15mm thick. The effect of surface to volume ratio was also investigated by Celasco and Fiorillo [16] who found that there was a drop in spectral density at low frequencies as the sample was thinned from 0.4mm to 0.1mm. In conclusion, they suggested that there should be a linear dependence between the number of Barkhausen jumps per cluster and the sample thickness;

$$\bar{\rho} \tau_0 \approx \bar{\mu}_{irr} d$$

where $\bar{\mu}_{irr}$ is the average irreversible permeability and d is the sample thickness. This is similar to a result obtained much earlier by Storm, Heiden and Grosse Nobis [17].

2.6 THE CORRELATION DOMAIN

The basis for the statistical treatment of Barkhausen noise is that the individual Barkhausen jumps are correlated in time and space. The idea of a correlation domain was introduced by Mazzetti and Montalenti [18] as being the volume over which domain wall movements were strongly correlated in a material. The coupling between domain wall movements could be in two forms [19]; direct magnetostatic coupling between the ends of each domain and its neighbours or indirect coupling due to changes in the local field caused by other domain wall motions. The former has a shorter range and is stronger than the latter. The correlation domain will start growing at some favourable site, such as a reverse spike at an inclusion, it will then continue to propagate by magnetostatic coupling in a continuous chain. The second coupling mechanism will cause a dendritic pattern of reversed volume to form. Depending on the material, there may be volumes between the branches caused by coupling which will reverse much

later in the magnetisation process. It is because of the inter-relationship between domain reversals that the application of Campbell's Theorem, which relates the power spectrum of uncorrelated pulses to the time distribution of the pulses and the volume of material changed, is now considered inappropriate for the analysis of Barkhausen noise as it relates only to random processes [20].

2.7 BARKHAUSEN NOISE IN NDT

The movement of domain walls in a magnetic material is related to the crystal structure in the region in which the wall is moving. The presence of voids, inclusions, dislocations and stresses may influence the irreversible movements of the walls. The dependence of Barkhausen noise on material properties was recognised as a possible means to investigate the state of a material.

It was clear that if instruments were to be used in a "non-destructive" test, the coil systems normally employed in laboratory measurements would be of little use. Systems which allowed for the measurement of Barkhausen noise from the surface were therefore developed. Transducers measuring Barkhausen noise use the same principles as those for laboratory work, but the coil geometry is adapted for surface techniques [21, 3, 22]. Lomaev [22] shows many different coil

geometries, each having a specific application.

Barkhausen noise transducers have been used to make some analysis of grain size [12], residual stress [23], plastic deformation [24], hydrogen content [25] and ferrite content [25].

2.8 GRAIN SIZE MEASUREMENTS

Grain size measurements were made by taking the median value of the amplitude distribution spectra of the Barkhausen jump clusters. The larger the grain size, the higher the probability of larger Barkhausen clusters. It was observed that this dependence of the amplitude of the jumps on grain size was most prominent in the steepest part of the hysteresis loop near to the coercive point. In terms of the clustering of Barkhausen jumps, the amplitude distributions were interpreted as meaning that for small grain sizes there would be more interaction between domain walls and grain boundaries causing the distance between pinning sites to be small. The time taken for the wall to travel between pinning sites would also be small. The correlation domain discussed earlier would grow by extending a small amount for each jump. The results of the grain size measurements were checked by more conventional optical techniques and a good agreement was found.

2.9 OBSERVATION OF DEFORMATION

The transducer electronics have also been used for the observation of residual stresses in welded materials [23]. Tensile stress increases the median value of jump amplitude of Barkhausen noise in steels when the stress is in the magnetising direction. The relationship of Barkhausen noise with stress can be displayed by the progressive annealing of a sample, the median value of Barkhausen noise amplitude gradually decreases as the stress is relieved.

Plastic deformation has been monitored with a Barkhausen noise method in mild steel [24] and in silicon iron [26]. In silicon iron it was found that the low frequency portion of the Barkhausen power spectrum was reduced as the deformation became greater. This can be interpreted by considering the increase in domain wall pinning locations as the strain is increased. The motion of the domain walls will be interrupted more often and the Barkhausen jumps will be smaller, the large jumps which had made up the low frequency part of the power spectrum are split into smaller, higher frequency jumps. Mild steel was deformed by Karjalainen and Moilanen [24]. They observed that large changes in Barkhausen noise amplitude occurred at the yield point of the steel. The change in Barkhausen noise when the steel was magnetised in the strain direction was in the order of

40%. They suggested that there may be a use for Barkhausen noise in detecting the fatigue limit of cyclically loaded materials without needing to know the exact straining conditions.

2.10 OTHER USES IN NON-DESTRUCTIVE TESTING

Hydrogen content and ferrite content are discussed by Lomaev et al. [25]. They conclude that ferrite content could be measured with Barkhausen noise but care was needed in selecting the correct magnetising parameters and that there were too many other factors involved to be able to make sensible estimates of hydrogen content.

2.11 RELATIONSHIP WITH BULK MAGNETIC PROPERTIES

There has been an attempt to relate Barkhausen noise power spectra to the bulk magnetic properties of a material for use in an NDT technique [27]. The factors influencing power spectra should be similar to those influencing coercivity, mainly impediments to domain wall movement. Rautioaho et al. [27] followed a method which gave a representation of relative coercivity of a material. The relative coercivity was given by the value in amperes of the magnetising current in their coil system required to give half the maximum Barkhausen noise voltage pick-up from the

material. The power spectra for the Barkhausen noise in the materials were plotted and the relationship between the relative coercivity and the frequency of the power spectrum maximum observed. There was no direct correlation found.

2.12 MAGNETO-ACOUSTIC EMISSION

The abrupt movements of domain walls in Barkhausen noise generate elastic waves in the material. These waves can be detected by a piezo-electric transducer [28] and can give information about the state of a material. The main difference between the elastic wave pick-up, magneto-acoustic noise, and Barkhausen noise is that magneto-acoustic noise is sensitive only to changes in 90° domain walls, as the movement of 180° walls does not change the local strain in the material. It has been shown by Buttle et al. [29] that there are two peaks in the magneto-acoustic voltage profile and three in the Barkhausen noise profile. The outer peaks of the Barkhausen noise profiles, taken at very low magnetising frequency, correspond to the 90° wall movements and the central peak to the 180° wall movements. The two magneto-elastic peaks correspond to the two outer peaks in Barkhausen noise voltage profile.

It was shown by Buttle et al. [29] that magneto-acoustic noise is sensitive to precipitates,

dislocations and tensile stress. A limited sensitivity to damage induced by neutron irradiation was found.

The sensitivity of magneto-acoustic noise to stress was noticed earlier by Burkhardt et al. [30]. They concluded that there was scope for the development of an NDT method. The main problem was to be able to quantify results, but used in conjunction with Barkhausen noise techniques, an effective treatment of results may be developed.

2.13 THE BARKHAUSEN EFFECT IN SILICON IRON

The methods of studying Barkhausen noise in silicon iron are those described earlier. Some specific work has been done on grain oriented silicon iron by British Steel for the European Coal and Steel Community (ECSC) [31]. The purpose of the work was to be able to infer the state of the steel during the production process in order to cut down on waste products. The analysis of the Barkhausen noise was made in the frequency domain in the form of power spectra and in the amplitude domain in the form of voltage profiles. It was found that the noise was concentrated in two regions in a half cycle of magnetisation, one at either side of the coercive point. The work was mostly carried out in a coil system modified to give a constant rate of change of magnetisation in the sample. A similar pattern would

be expected for a constant rate of change of applied field but the peaks would be of a different shape and size. The power spectra plotted in the second phase of the work [5] were also from a system with a constant rate of change of magnetisation. It was concluded that grain size and stress affect the power spectra. The grain size dependence was, however, too limited to be of use in grain oriented silicon iron as the variation in grain size is small.

Bertotti et al. [32] studied the power spectra of Barkhausen noise at different points of the hysteresis loop in silicon iron. The system used applied a constant rate of change of induction and it was shown that the Barkhausen noise did not give similar power spectra at different points on the loop. The noise power, P , was shown to be inversely proportional to the average mobility of a domain wall during a cluster of Barkhausen jumps and directly proportional to the effective field applied to the domain wall in the material.

The influence of strain on Barkhausen noise in silicon iron has been observed by Tiitto [33]. The measurements made are in the amplitude domain, a magnetic parameter, M , being defined as the median voltage of the distribution. It was found that M increased for both plastic and elastic deformation when the sample was magnetised parallel to the strain direction.

CHAPTER 3 - EQUIPMENT AND EXPERIMENTAL PARAMETERS

3.1 COIL GEOMETRY

There have been two main coil geometries used to investigate Barkhausen noise. One; a system of coaxial coils, one coil to provide a magnetising field, the other to detect the Barkhausen discontinuities. A system such as this was used by Tebble et al. [1]. The other geometry uses a magnetising coil with a pick-up coil whose axis is perpendicular to the magnetising direction. The second system, used by Rulka, [2] has been used for the work described here. The coil system used by Rulka was chosen as it had been used as part of a large project on Barkhausen noise which was successful in producing a transducer suitable for use in non-destructive testing (NDT). In the process of NDT by the Barkhausen noise method it would, in most instances be impossible to surround the sample to be tested by a coil. The coil system used by Tebble et al. [1] would therefore be of limited use in the field. As it was anticipated that the project here might lead to the measurement of magnetic parameters of steels in situ, a proven coil design was essential.

3.2 GENERAL LAYOUT OF APPARATUS

The block diagram (figure 3.1) shows the layout of the apparatus. The magnetising current for the main coil was provided by a standard feedback oscillator (Feedback Function Generator, FG601) with variable frequency and waveform output. The signal from the oscillator was amplified by a power amplifier (Crown M600 type) stable over a wide range of input frequencies and output impedances.

3.3 SIGNAL AMPLIFICATION

The Barkhausen noise signal from a material is small, typically between 0.01mV and 10mV [3]. It was necessary to amplify the signal to be able to capture the noise on a recording instrument. The minimum input range of the transient recorder (Thorn EMI Waveform Analyzer SE2550) chosen for the Barkhausen noise work was $\pm 0.1V$. The range was divided into 522 discrete levels. At the minimum setting of 0.1V each level represented approximately $2 \cdot 10^{-4}V$. It was decided therefore that the Barkhausen signal should be amplified 1000 times so that a signal of 0.01mV would be represented by 50 of the discrete levels of the transient recorder and the small Barkhausen jumps would still be adequately represented. Two amplifiers were considered for this purpose, one an EG+G standard low

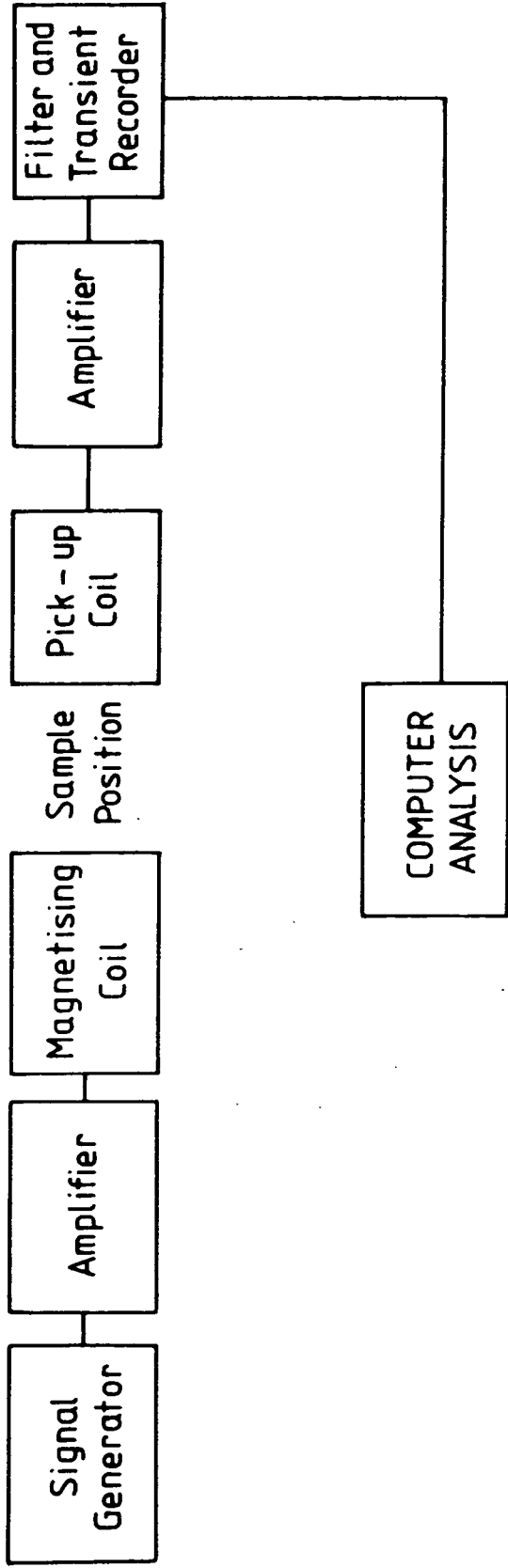


Figure 3.1 Block Diagram of Apparatus

noise amplifier, the other an amplifier designed by C. D. H. Williams in the Physics department (referred to as CW amplifier). The CW amplifier, driven by batteries, was based on a ZN459CP low noise circuit. Figure 3.2 shows the circuit diagram. The EG+G amplifier was designed to be an input stage to a lock-in amplifier, it was driven by two Farnell DC supplies providing the required input voltage of $\pm 15V$. The amplifiers were tested with a resistance box as the input load, the resistance being set to 16.3Ω (approximately the resistance of the pick-up coil). The signal from each amplifier was recorded, and having first been filtered by the transient recorder anti-alias filter, Fourier analyzed. The cut-off frequency of the filter was automatically selected to suit the sample rate. The graphs plotted show the Fourier transform, each point representing the mean of 50 values and the crosses representing the standard error in the mean of the 50 values. Figures 3.3 and 3.4 show the spectra for each of the amplifiers. The multiples of 50Hz are clear on both. It can be seen that the CW amplifier contributes considerably less background noise than the EG+G amplifier. The CW amplifier was tested with the pick-up coil and a large peak near the zero point of the graph was found (figure 3.5). It was investigated and found to be at 0.1Hz, the frequency of the signal being used as the external trigger to the transient recorder. The peak was therefore attributed

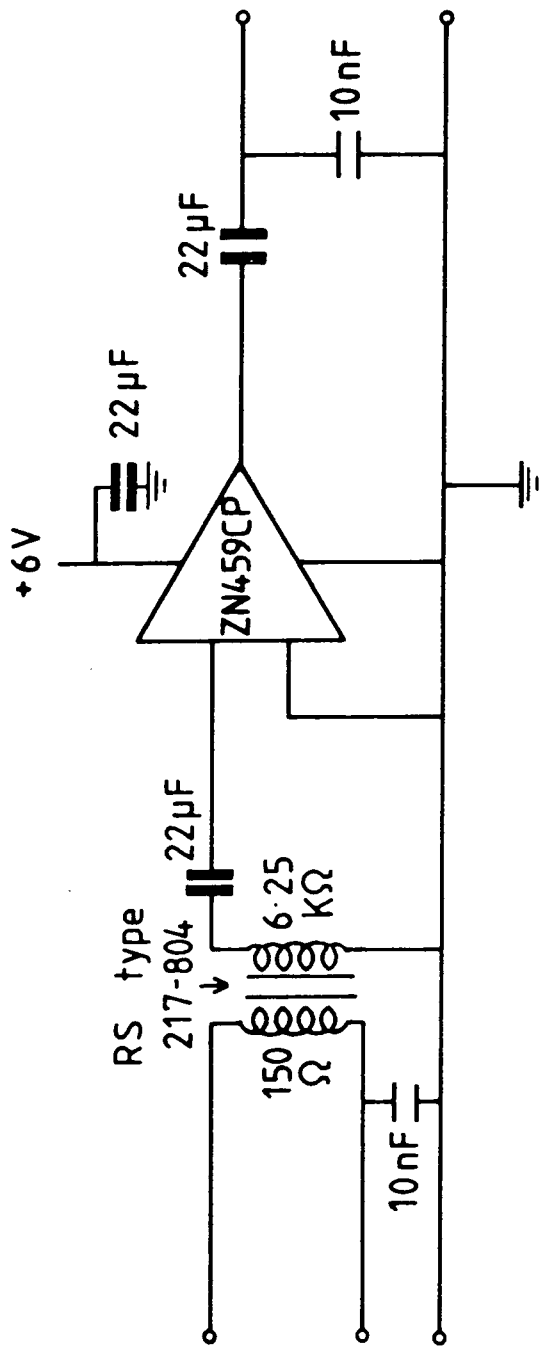
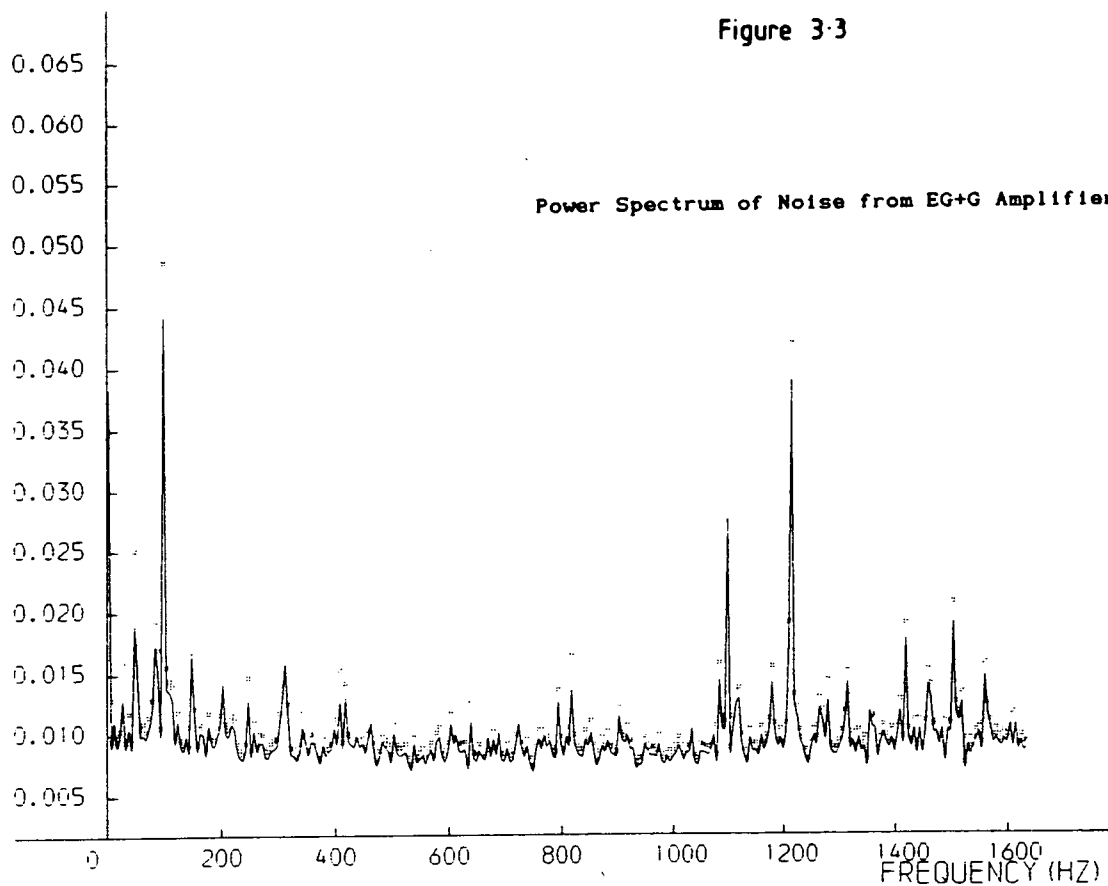


Figure 3.2 Circuit Diagram of Low Noise Amplifier

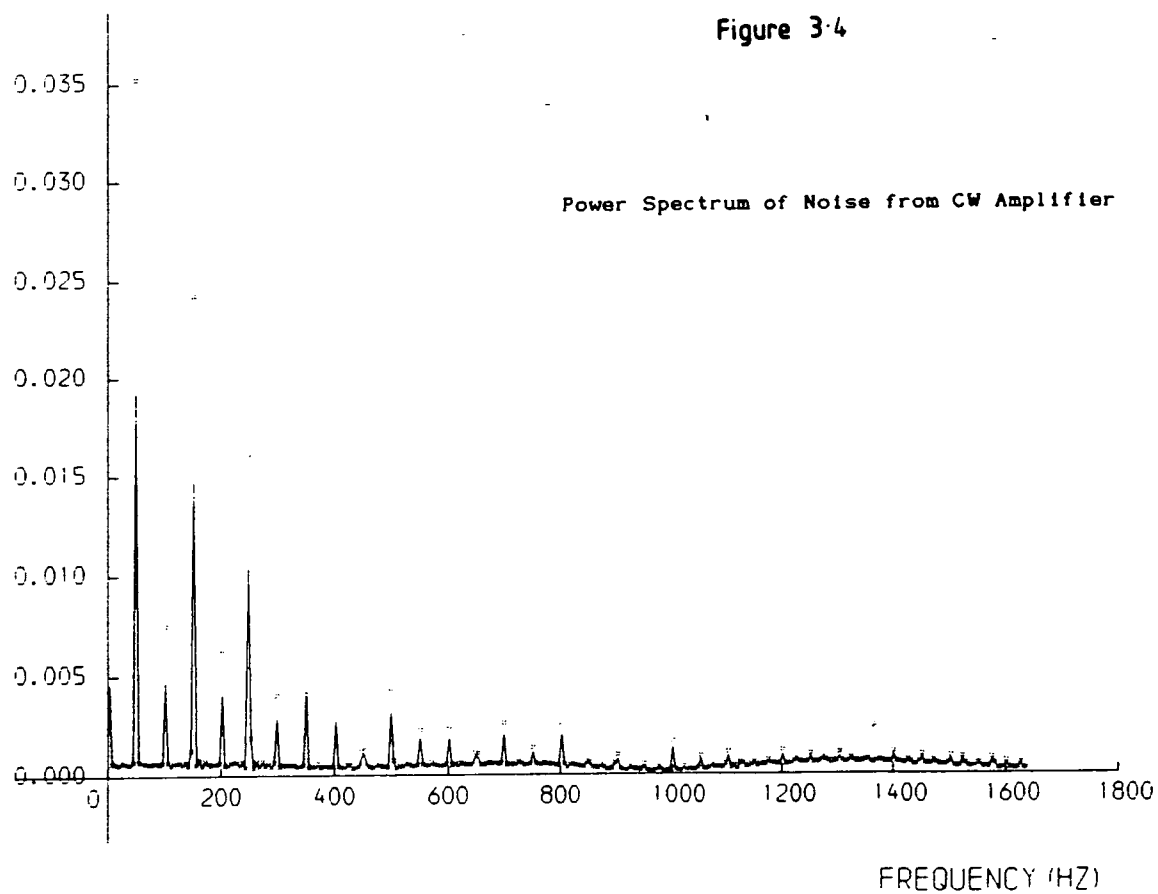
POWER
(W/HZ)

Figure 3-3

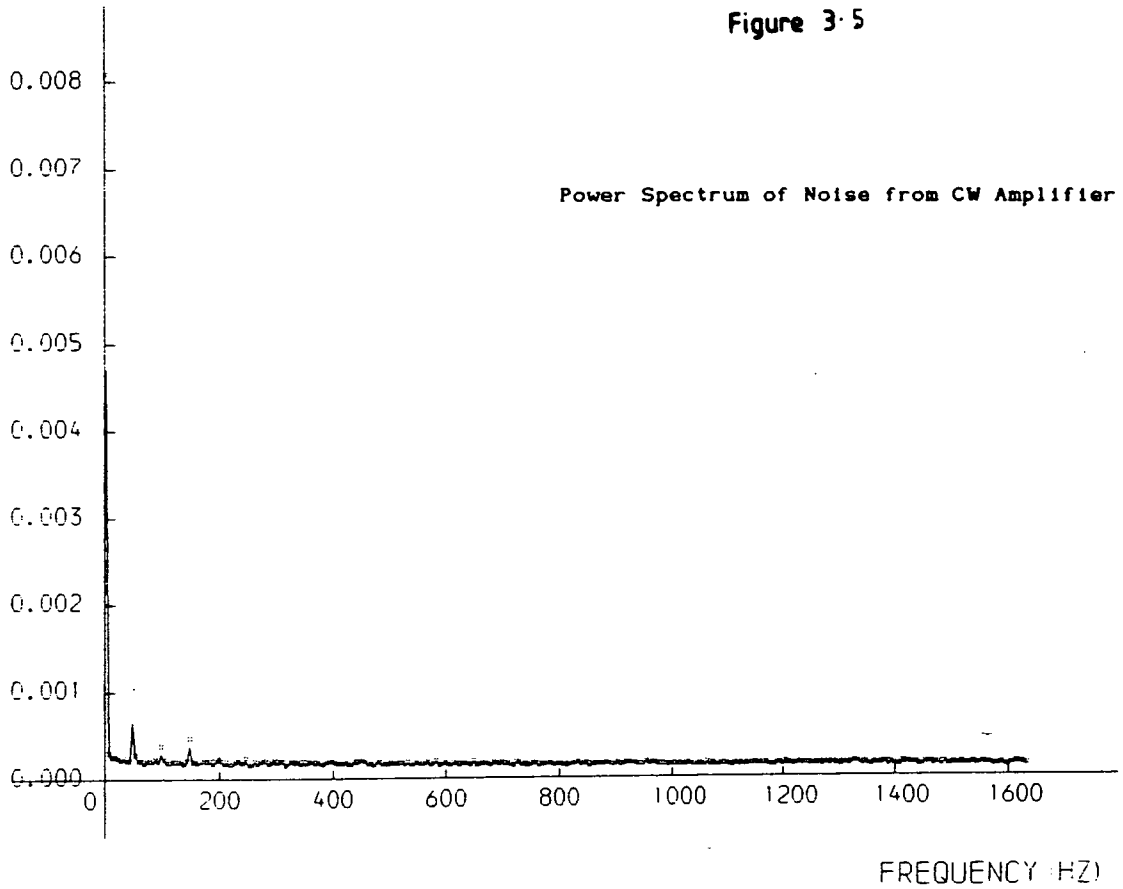


POWER
(W HZ)

Figure 3-4



POWER
(W/HZ)



to this source and, as this was to be used as the triggering mechanism for the experimental work, the FFT was plotted in more detail. Figures 3.6a and 3.6b show the peak. Figure 3.6a shows the first 10 points of the FFT and figure 3.6b the first 50. It can be seen that there is no significant contribution to the spectrum in that region at any frequency other than 0.1Hz.

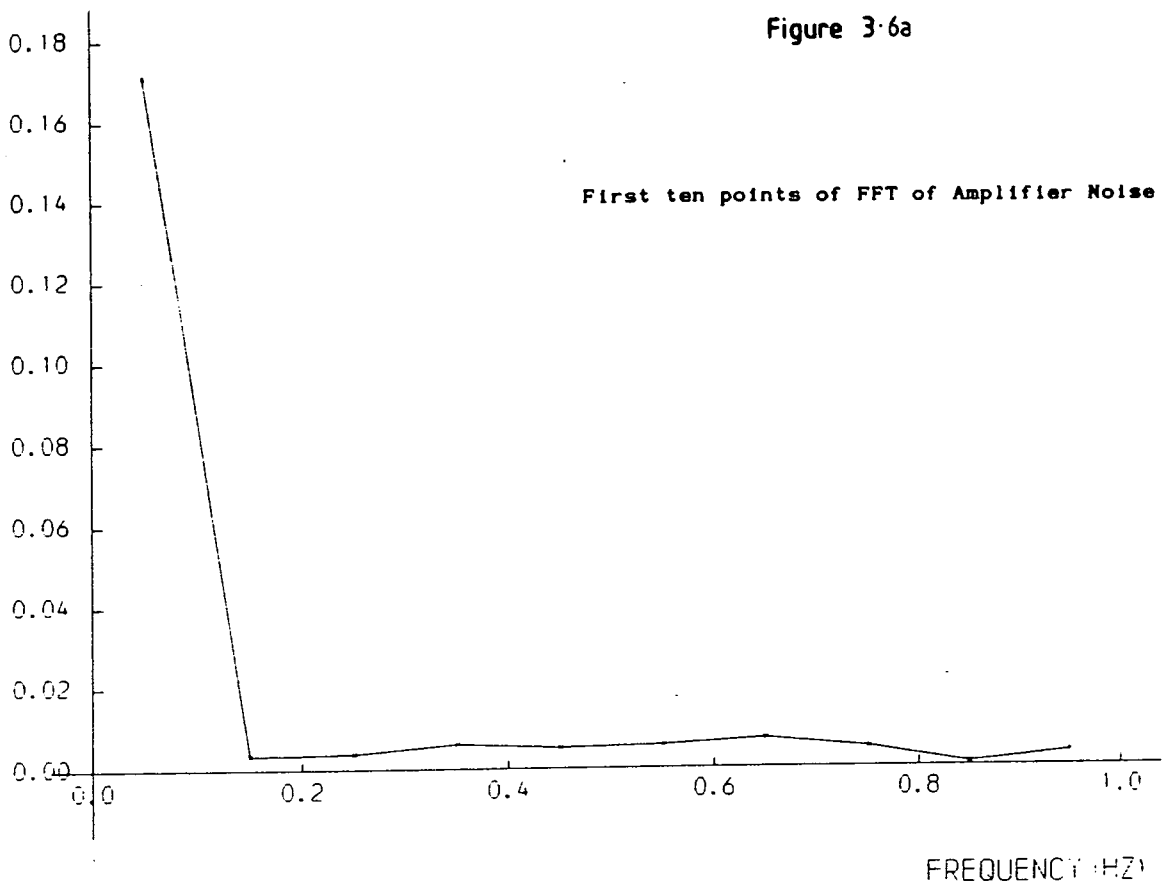
3.4 ENVIRONMENTAL SHIELDING

The preliminary tests on the equipment were carried out with the coil system unshielded from the environment. It was apparent that there was interference from sources in the laboratories. The main problems being 50Hz pick-up, as shown in figure 3.3, the signal from the lights being switched and the radio frequency generator in the room.

In order to alleviate the problem a steel box was built, large enough to accommodate the coil system and sample. The box was of dimensions 45x25x20cm and was made from 1/4inch thick steel; the choice of material being made from a consideration of the electrical shielding properties of metals [4]. There are two ways in which environmental shielding is provided by enclosing equipment; absorption and reflection. In the near field i.e. $< \lambda/2\pi$ metre from the source, there are two main types of noise source, electric field type and magnetic field type. In the far field, $> \lambda/2\pi$ metre

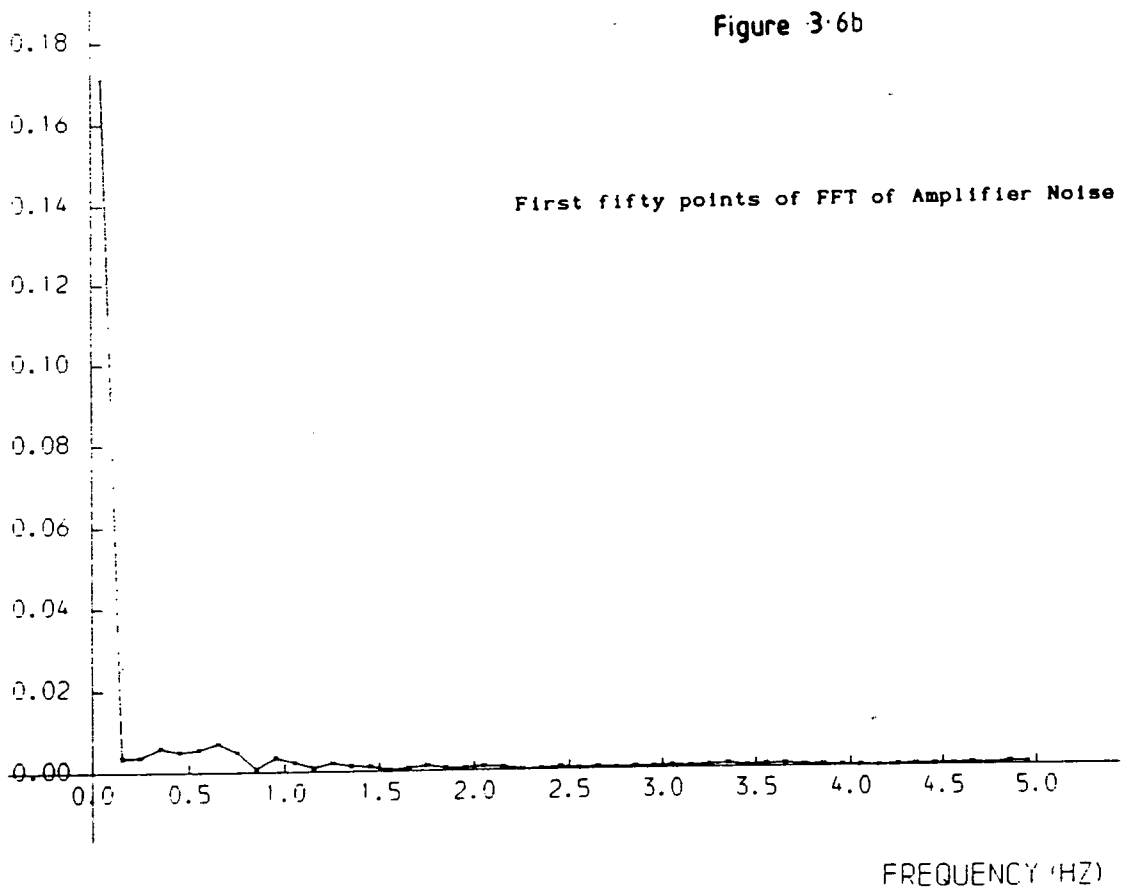
POWER
(W/HZ)

Figure 3-6a



POWER
(W/HZ)

Figure 3-6b



from the source, the waves are considered to be plane. The noise sources considered for the box design were mainly of the electric field type i.e. from a high impedance source. The distances of the noise sources from the coil system were not known precisely, but it can be seen from figure 3.7 that at a distance of 30 metre a copper shield will provide considerable reflection shielding. The type of metal used in shielding has little effect on the reflection loss in the near field i.e. $< \lambda/2\pi$ metre from the source. The choice was therefore based on the absorption properties of the material. Figure 3.8 shows the relationship between the ratio of thickness of shield, t and skin depth, δ with absorption loss in the material. The following values were used for an approximate calculation of the absorption of a 60Hz noise signal.

$\delta_{\text{STEEL}} = 0.034\text{in}$
$\delta_{\text{COPPER}} = 0.335\text{in}$

The absorption loss A , is equal to;

$A = 20t \log(e) / \delta \quad \text{or} \quad A = 8.69t / \delta$

A thickness of $\frac{1}{4}$ inch gives the following absorption losses:

Loss in steel = 63.90dB
Loss in copper = 6.485dB

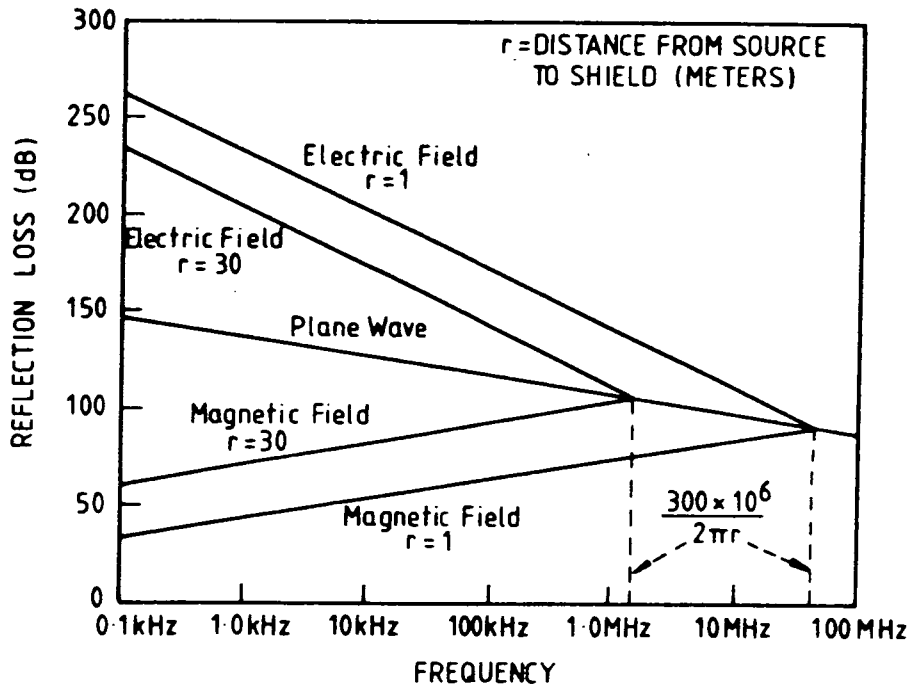


Figure 3.7
Reflection Loss in a Copper Shield (after Ott)

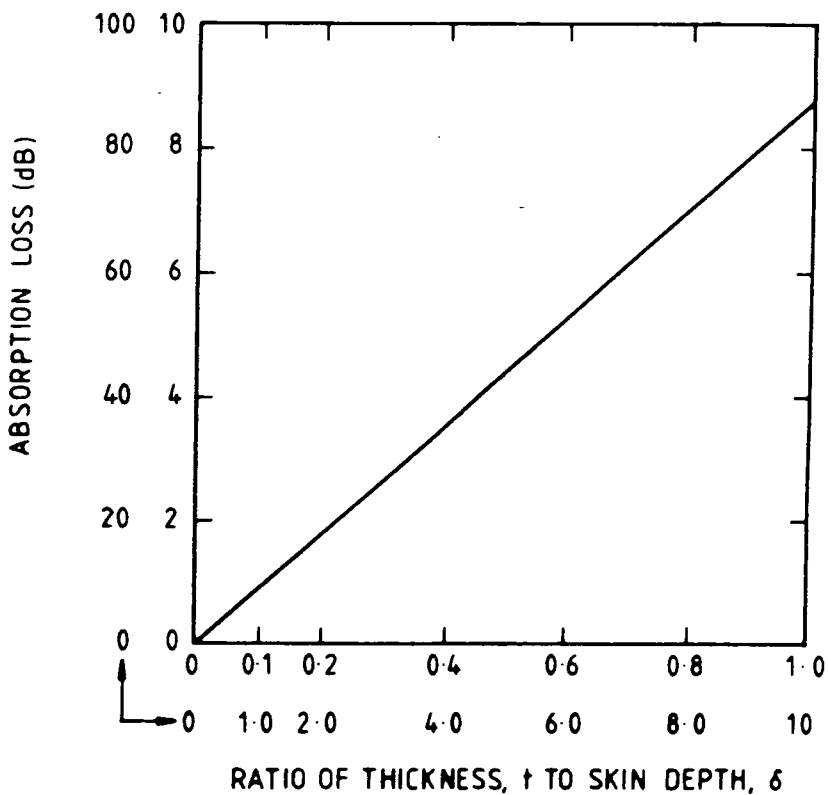


Figure 3.8
Absorption Loss against
Ratio of Thickness to Skin Depth
in an Electrical Shield (after Ott)

The loss in steel is therefore very much greater than that in copper so steel was chosen for the box, the thickness of steel providing approximately 64dB attenuation for a noise signal of frequency 60Hz.

3.5 DATA HANDLING

As part of the analysis of the Barkhausen noise was to be in the form of a Fourier Transform, it was necessary to be able to use the University mainframe computer (NUMAC) for calculations. The noise signal was therefore captured on the transient recorder and recorded to CBM PET disc via the IEEE interface of the transient recorder. The data were transferred to a BBC microcomputer disc before the final transfer to a magnetic tape at NUMAC.

3.6 COIL SYSTEM

The dimensions of the coil system were based on those of Rulka [2].

3.6a Magnetising Coil

The magnetising coil was wound in two sections on Tufnol formers. The dimensions of the system are shown on figure 3.9. The two section design was to allow access to the small pick-up coil located at the centre of the coil, the two halves were held together by three

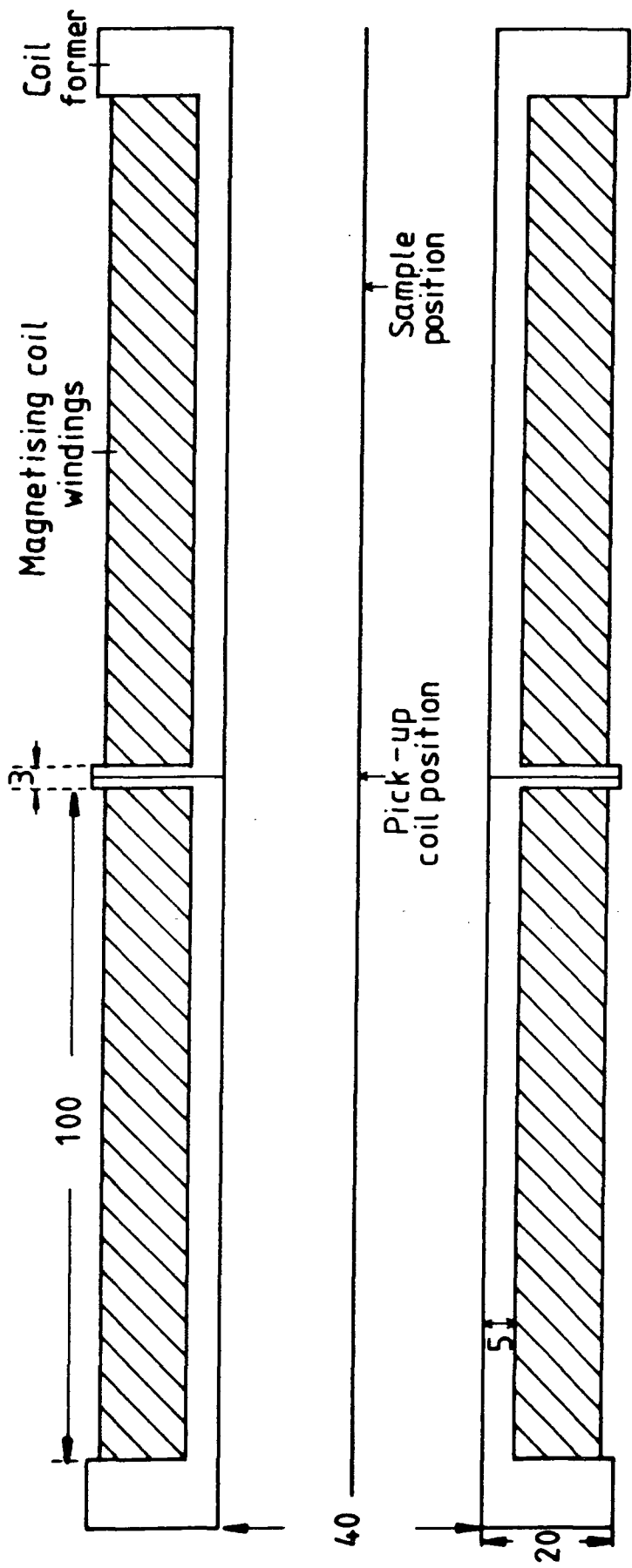


Figure 3.9 The Coil System

Dimensions in millimetres

brass nuts. The coils were wound with 0.8mm diameter wire and varnished after each layer was complete to ensure there could be no contact between windings. The properties of the coils were as follows:

	COIL 1	COIL 2
TURNS	901	897
RESISTANCE	5.5Ω	5.5Ω
INDUCTANCE	20mH	19.85mH

As the magnetising coil was built in two sections it was necessary to investigate the field on the axis of the coils in the region where the sections joined. A method by Zijlstra [5] was used to calculate the field on the axis of a coil (see figure 3.10).

$$\text{Thickness of windings} = \rho_2 - \rho_1$$

$$\alpha = \rho_2 / \rho_1 \quad \beta = z / \rho_1$$

$$\tau = \text{current density}$$

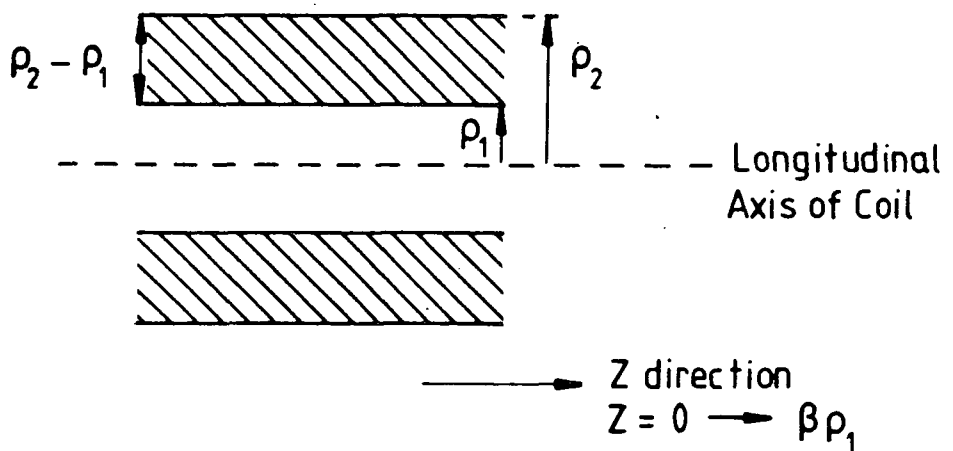
$$H_z = \frac{\tau}{2} \rho_1 \beta \ln \left(\frac{\alpha + \sqrt{\alpha^2 + \beta^2}}{1 + \sqrt{1 + \beta^2}} \right)$$

EQUATION 1

The above relationships were used to calculate the field on the axis, H_z . The value of z was varied between zero and $\beta\rho_1$.

The field, H_z at a distance z_1 from the end of a coil length z_2 was found by the relationship,

$$H_z = H_{(z_1 + z_2)} - H_{z_1}$$



$$\beta = \frac{Z}{\rho_1} \quad \alpha = \frac{\rho_2}{\rho_1}$$

Figure 3-10

Diagram to show Parameters
for Field Calculation (after Zijlstra)

The space between the coils in the case of the magnetising coils was 3mm; the field at a distance of 1.5mm from each coil was calculated and the effect of joining two similar coils considered. It was calculated that a 3mm space between two similar coils each providing a field would give approximately a 5% reduction in field at the centre of the space.

The uniformity of the magnetising field at the centre of the coils was measured with a commercial Hall probe and gaussmeter. The Hall probe was mounted on a travelling microscope stand to allow accurate movement in two directions. The stand was positioned in the coils so that the probe could be used to take measurements of field over the cross section of the coils. Figure 3.11(a) shows the region over which measurements were taken on the axis of the coil, A-B. Figure 3.11(b) shows the cross section of the coil. The maximum variation found over a cross section was in the order of 2%, the variation representing the difference between the edge of the coil next to the windings and the centre of the coil, i.e. the difference between positions 2, 3, 4 or 5 and position 1 on figure 3.11(b). In the region occupied by the pick-up coil on the axis of the magnetising coil i.e. between A and B on figure 3.11(a), the field variation was <1%.

The magnetising field provided by the coils was calculated by the method of Zijlstra. Equation 1 was used to calculate the field on the axis of the

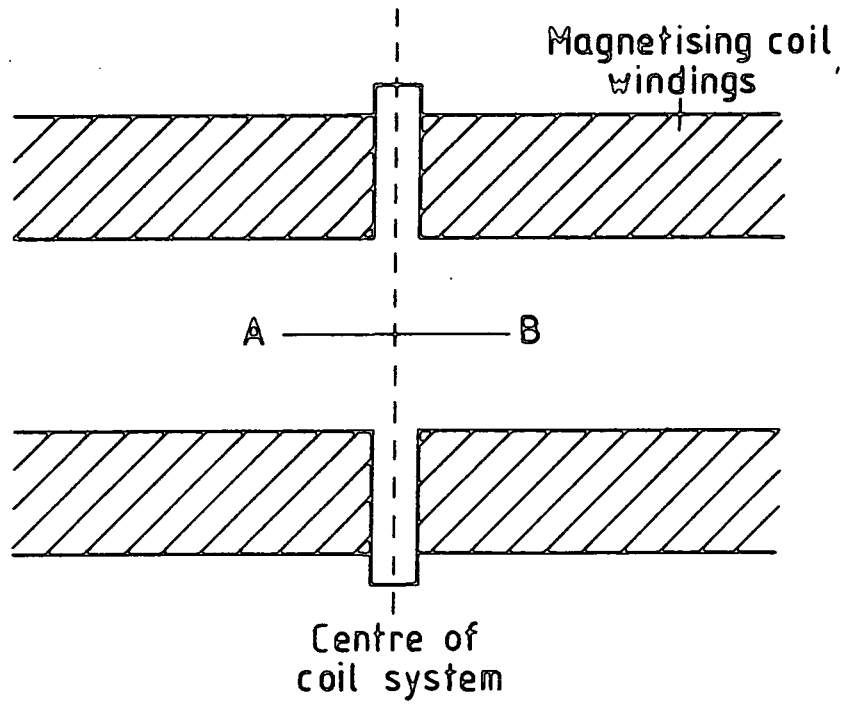


Figure 3.11(a)

Region of Measurement of Magnetic Field on Axis of Coil

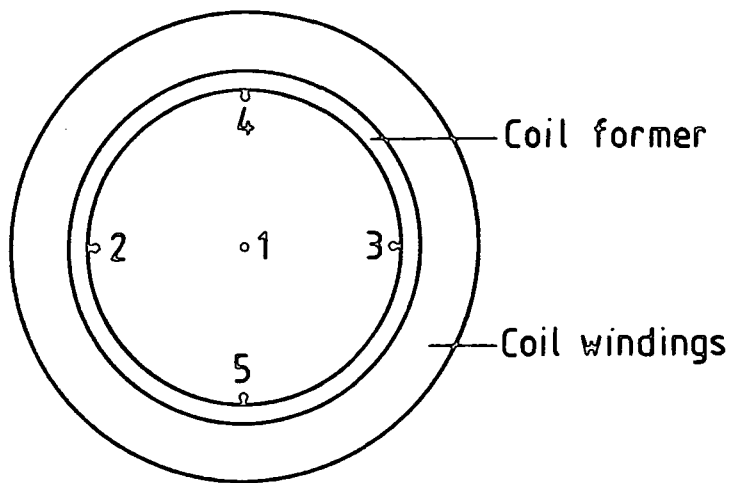


Figure 3.11(b)

Positions of Measurement of Magnetic Field on Cross Section of Coil

magnetising coil with a current density provided by one ampere of magnetising current. The field calculated was $4700 \pm 100 \text{ Am}^{-1}$. The current density is directly proportional to the field so the value calculated was used to find the field value at other values of magnetising current.

3.6b Pick-up Coil

The pick-up coil was wound on a ferrite core of Mullard type 4B1, diameter 1.5mm and length 12mm. The coil was wound with 0.1mm diameter wire, each layer being insulated with varnish. The coil had 804 turns, the limiting factor on the number of turns being the physical size of the coil. The resistance of the coil was measured to be 16.28Ω and its inductance found to be 3mH. The coil was mounted on a Tufnol holder so that it could be held in position at the centre of the magnetising coil. The holder also provided support points for the steel samples to be positioned above the pick-up coil.

3.7 EXPERIMENTAL PARAMETERS

3.7a Constructional Steels

The frequency of the magnetising waveform has been shown to be important in the study of Barkhausen noise spectra. A frequency of 0.1Hz was chosen as a suitable frequency as it has been observed that in the range of

10^{-2} - 10Hz it is possible to differentiate between the Barkhausen noise signal and a white noise signal [6]. The shape of the magnetising waveform was chosen to be a triangular wave as this would give the most steady rate of change of magnetising field.

The variation of Barkhausen noise around the hysteresis loop has been observed by many workers [7]. It has been observed, for example, that for small Barkhausen jumps, the majority of jumps occur close to the coercive point. In order to make use of the full memory of the transient recorder, it was necessary to locate the region of maximum Barkhausen activity on the hysteresis loop. The full loop was observed on the transient recorder; it was broken down into sections using the external trigger facility until the maximum noise could be observed in detail. The area of maximum noise was split up into ten sections. It was found that for the constructional steels a period of 1.638 seconds during the half loop of 5 seconds could be used to cover the full Barkhausen noise burst. The noise burst was therefore divided into ten sections each of 0.1638 seconds. Analysis could thus be carried out on the full noise burst or on the individual sections. The sectioning was carried out by using an external trigger to the transient recorder. Recording was started a number of μ s after the trigger signal was received. By adjusting the time after the trigger by 163800 μ s after each section, the consecutive time

periods could be recorded. Figure 3.12 shows the position of the sections on the magnetising waveform. A sample interval of $5\mu\text{s}$ was used in order that the 0.1638 seconds of noise data filled 32760 memory positions of the transient recorder. The other 8 available memory locations were used to record pre-trigger information and were not used in the data analysis.

The noise signal was filtered by the low pass filters of the transient recorder, the cut-off frequency being set at 19.9kHz. The frequency of cut-off was selected to be approximately $1/10T$, where T is the sample interval. The cut-off should be at most $1/2T$, the Nyquist frequency [8] which is the required frequency for aliasing of signals to be suppressed. The results graphs were plotted to a point at which there would be <1dB attenuation of the signal due to the cut-off characteristics of the filter, a standard 6 pole Bessel filter [9].

The size of the magnetising field was sufficient to magnetically saturate the steel, the demagnetising factor of the samples being taken into account [10].

3.7b Silicon Iron

The parameters for the silicon iron experiments were chosen to be similar to those in the reports of the ECSC Sponsored Research [11]. The magnetising field was $\pm 800\text{Am}^{-1}$, the frequency of the magnetising

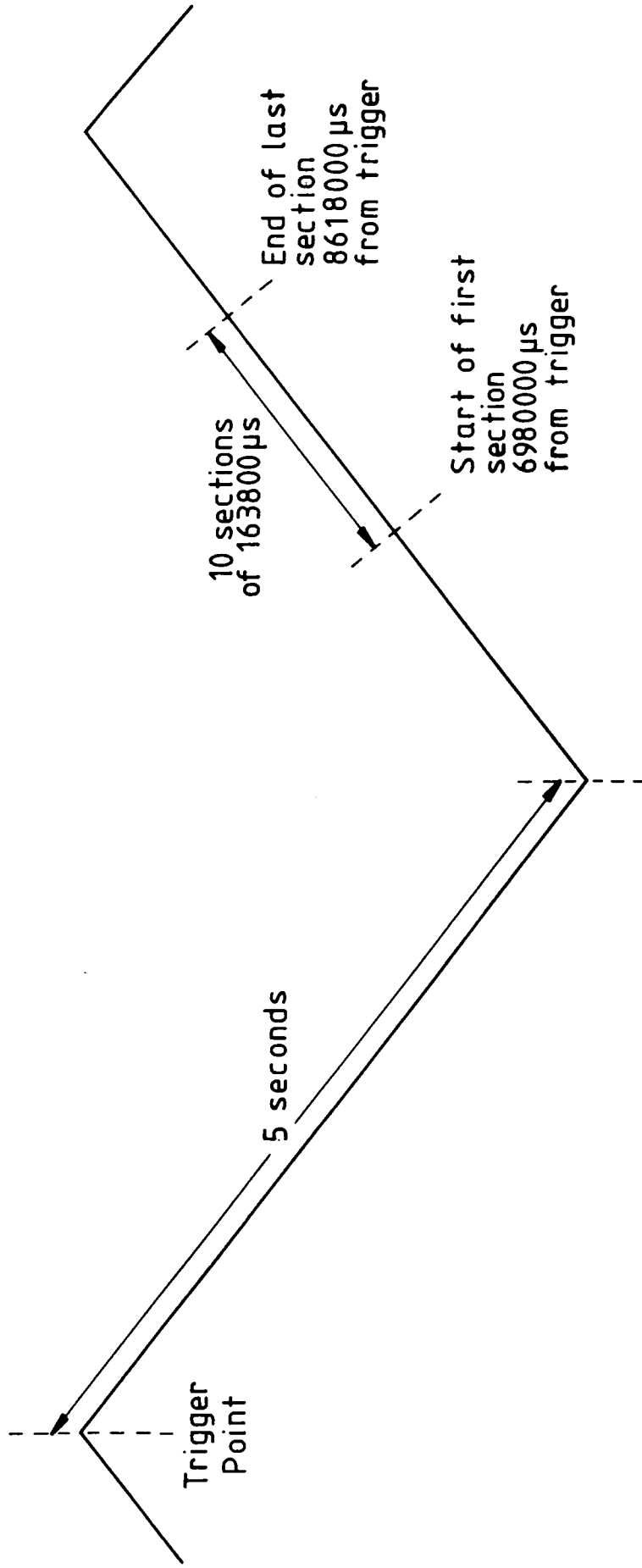


Figure 3.12 Position of Recording of Barkhausen Noise on Magnetising Waveform

waveform 0.14Hz. The sample interval and the filter cut-off frequency were chosen to fully use the memory available on the transient recorder. The values used were 14 μ s and 4.18kHz.

3.8 SAMPLES

3.8a Constructional Steels

The majority of the samples chosen for the experimental work were selected from a set of steel bars cut in a spiral pattern around a piece of 12 inch gas pipe. The magnetic properties of the set of samples had been measured so any relationship between these properties and the Barkhausen noise could be found. Figure 3.13 shows the variation of coercive field with circumferential position for the full set of samples [12]. The samples chosen to work on were 34, 40, 33, 39, 5, 11, 15, 16, 2, and 20. In addition to these samples two samples were cut from pieces of steel labelled DFD and DHP. The dimensions of all the samples were 250x20x5mm.

The samples were chosen on the following basis: 34 and 40 were adjacent to the samples showing the most extreme values of magnetic parameters; 33 and 39 displayed large differences in power spectra in a shortened version of the experiments; 5 and 11 were of similar coercive field to 40; 15 and 16 were of similar coercive field to 34; 2 and 20 were chosen as

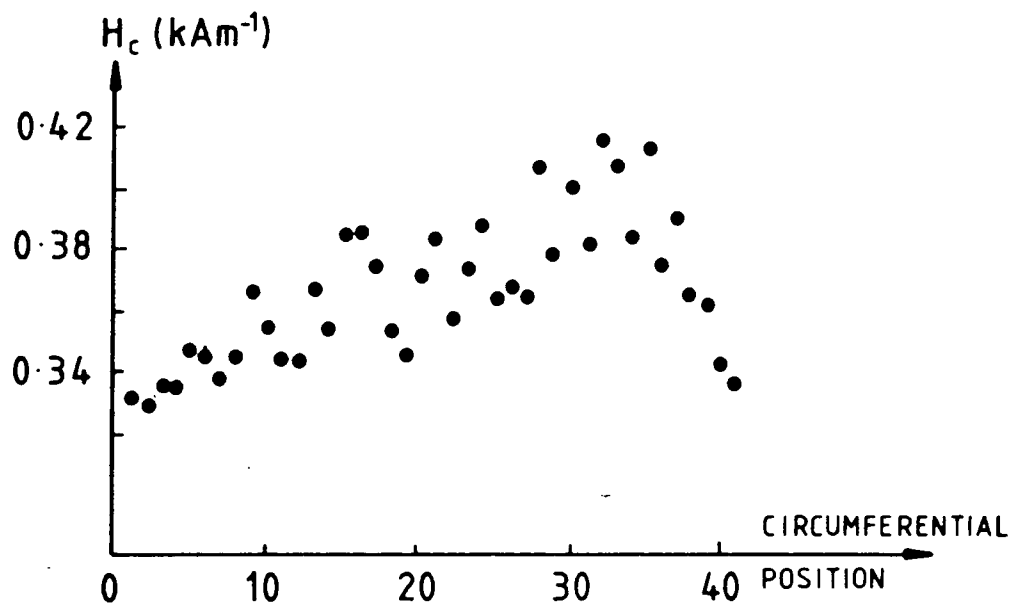


Figure 3.13 Variation of Coercive Field with Circumferential Position for 12 inch Pipe Steel Samples [after Willcock] [12]

representing opposite sides of the pipe; DFD had a much larger coercive field than the 12 inch set of samples; DHP had a similar coercive field to the 12 inch set.

The thickness of the steel is important in the analysis of Barkhausen noise as damping of the signal occurs in the material [6]. It was found that the signal from the 12 inch set of steels was sufficiently strong to be detected by the equipment, the choice of a thick sample being offset by the choice of magnetising frequency.

3.8b Silicon Iron

The silicon iron samples used were as supplied by British Steel, Newport. Two sets of samples were finished grain oriented material which is used mostly for transformer cores and is made specifically to have a low loss characteristic at 50Hz. The samples were of a standard Epstein sample size used to test the properties of the steel at the Newport works. The dimensions were 300x30x0.25mm.

CHAPTER 4 - SILICON IRON

4.1 RESULTS

The voltage plots of the silicon iron finished samples were as expected from the ECSC reports [1, 2] in that they showed a peak of activity either side of zero applied field (figure 4.1). The size of the peaks was small compared with the peak of activity observed from the constructional steels.

The power spectra were plotted for the half hysteresis loop and for the individual sections into which the loop was divided for analysis. Figures 4.2 to 4.10 show the power spectra. It can be seen from the power spectra that the level of the spectra varies between $0.0001V^2$ and $0.00065V^2$ in the first three sections of the loop but then increases to a maximum level of $0.0085V^2$ in the section where the first of the peaks of activity was displayed. There is a drop again to $0.0039V^2$ in the section between the peaks and a rise to $0.0029V^2$ at the next peak. The order of the individual spectra is not exactly the same as the order given by the ECSC but it is similar in that sections A and H are very much smaller than all the others and the others vary upwards from there (figure 4.11). The low frequency roll-off, attributed to the measuring system in the ECSC work, is deceptive as the gradients of all the segments beyond the roll-off are different. The

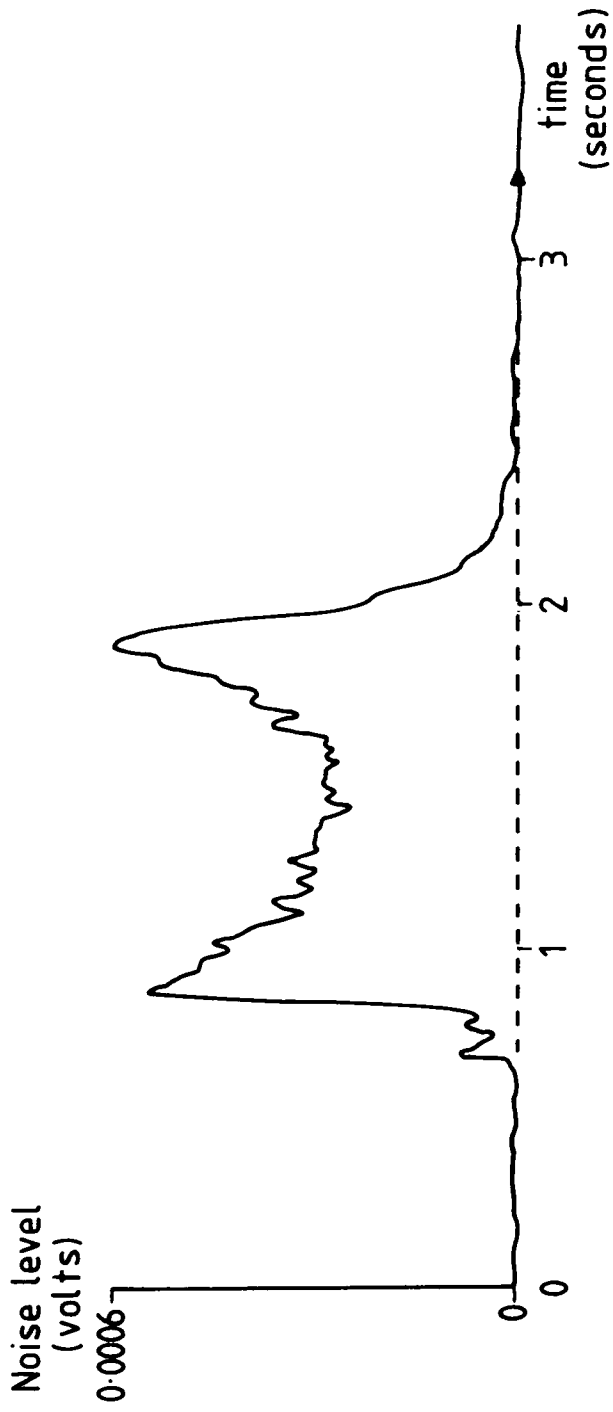


Figure 4.1 Typical Barkhausen Voltage Profile for Grain Oriented Silicon Iron [1]

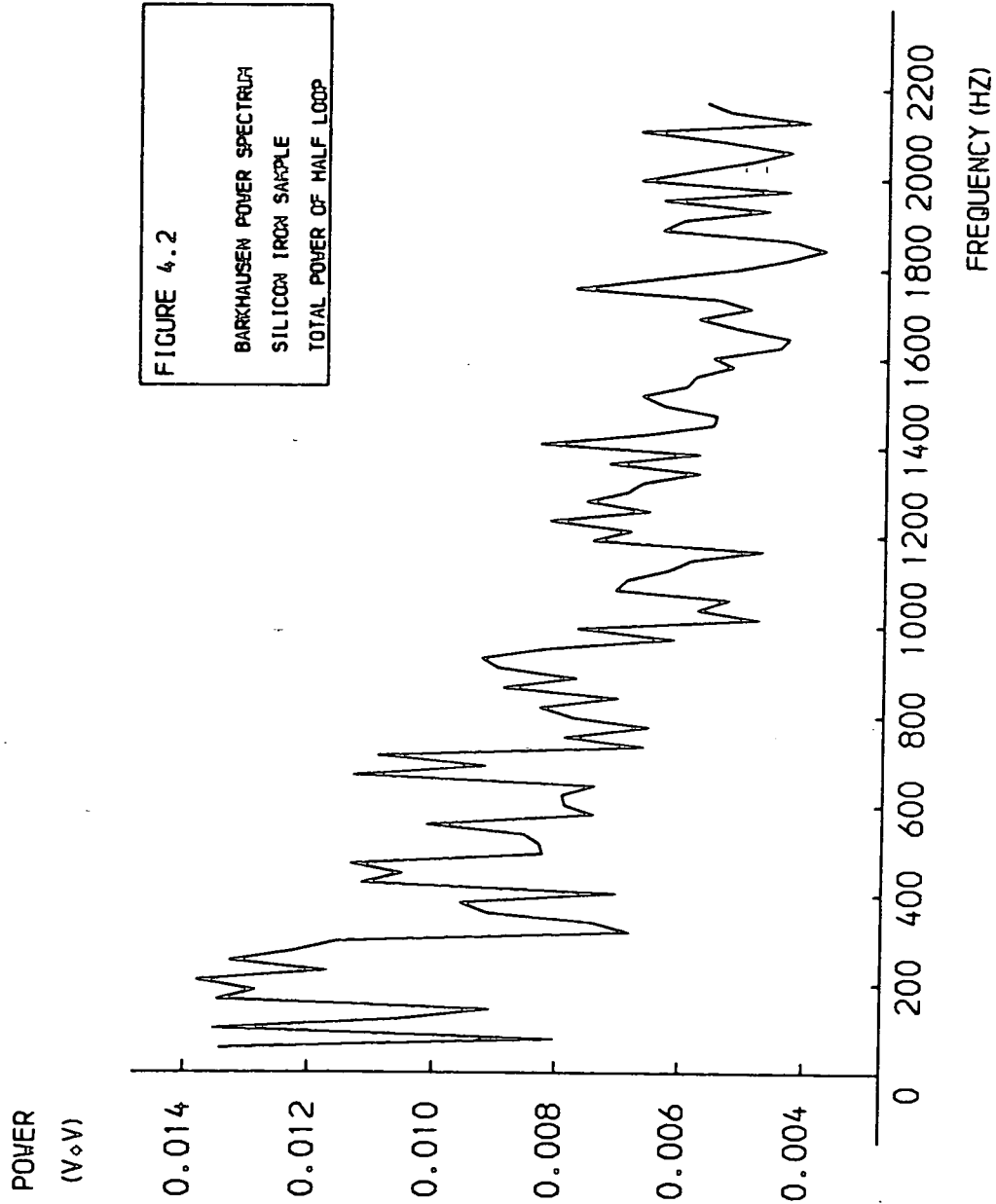


FIGURE 4.2

BARKHAUSEN POWER SPECTRUM
SILICON IRON SAMPLE
TOTAL POWER OF HALF LOOP

POWER
(V_oV)

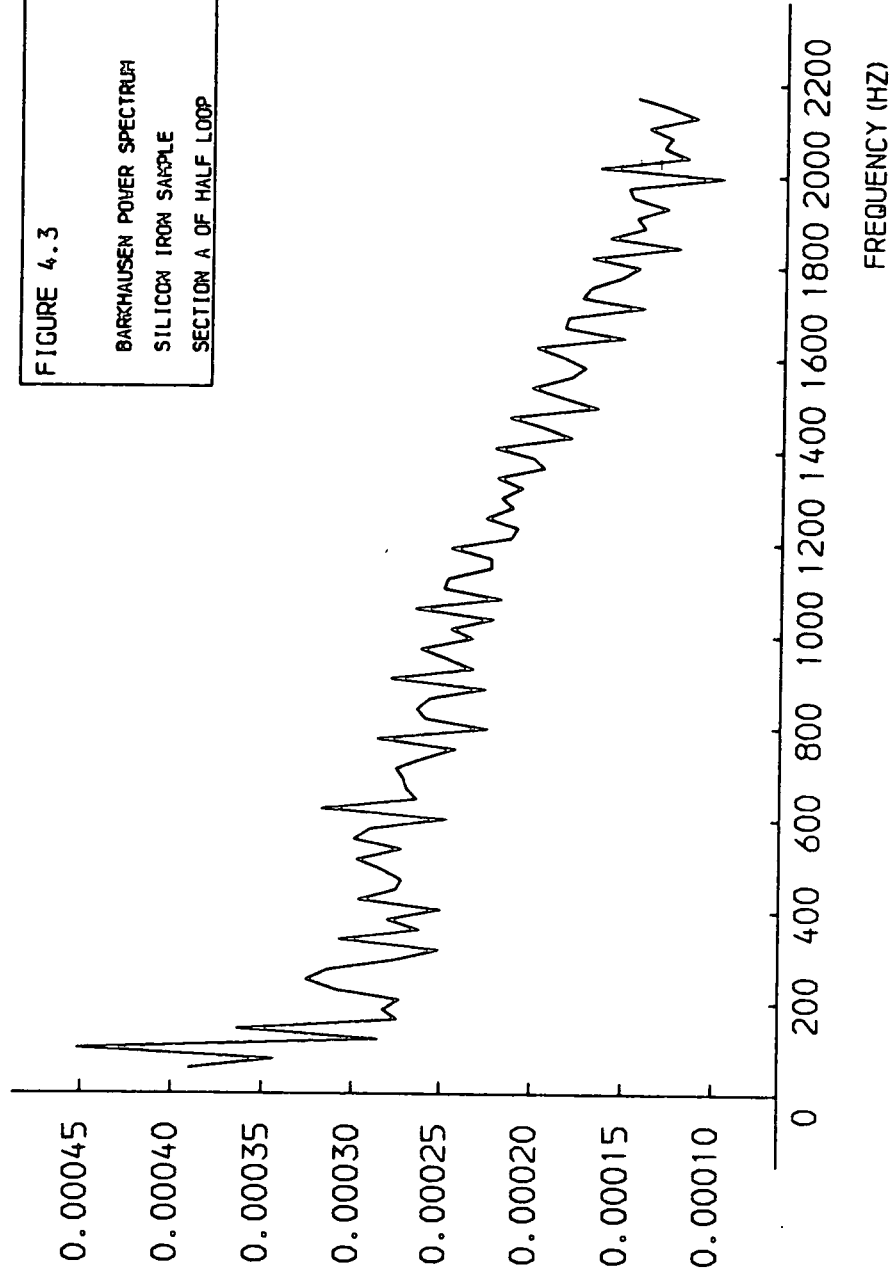


FIGURE 4.3
BARKHAUSEN POWER SPECTRUM
SILICON IRON SAMPLE
SECTION A OF HALF LOOP

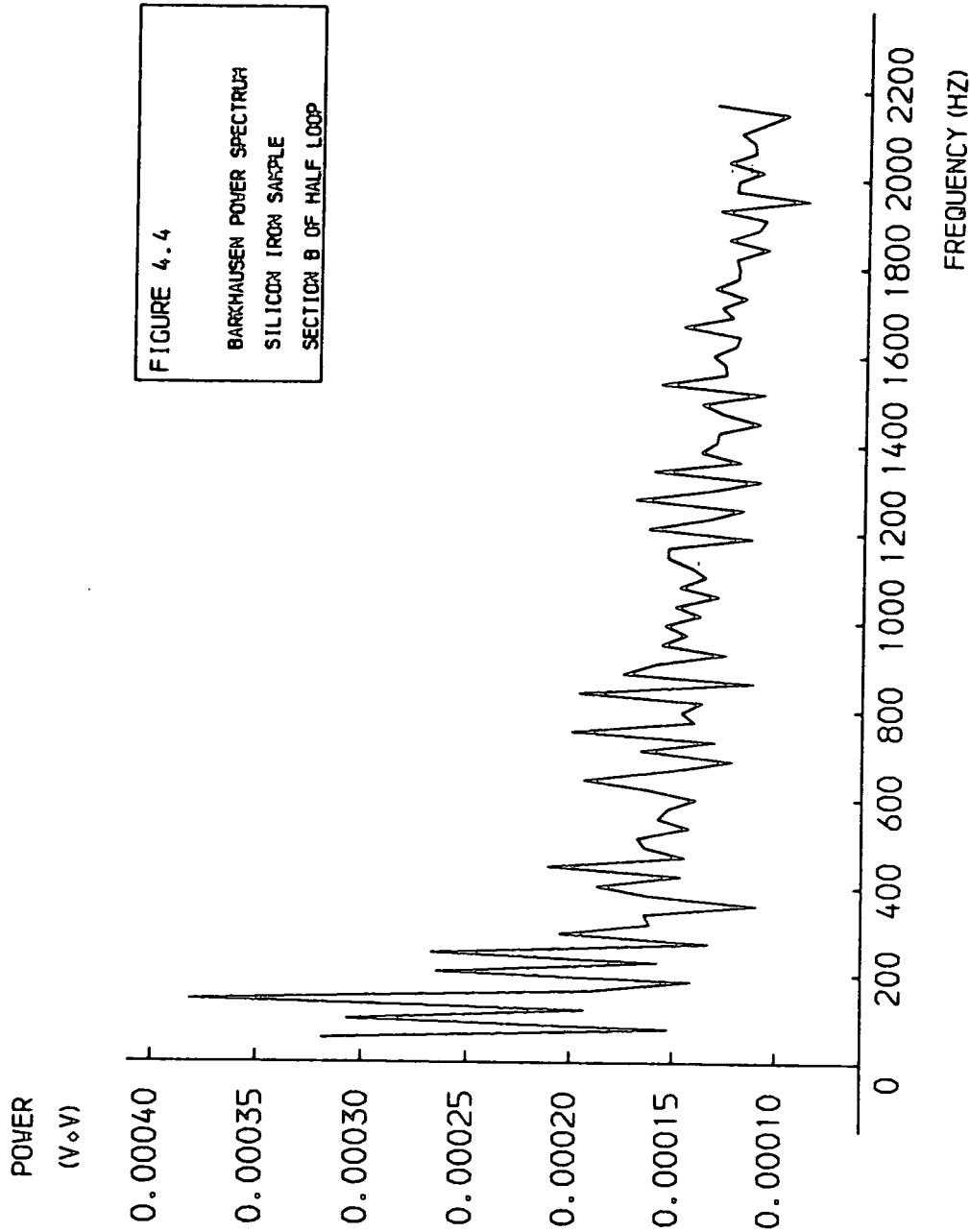


FIGURE 4.4
BARKHAUSEN POWER SPECTRUM
SILICON IRON SAMPLE
SECTION B OF HALF LOOP

POWER
(V²/V)

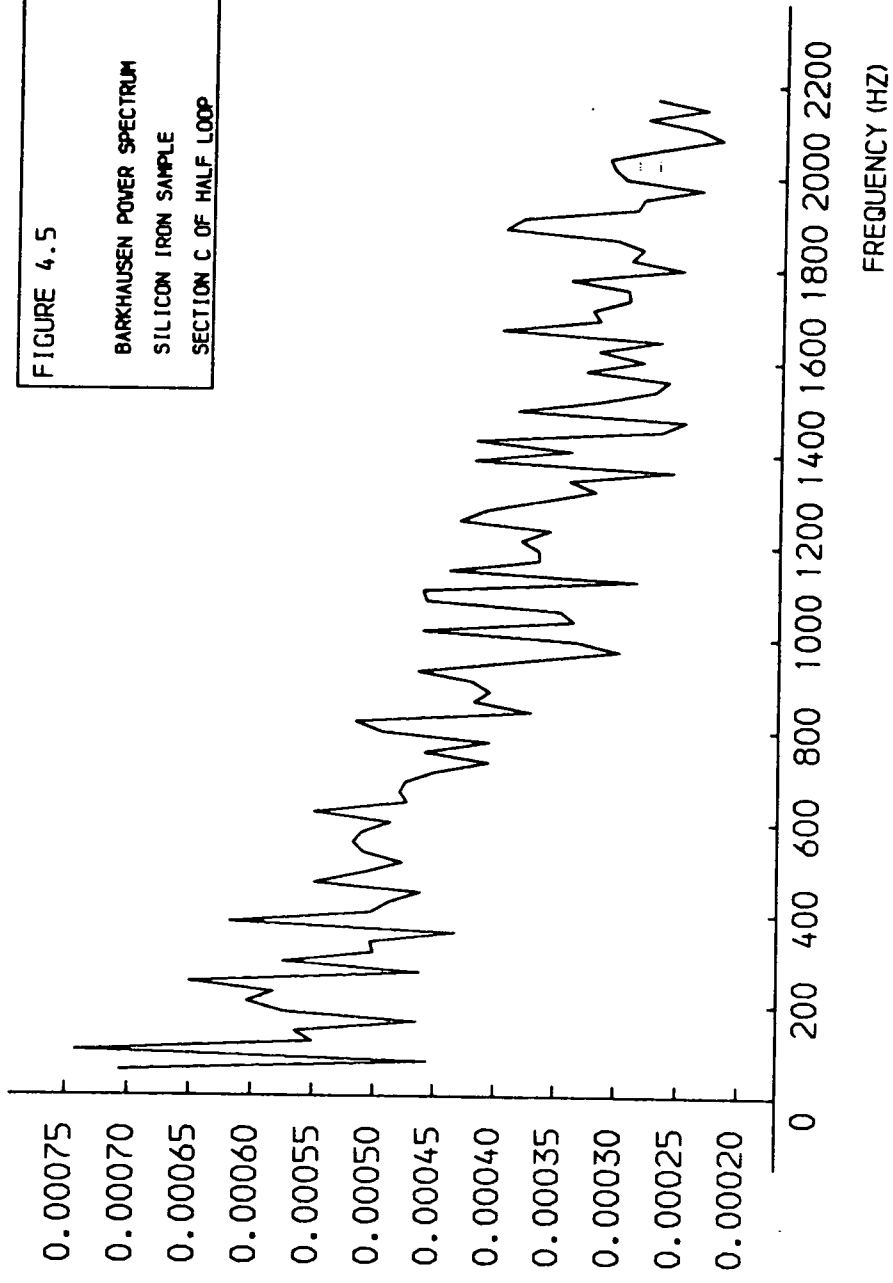


FIGURE 4.5
BARKHAUSEN POWER SPECTRUM
SILICON IRON SAMPLE
SECTION C OF HALF LOOP

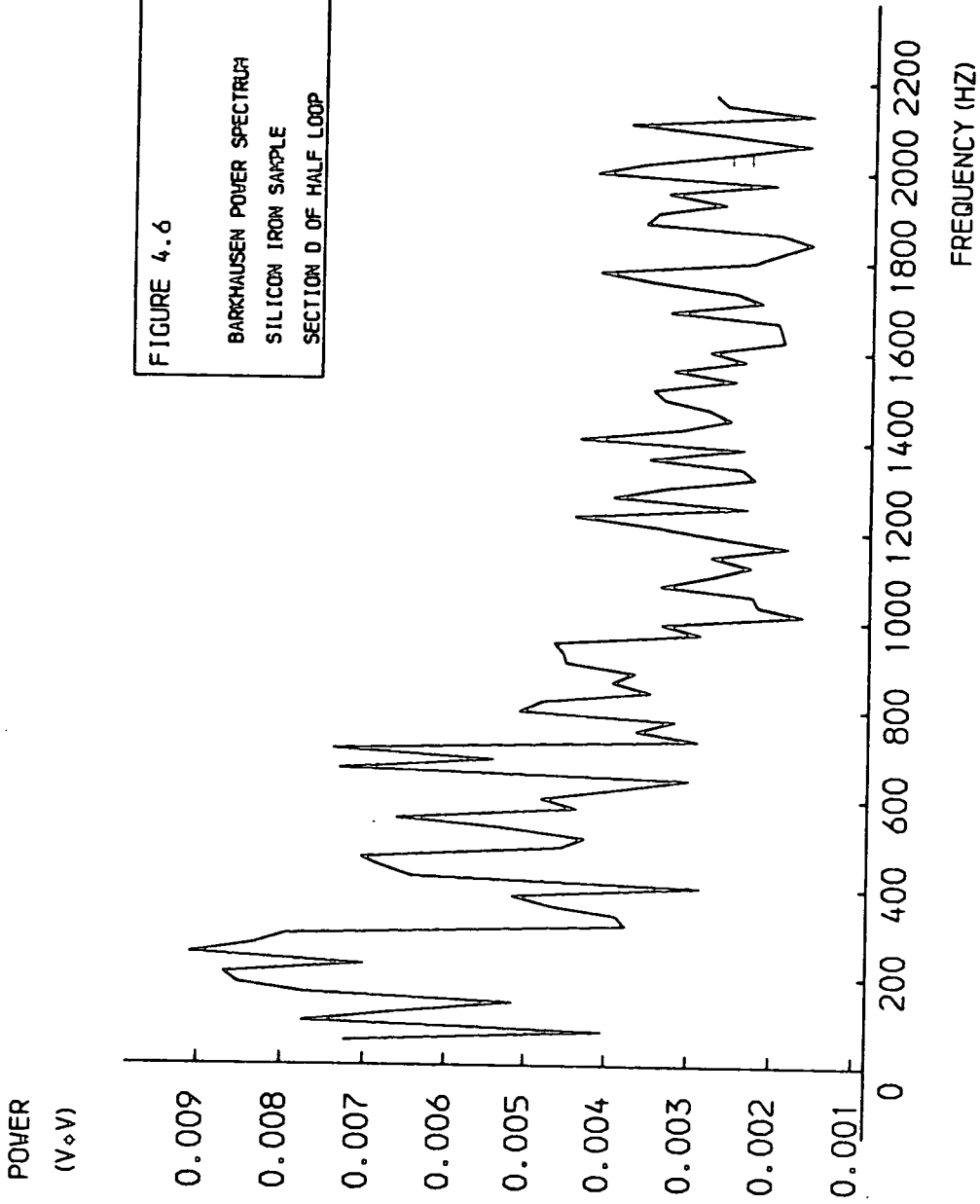


FIGURE 4.6
BARKHAUSEN POWER SPECTRUM
SILICON IRON SAMPLE
SECTION D OF HALF LOOP

POWER
(V²/V)

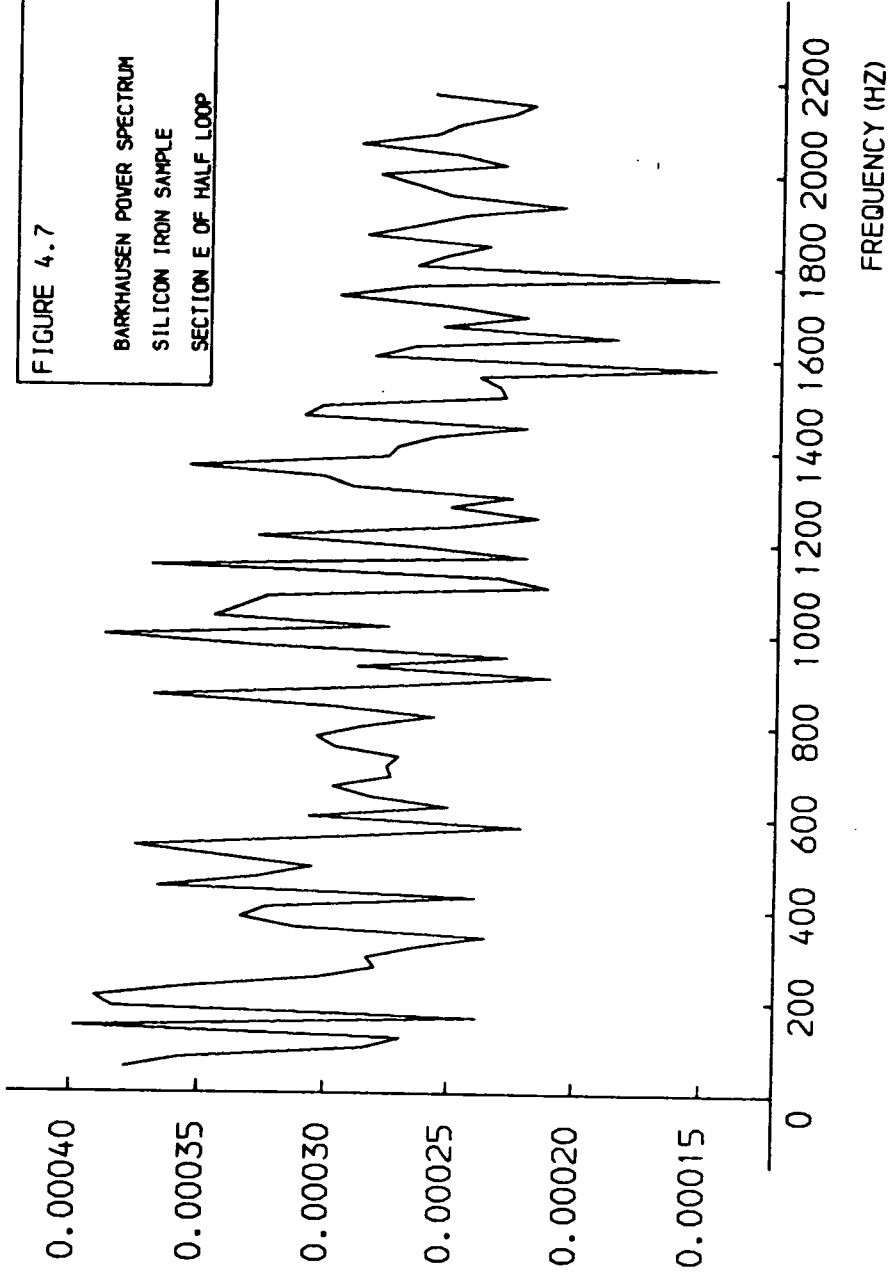
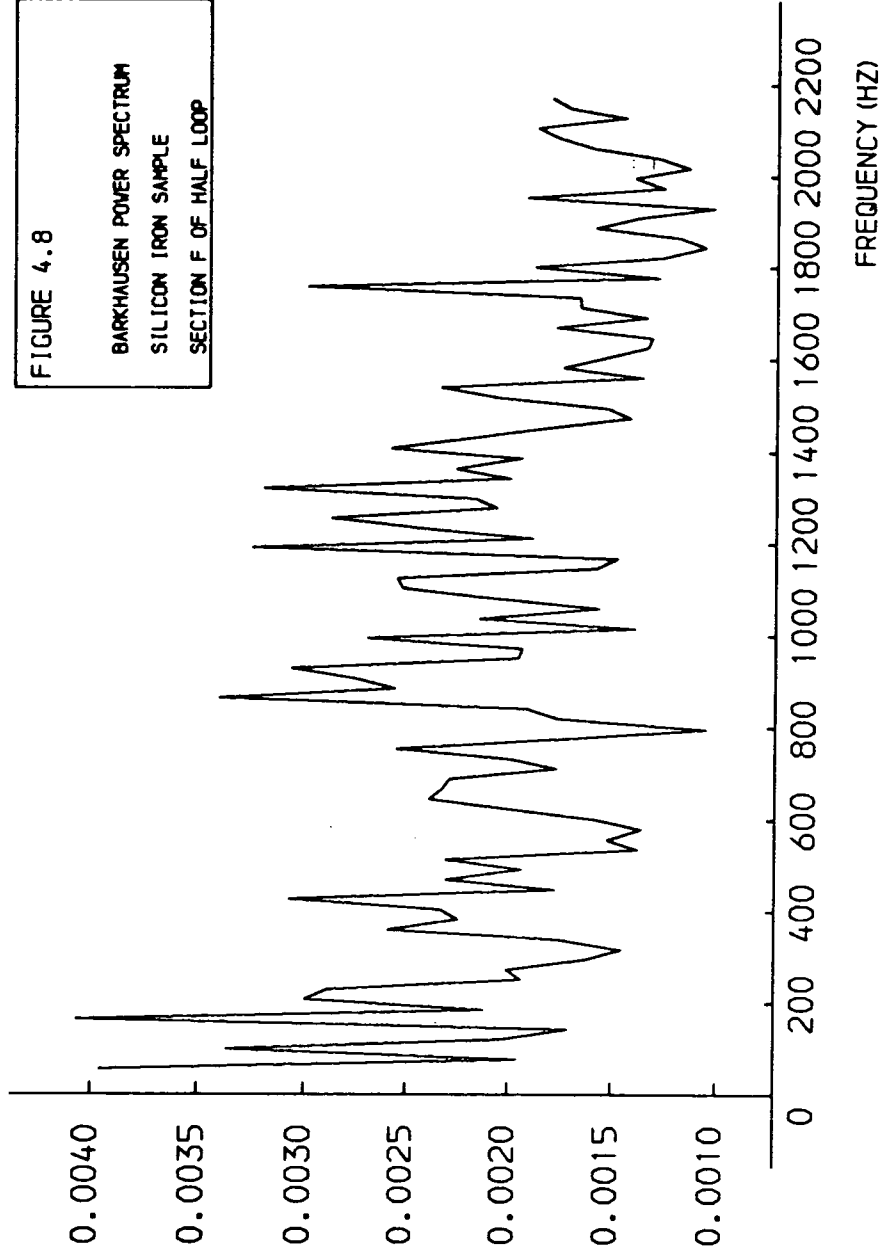


FIGURE 4.7
BARKHAUSEN POWER SPECTRUM
SILICON IRON SAMPLE
SECTION E OF HALF LOOP

POWER
(V \cdot V)



POWER
(V \cdot V)

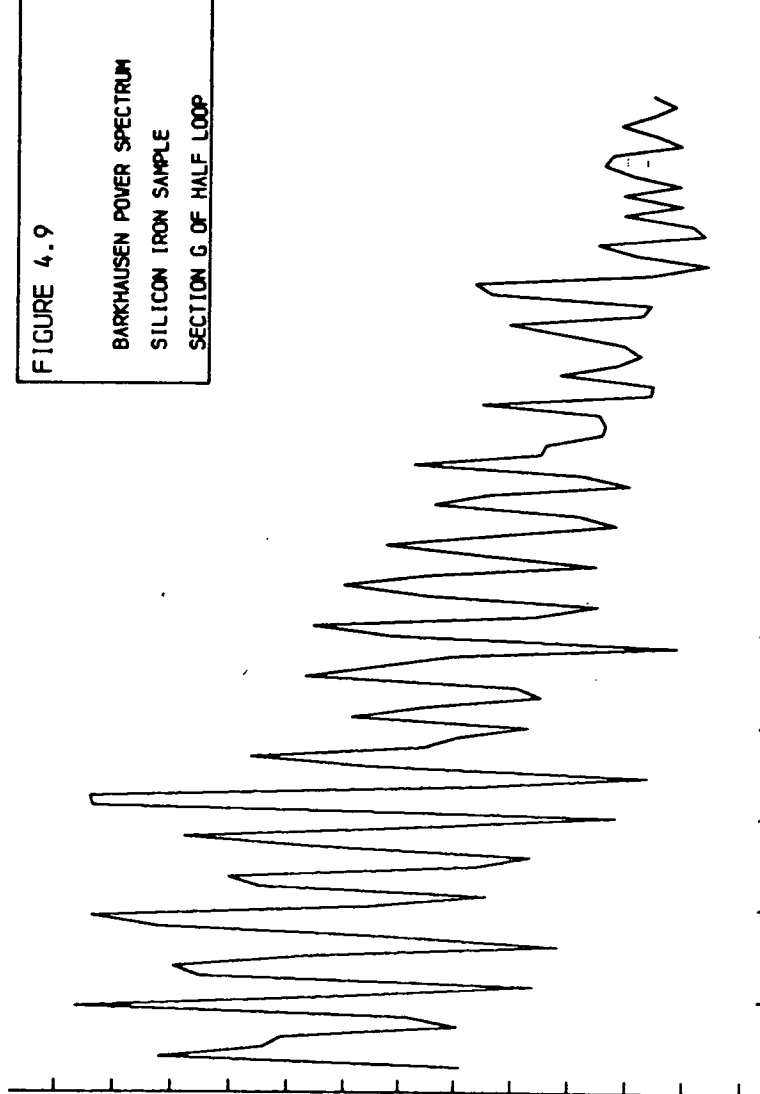
0.00070
0.00065
0.00060
0.00055
0.00050
0.00045
0.00040
0.00035
0.00030
0.00025
0.00020
0.00015
0.00010

0 200 400 600 800 1000 1200 1400 1600 1800 2000 2200

FREQUENCY (HZ)

FIGURE 4.9

BARKHAUSEN POWER SPECTRUM
SILICON IRON SAMPLE
SECTION G OF HALF LOOP



POWER
(V \cdot V)

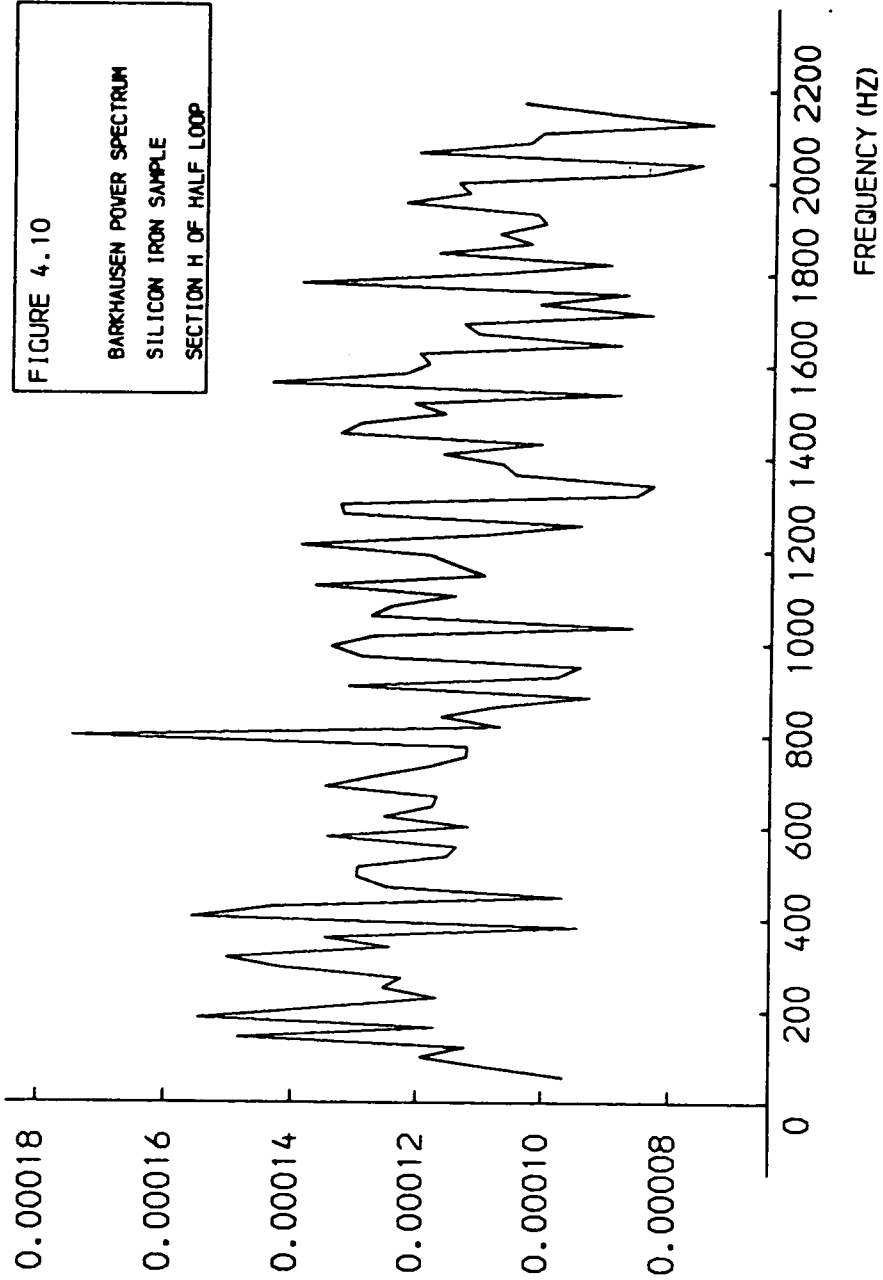


FIGURE 4.10

BARKHAUSEN POWER SPECTRUM
SILICON IRON SAMPLE
SECTION H OF HALF LOOP

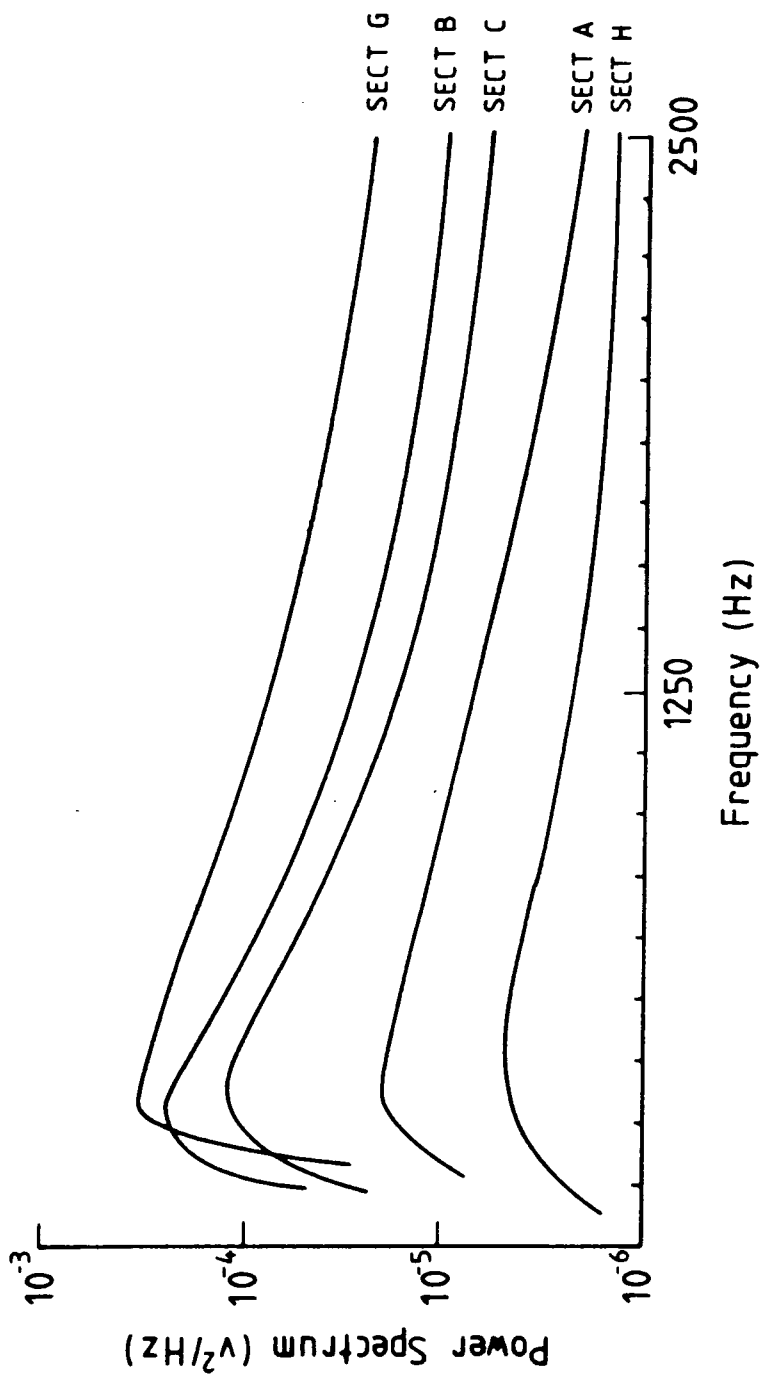


Figure 4.11 Power Spectra of Grain Oriented Silicon Iron showing Sections of Half Loop [1]

general trend is very similar and the order of the difference between the highest and lowest spectra is similar. The power spectrum for the half hysteresis loop of the eight sections together is as expected. It shows a fall off in the power from low frequency to high frequency. The amount of decrease for an interval corresponding to the ECSC roll-off point up to 2000Hz is in the order of one order of magnitude which is similar to the ECSC drop in power. The actual numbers on the power axis have little meaning as there are many different FFT algorithms all of which will give different values of power.

4.2 DISCUSSION

The power spectra may simply be interpreted as being the result of the addition of many similar pulses of Barkhausen noise. If a Barkhausen cluster could be represented by a single box function and the avalanches of clusters expected in this type of experiment as a series of these functions; it would be expected that the FFT would be something like that of a continuous square wave, the harmonics of the FFT dropping in height according to a relationship with the time period of the square wave. In practice the clusters are not separated sufficiently to allow the 'square wave' to develop and the shape of the cluster is modified according to the measuring system. The effect however

may be similar and a rapid drop in the noise power would be expected over a small frequency range.

It would be expected in a material such as a grain oriented silicon iron that the clusters would be of a similar size and duration from sample to sample as the quality control of the production system demands strict rules for certain material parameters. The grain size should be very similar for samples from the same production process. This would imply a fairly consistent level for the Barkhausen noise, although for varying grain sizes it was found that there was little difference in the power spectra (ECSC reports) and that the results were not always as expected. For these reasons there seems little point in developing an NDT system based on power spectra.

The results of the tests carried out on the Epstein strips of silicon iron were in general consistent with those obtained by other workers, in that there was;

- a) a considerable difference in power spectrum at different points on the hysteresis loop.
- and b) the power spectra plotted displayed a similar shape and reduction in power over the frequency range considered.

4.3 CONCLUSION

The results show that the Barkhausen noise measuring system developed was indeed measuring the Barkhausen noise from the silicon iron and that the measurements to be carried out on constructional steels could be expected to be appropriate to the noise from those materials.

CHAPTER 5 - DATA HANDLING - CONSTRUCTIONAL STEELS

5.1 DATA HANDLING

The equipment was used with the parameters described in Chapter 3. The data collected were stored on a magnetic tape at NUMAC in the form of matrices of dimensions (8, 4095). Each data file represented one experimental run; ten such files formed the data for one steel sample. The data were treated in two different ways; the first involving the Fourier transform of the data, the second involving the voltage pick-up alone.

5.1a Power Spectra

The Fourier transform of the data was performed by a FORTRAN program on NUMAC, the transform algorithm being provided by a standard NAG library routine. The full program is shown in appendix A. The voltage values were squared before transforming. The transform algorithm used by the routine, a Fast Fourier Transform (FFT), for a series of N observations of a real value, x , was;

$$\hat{z}_k = \frac{1}{\sqrt{N}} \sum_{j=0}^{N-1} x_j \exp \left(\frac{-i 2\pi jk}{N} \right)$$

$$k = 0 \dots N-1$$

$$j = 0 \dots N-1$$

The result of running the program was a series of spectral estimates at divisions of frequency related to the total time of the original time series;

$$f = 1 / T$$

where, T is the total time of the original series

f is the frequency division of the spectral estimates.

For the constructional steel samples this gave a frequency division of 6.11Hz.

The spectral estimates ω_k formed a Hermitian sequence, that is for a series of N data points;

$$\omega_k = \omega_{N-k}$$

The number of appropriate spectral estimates was therefore half the number of original data points. For convenience in plotting, the spectral estimates were grouped into 'bins', each bin containing 20 estimates. The mean of the bin was found and plotted at the appropriate frequency. The total FFT for each sample was found by adding the appropriate bins for the 10 sets of data. It was possible to do this as all the time series were of the same length and the spectral estimates therefore at the same divisions of frequency. It was not possible to treat the ten sets of data as one continuous time series as the data file was too large for the NUMAC routine to handle and in the

Joining there would be a discontinuity at each boundary causing a component of the Fourier series to be passed in the analysis which was not appropriate to the experimental data. Initially, the standard error in the mean of each bin was found and used as an estimate of the experimental error involved; this was later not used, as it seemed more appropriate to estimate the size of experimental errors by considering the repeatability of the experiments and the errors involved in the fitting of a straight line to the spectrum.

Graphs of the power spectra were plotted using a FORTRAN program on NUMAC. The plotting routine is made up by a series of calls to the GHOST graphics library. An example program is shown in appendix A. The plotting routine is fairly flexible and could be adapted for all the plots required.

5.1b Voltage Plots

In order to make plots of the voltage profiles of the Barkhausen noise every 80 points of the individual data files were averaged. This step was necessary as the full data set would have been too large to be held on NUMAC. The averaged sets of data were concatenated to form a single data file which was plotted using a FORTRAN program on NUMAC. The average voltage was plotted as the ordinate and the appropriate time as the

abscissae. It should be noted that it is modulus voltage that is plotted.

5.2 GRAPHICAL PRESENTATION OF DATA

5.2a Appearance of Power Spectra

The results obtained from the Fourier transform of the individual sections of the experiments on steel sample 40 are shown in figures 5.1 to 5.10. Figure 5.11 shows the total FFT made up from the addition of the components of the individual sections.

It can be seen from the voltage profile plots, for example figure 5.12, that the separate sections which are Fourier transformed will be of very different shapes. The effect of this on the total FFT will be to introduce low frequency components and their harmonics. For example an upward trend in the positive voltage squared will be interpreted by the FFT program as part of a triangular waveform with a period equal to the observation window length. Slower variations will not be revealed by the FFT as they will not be continuous. In a region where there is no significant gradient to the positive voltage squared but there is an offset from zero there will be a low frequency component introduced. In theory if the offset were perfectly level the component introduced would be a delta function at zero frequency with height proportional to the offset. The peak, X, observed from some of the

POWER
(V²/V)

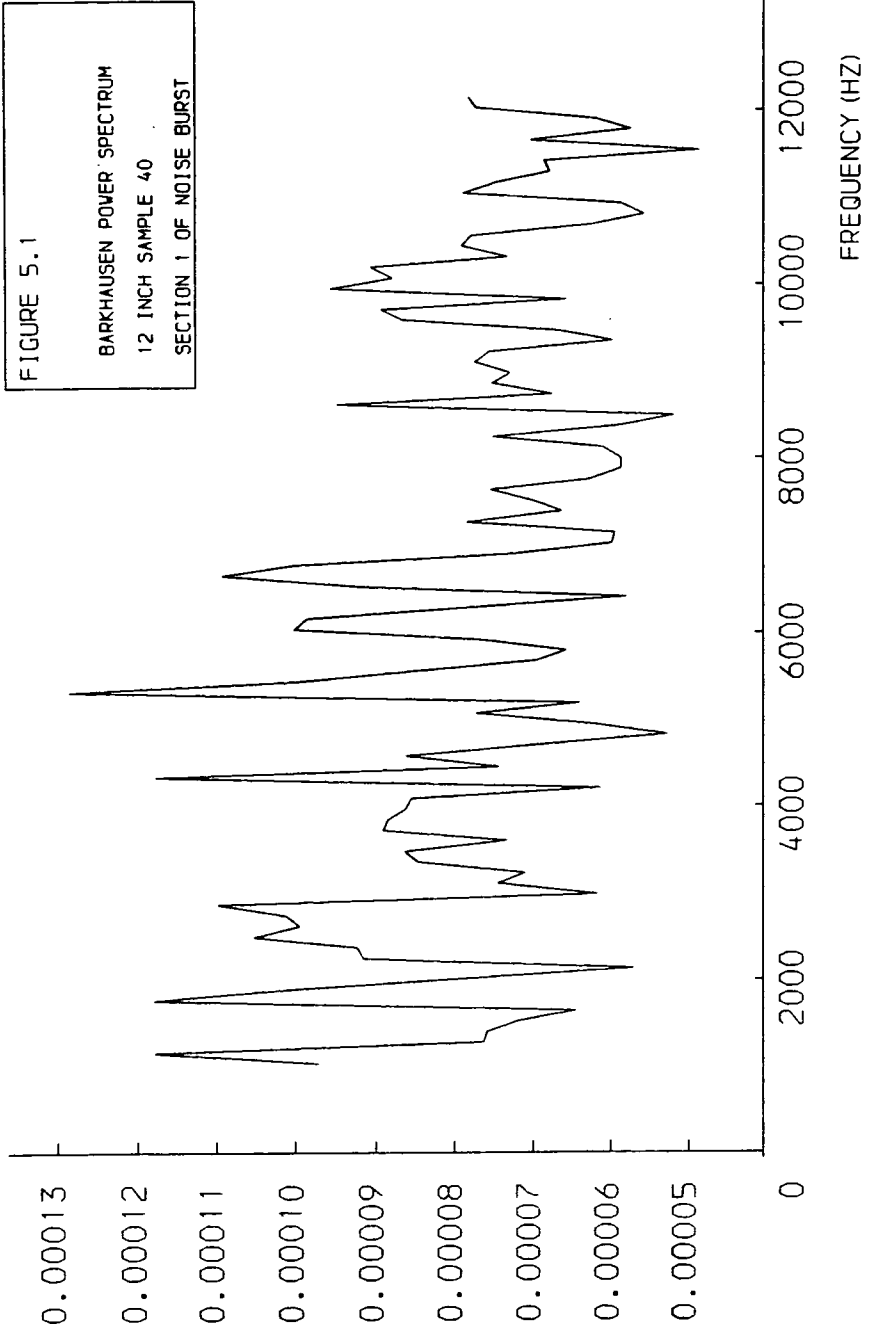


FIGURE 5.1

BARKHAUSEN POWER SPECTRUM
12 INCH SAMPLE 40
SECTION 1 OF NOISE BURST

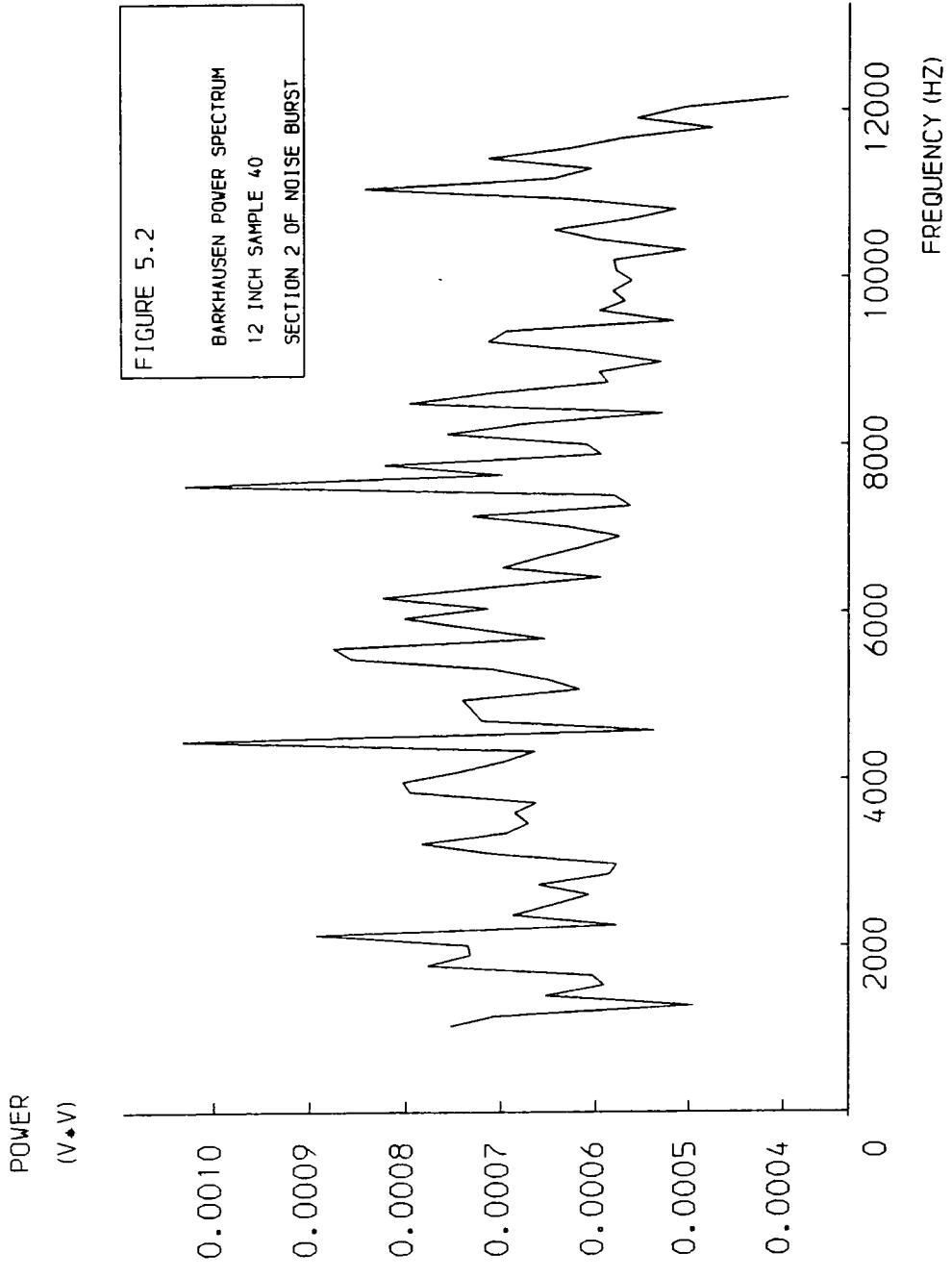


FIGURE 5.2
BARKHAUSEN POWER SPECTRUM
12 INCH SAMPLE 40
SECTION 2 OF NOISE BURST

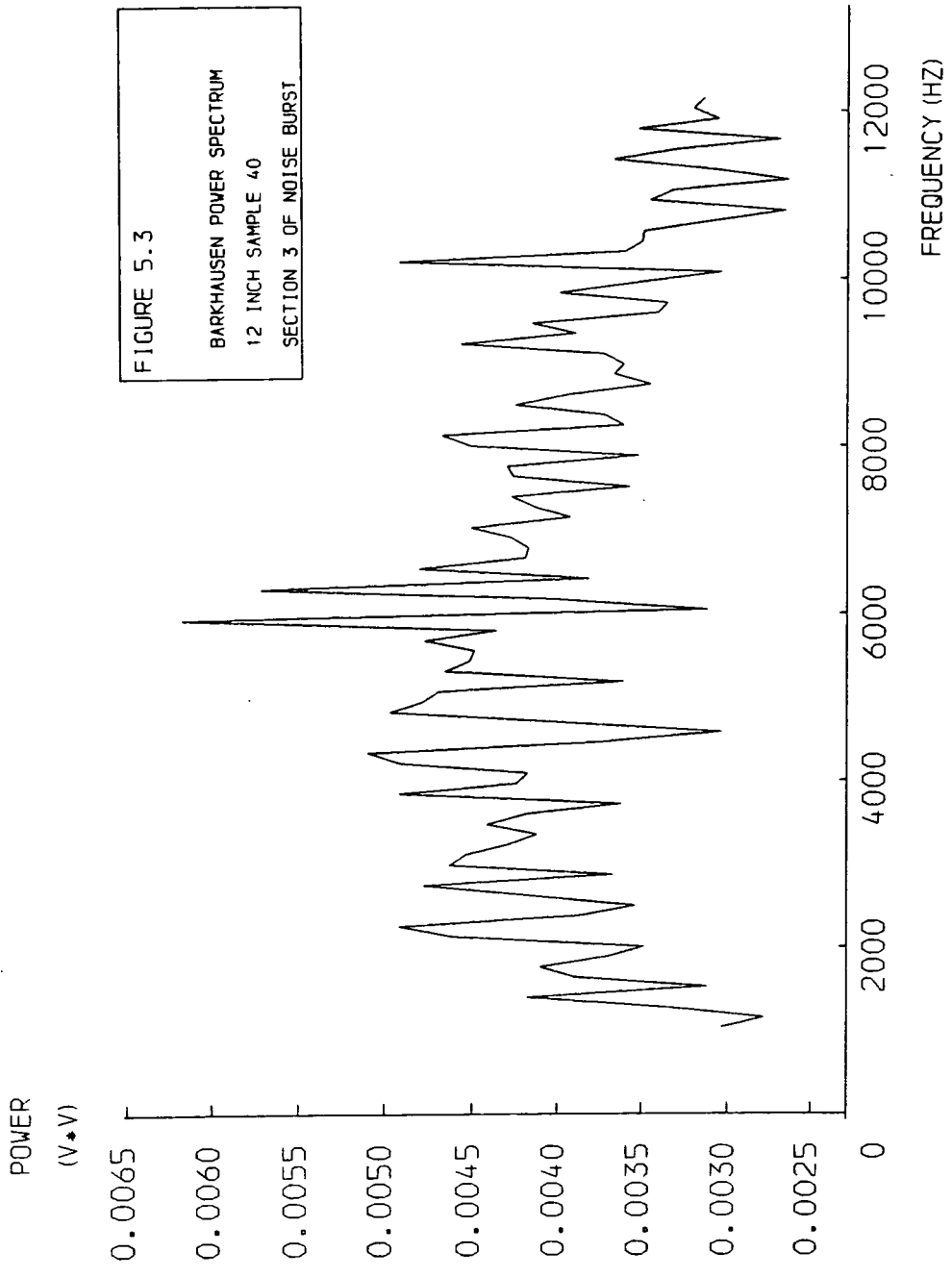


FIGURE 5.3
BARKHAUSEN POWER SPECTRUM
12 INCH SAMPLE 40
SECTION 3 OF NOISE BURST

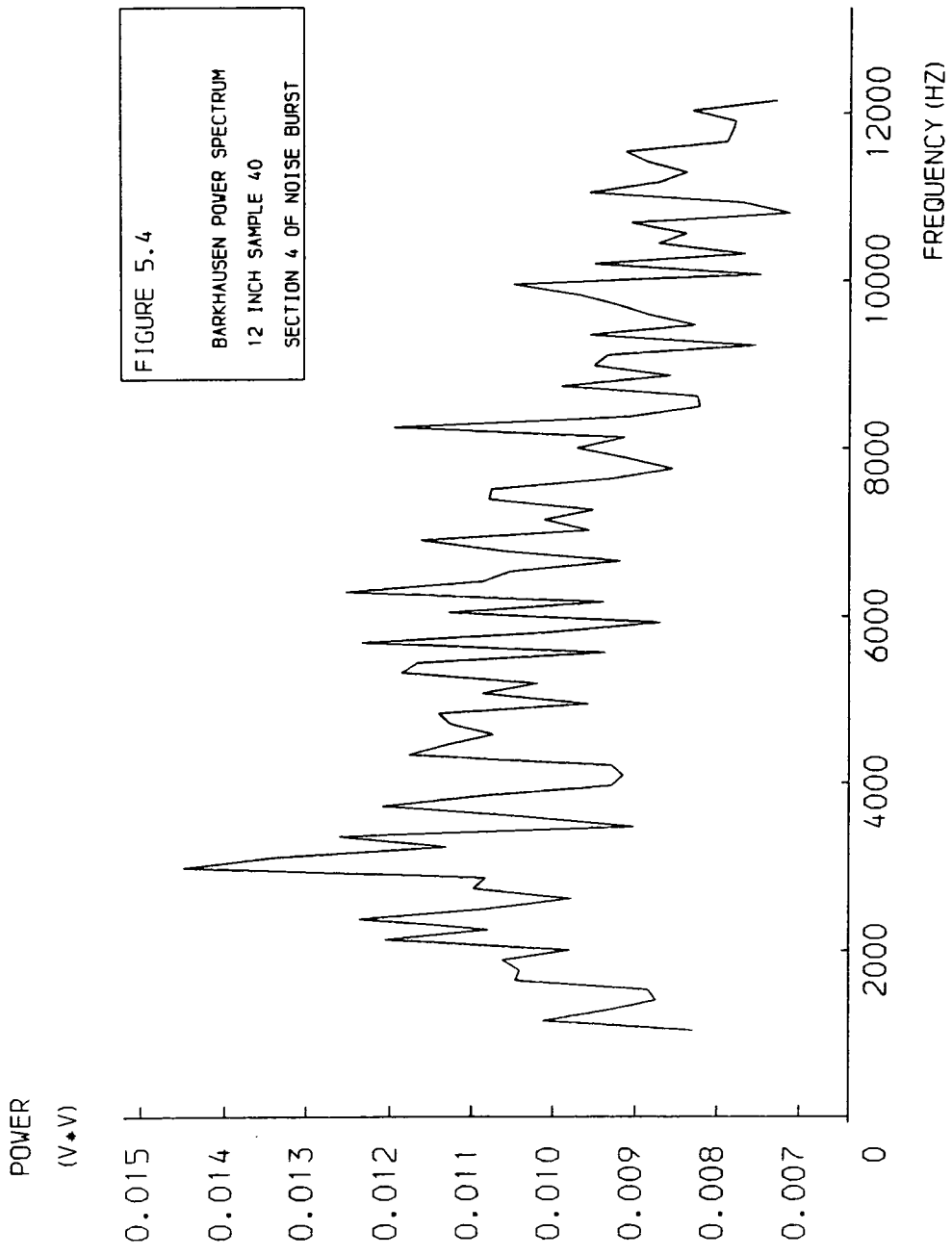


FIGURE 5.4
 BARKHAUSEN POWER SPECTRUM
 12 INCH SAMPLE 40
 SECTION 4 OF NOISE BURST

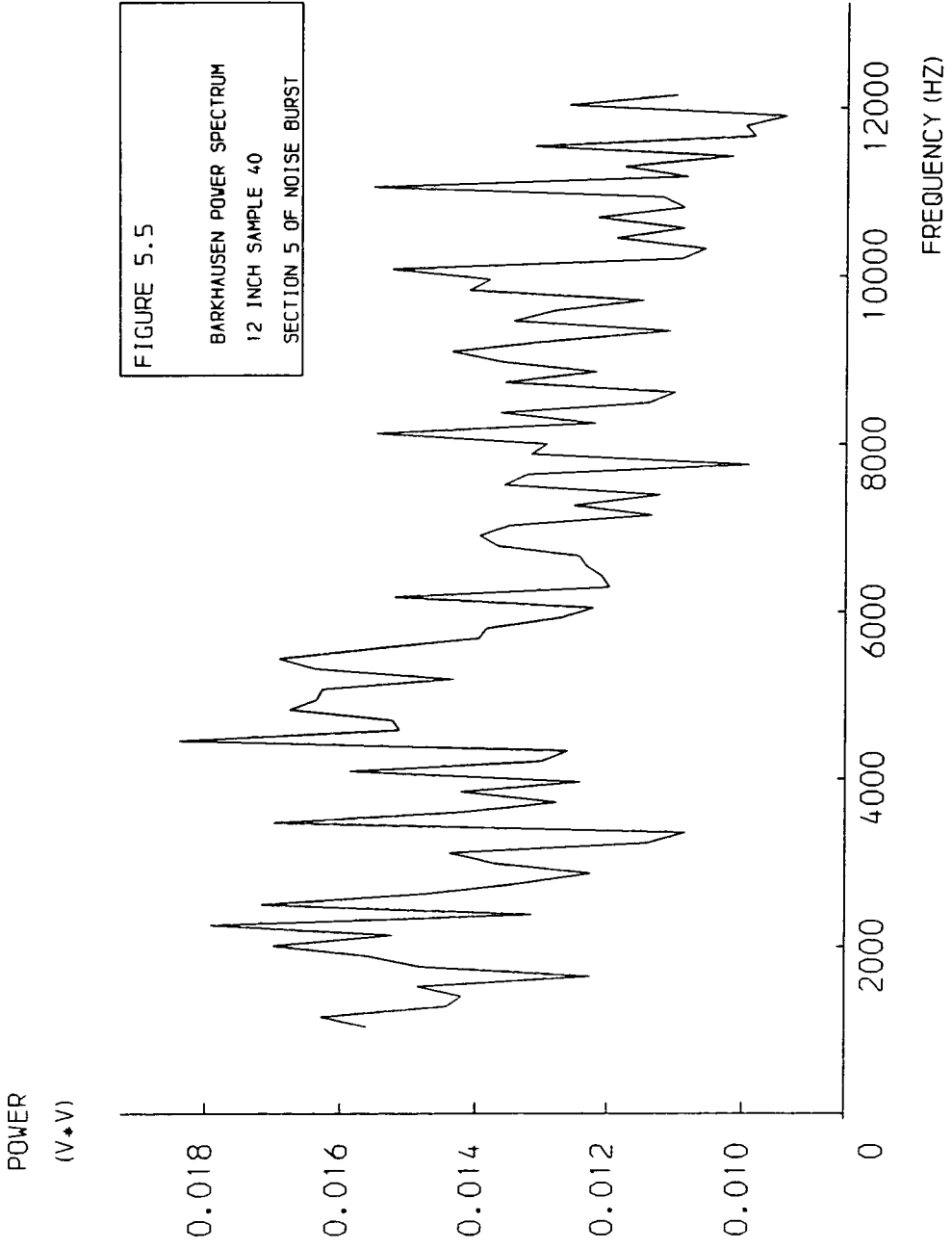
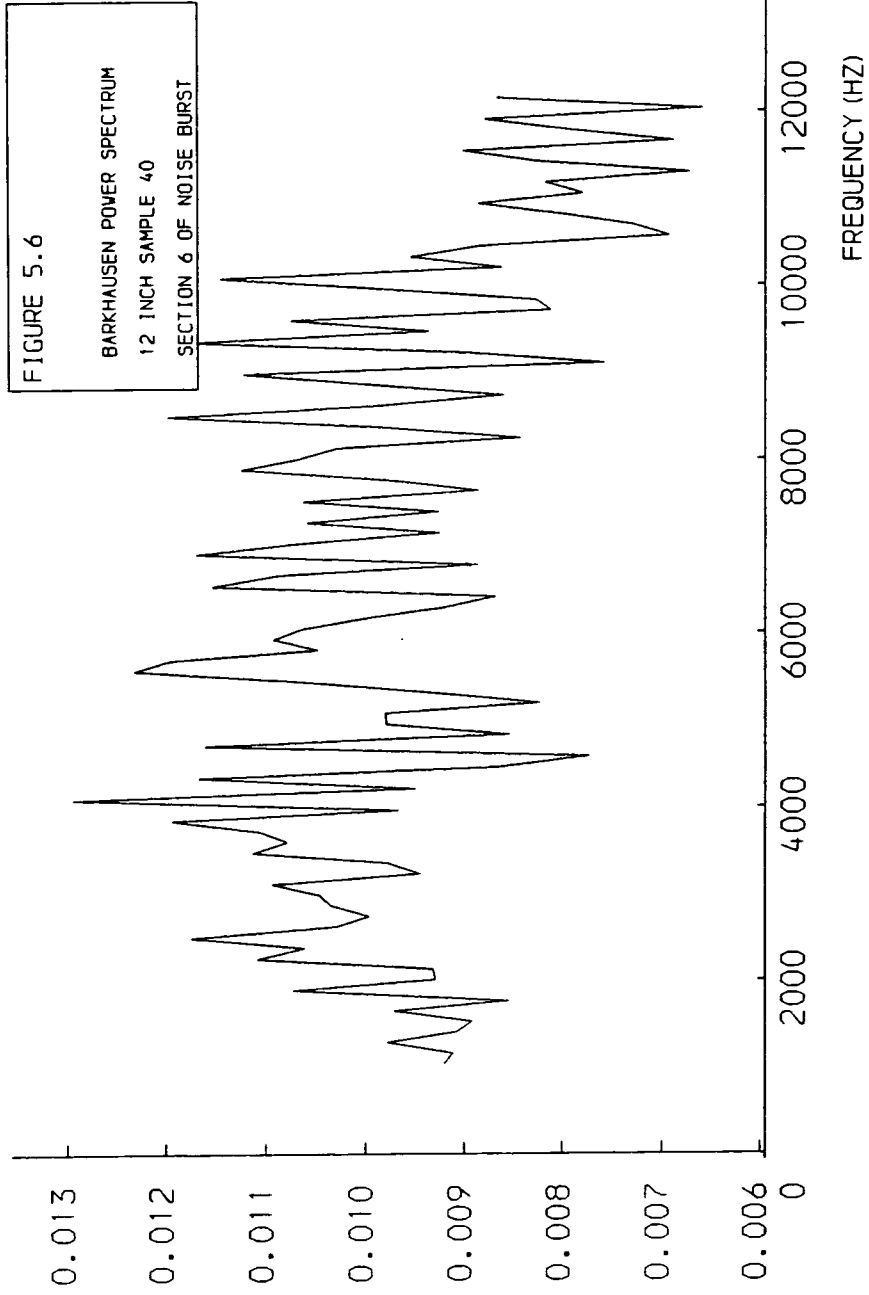
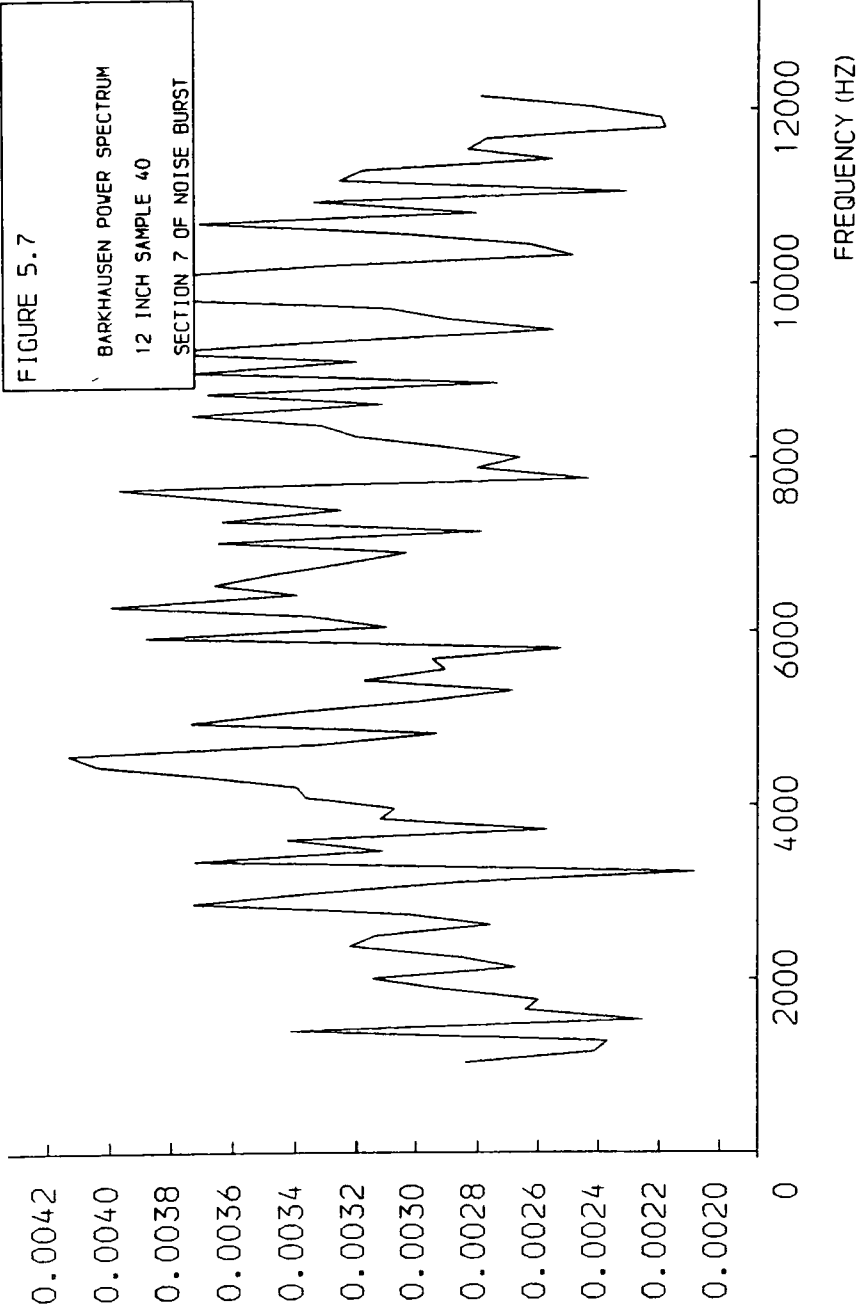


FIGURE 5.5
BARKHAUSEN POWER SPECTRUM
12 INCH SAMPLE 40
SECTION 5 OF NOISE BURST

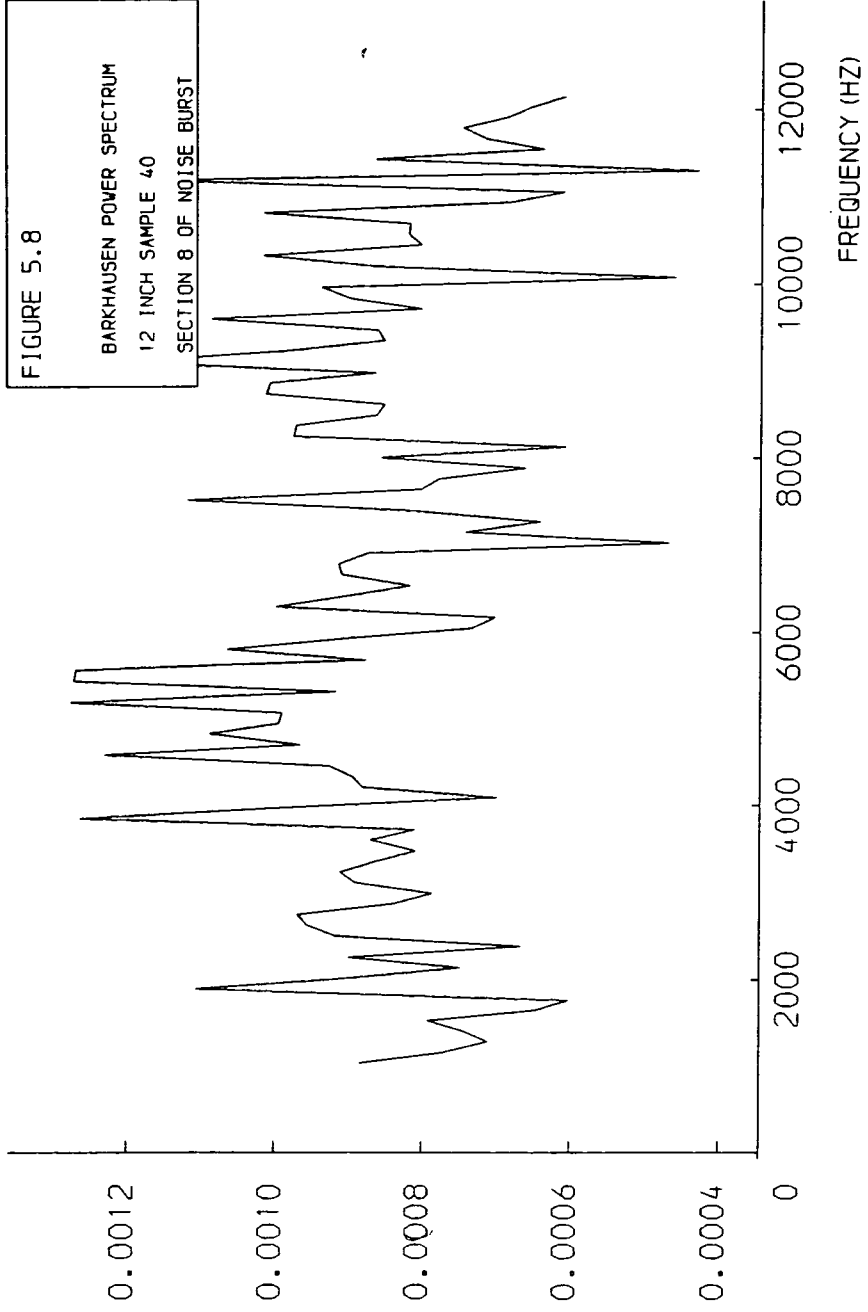
POWER
(V²/V)



POWER
(V²/V)



POWER
(V²/V)



POWER
(V*V)

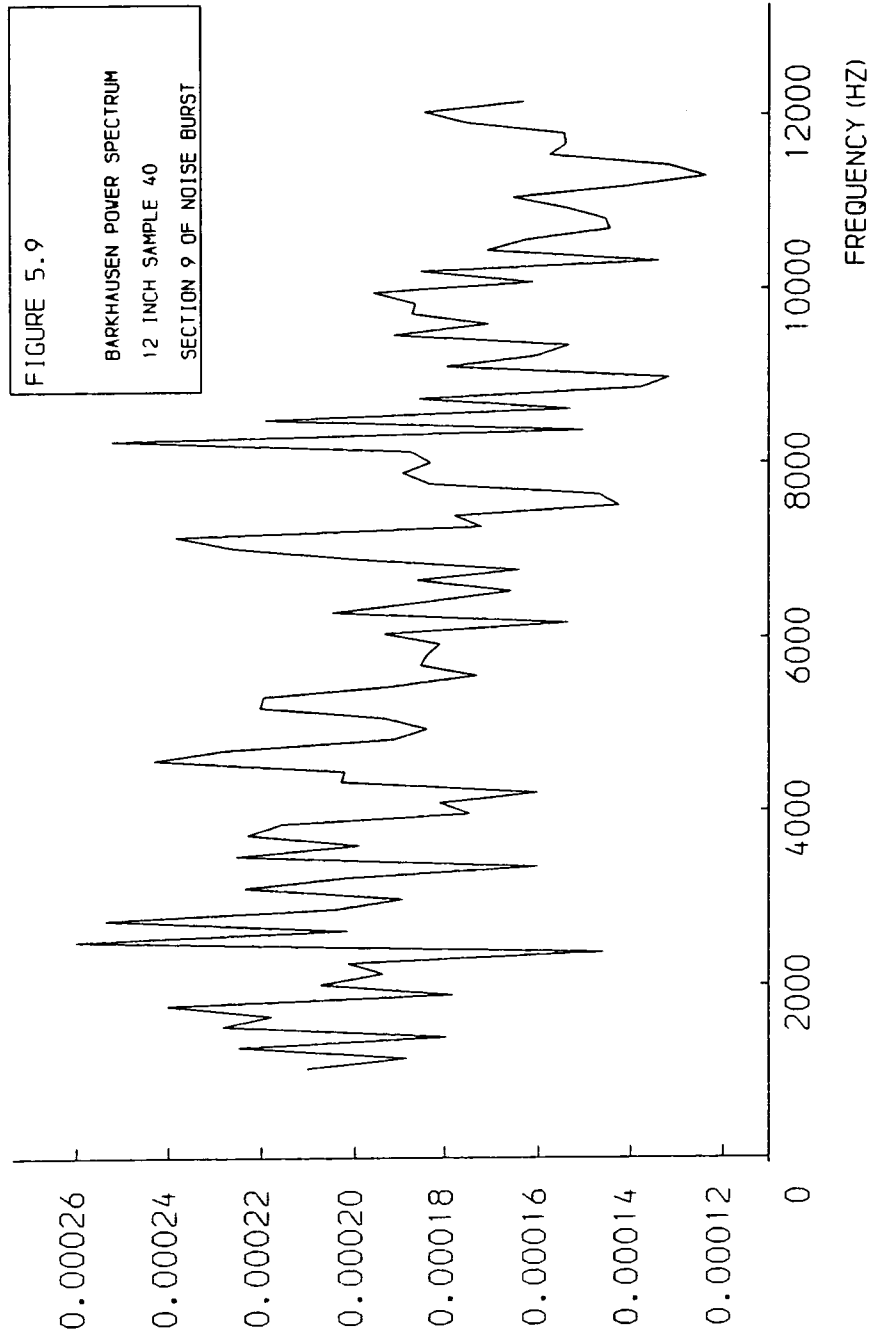


FIGURE 5.9
BARKHAUSEN POWER SPECTRUM
12 INCH SAMPLE 40
SECTION 9 OF NOISE BURST

POWER
(V*V)

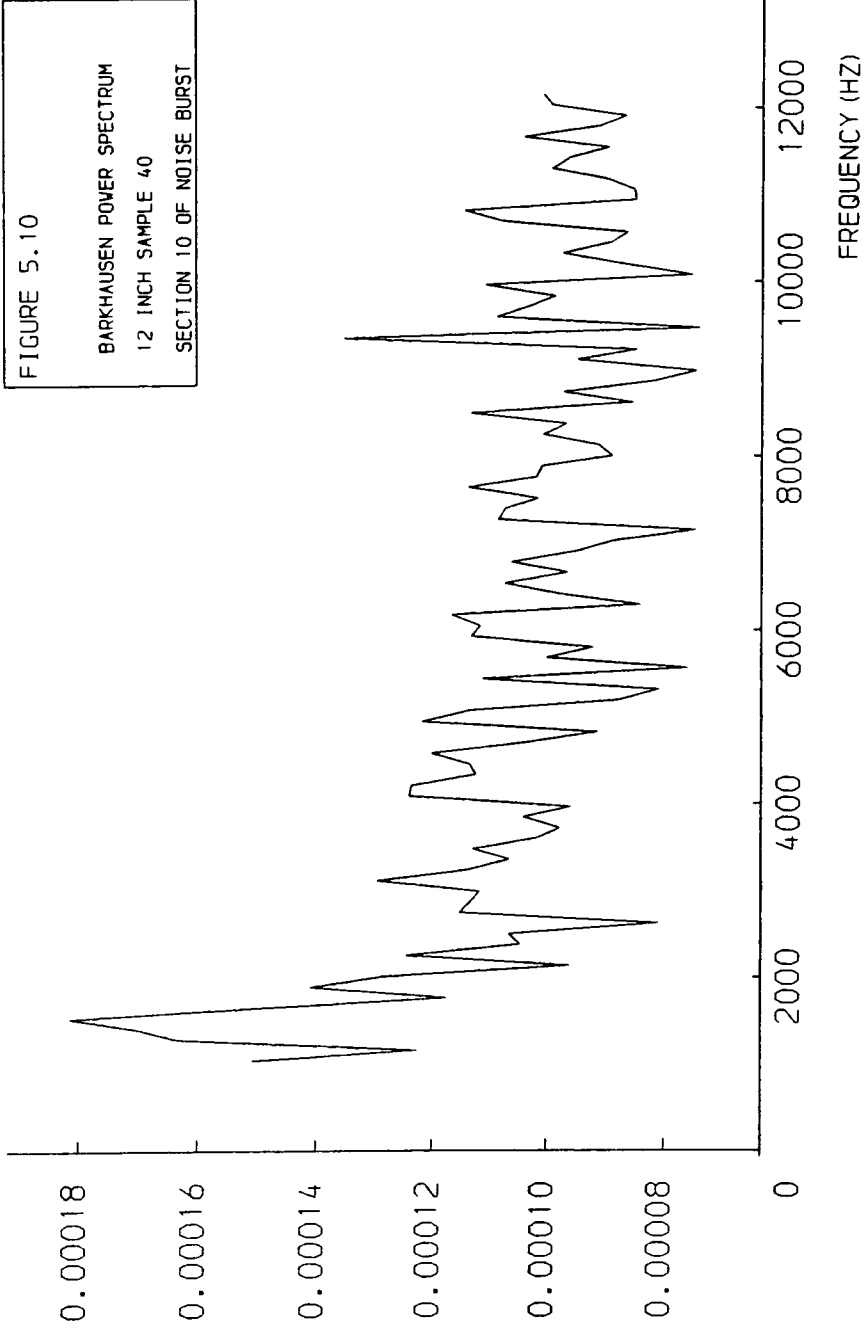


FIGURE 5.10

BARKHAUSEN POWER SPECTRUM
12 INCH SAMPLE 40
SECTION 10 OF NOISE BURST

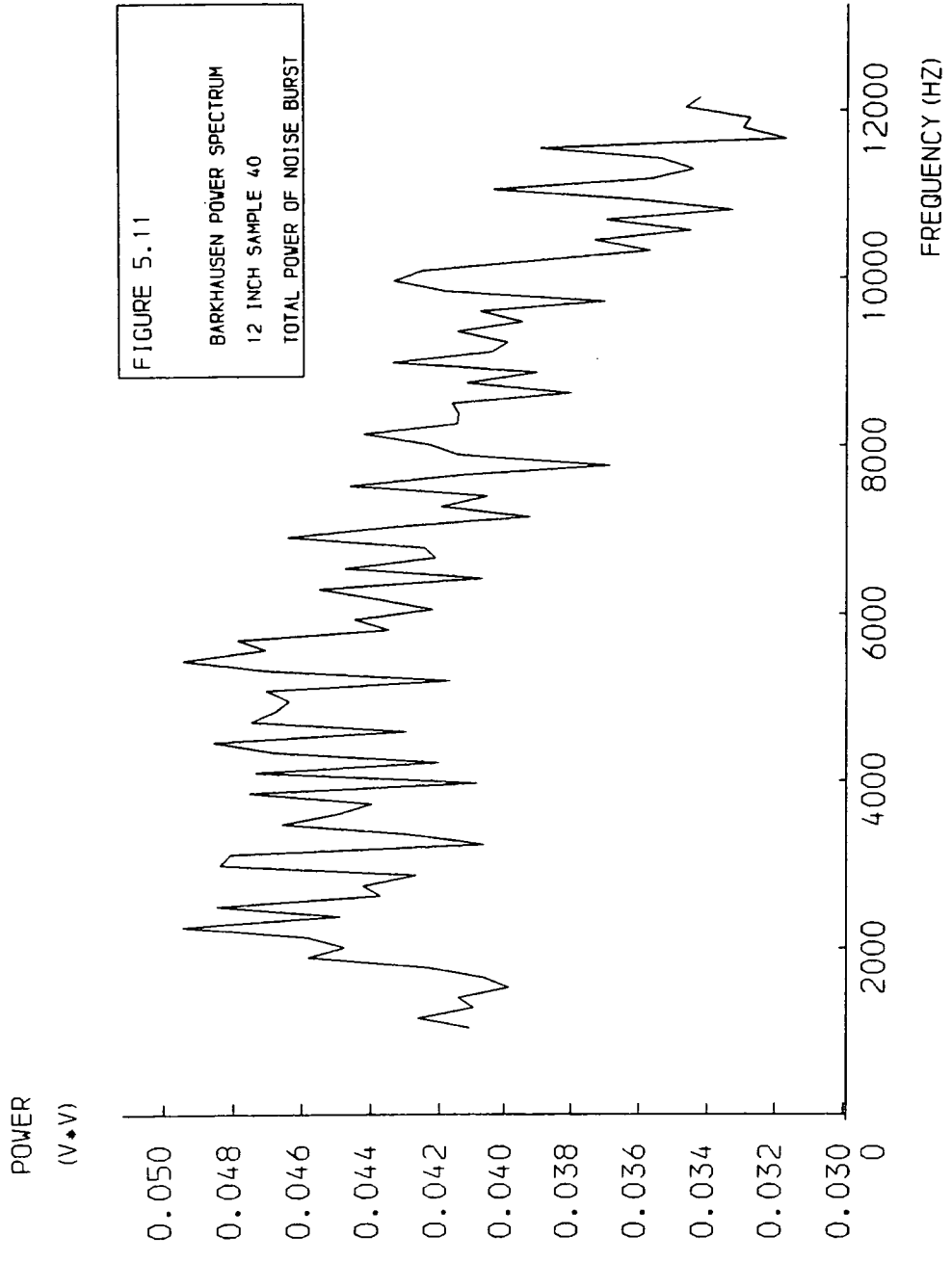
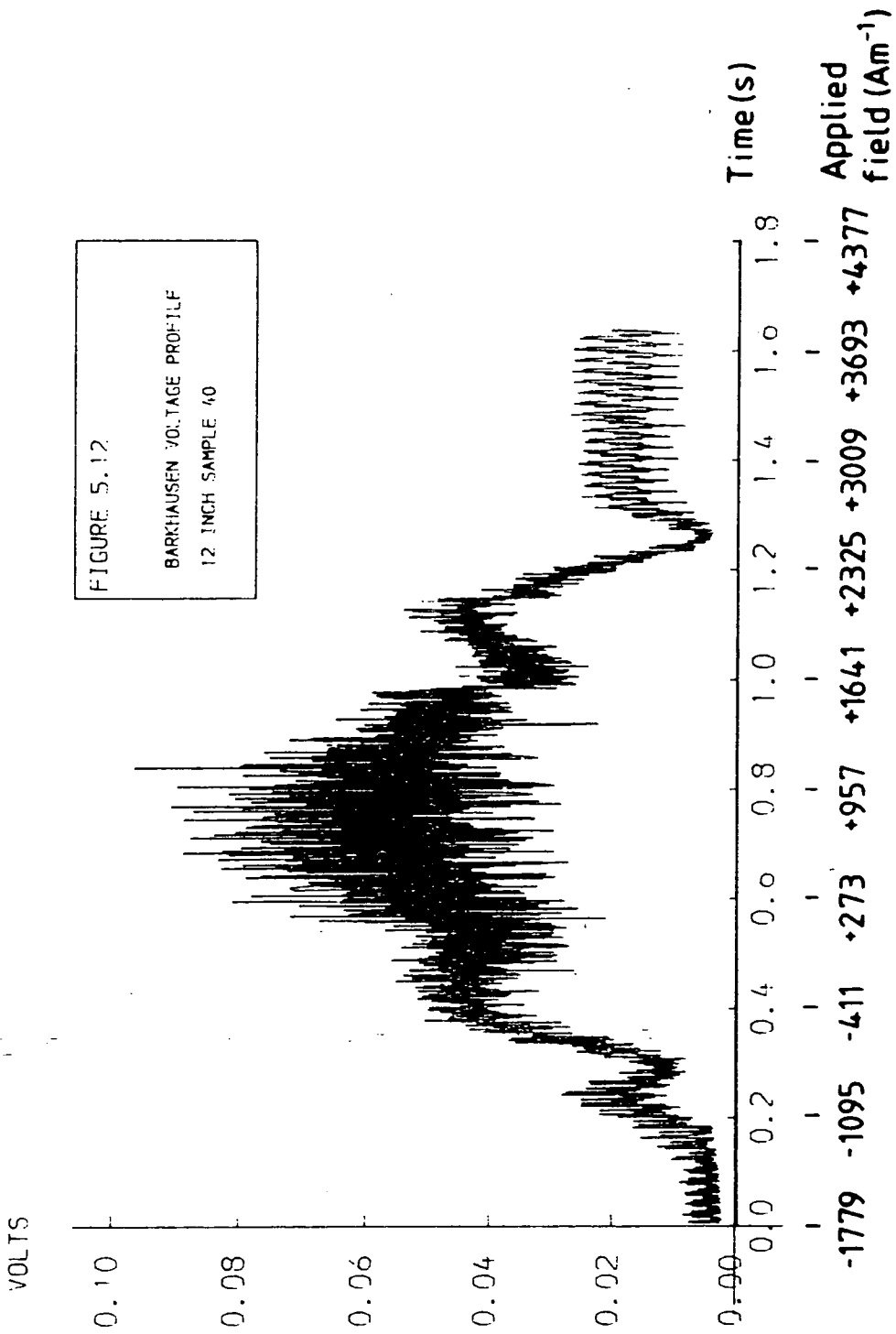


FIGURE 5.11
 BARKHAUSEN POWER SPECTRUM
 12 INCH SAMPLE 40
 TOTAL POWER OF NOISE BURST



samples and shown in figure 5.13 is positioned over more than one data window. The peak will therefore introduce low frequency components to the FFT but will not significantly affect the plotted power spectra.

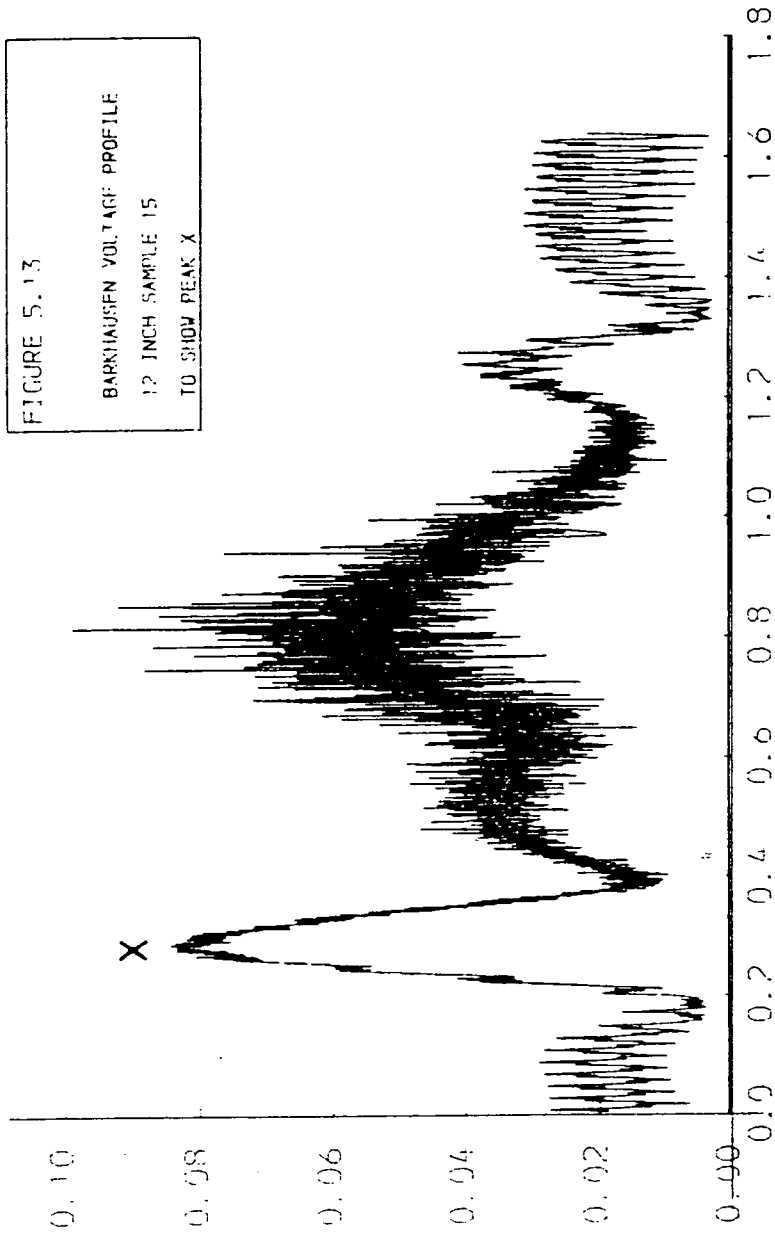
The level of the spectrum can be seen to increase from section 1 to a peak value then decrease to section 10. This would be expected as the Barkhausen activity increases and decreases across the time interval. The spectra for all the 12 inch samples showed similar behaviour. The lack of smoothness in the plots is a characteristic of an FFT used without any data manipulation and it was not considered necessary to alter the analysis procedure as the results were to be least squares analyzed.

5.2b Appearance of Voltage Plots

An unusual feature of the voltage plots was the large peak before the main Barkhausen activity peak shown on figure 5.13 and labelled X. The peak, X, occurred on several but not all of the plots.

It was firstly considered that it may be a function of surface condition. Samples 15 and 5 were chosen to assess the surface effect. The surface of 15 was etched in a 95% ethanol, 5% nitric acid solution until approximately 0.02mm of material had been removed. The depth of surface removal was decided by considering the damage to the surface by grinding [1]. The experiment was run on the sample. The peak was

VOLTS



Time (s)

Applied field (Am⁻¹)

-1779 -1095 -411 +273 +957 +1641 +2325 +3009 +3693 +4377

still clearly visible. Plots of the hysteresis loops of the samples were checked for any apparent discontinuities but none were found. Sample 16, which had had its surface etched in a similar manner, had its loop re-assessed on the British Gas On Line Inspection Centre (OLIC) permeameter and was found to have no major differences in its loop shape to the last measurement.

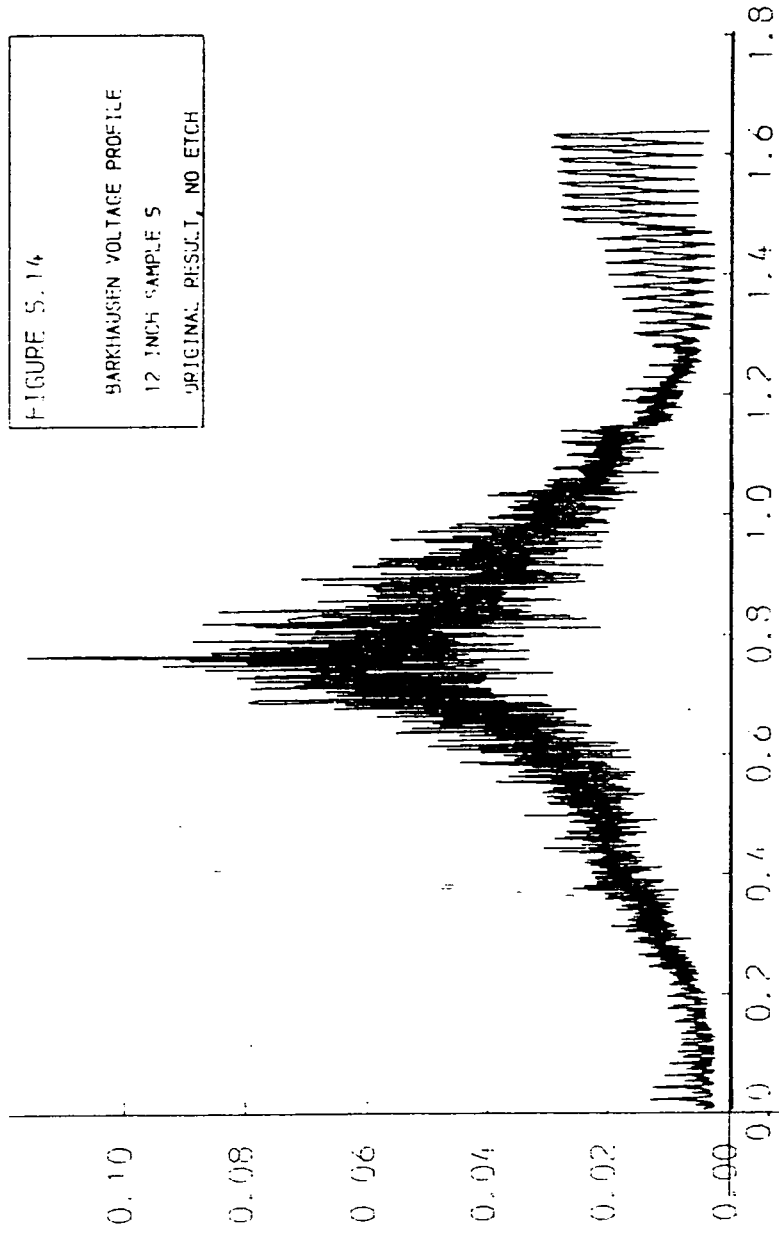
It was considered that the depth of removal of material was not sufficient to remove all damage done in machining, the exact nature of the cutting process not being known. It was decided to remove several layers of material by etching from the surface of sample 5 which had not shown a peak, X, to investigate the possibility of a peak appearing. The layers were removed at the following intervals.

	Mean thickness at centre(mm)	Amount of removal (mm)
original	5.22	—
etch 1	5.19	0.03
etch 2	5.17	0.02
etch 3	5.15	0.02
etch 4	5.13	0.02

The thickness was measured at five places at the centre of the sample near to the expected position of the pick-up coil.

Figures 5.14 to 5.18 show the plots of the above experiments. It can be seen that there is a peak, X, on the plots but it is not apparent after the fourth etch.

VOLTS



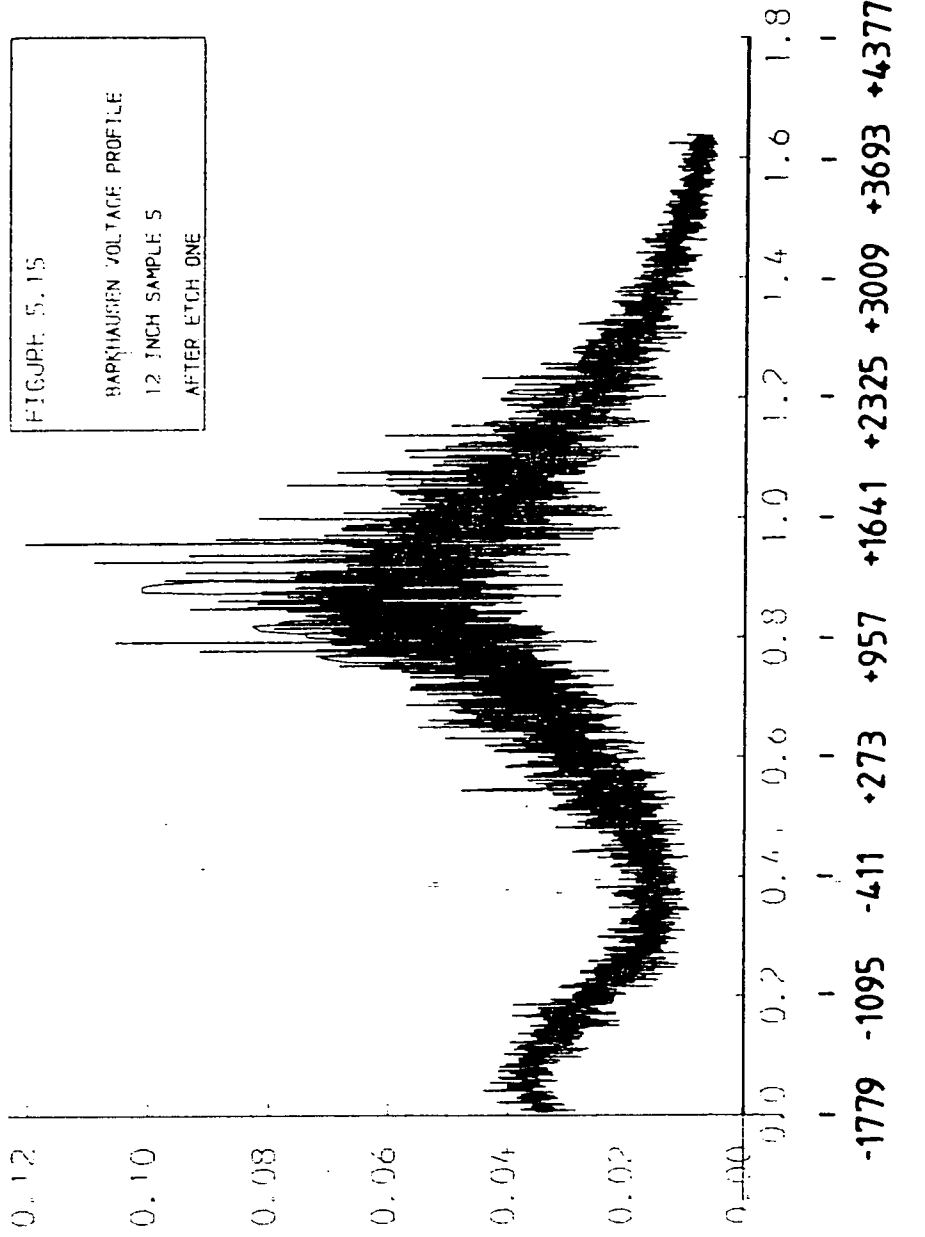
Time (s)

Applied field (Am^{-1})

-1779 -1095 -411 +273 +957 +1641 +2325 +3009 +3693 +4377

VOLTS

FIGURE 5.15
BARKHAUSEN VOLTAGE PROFILE
1.2 INCH SAMPLE 5
AFTER ETCH ONE



VOLTS

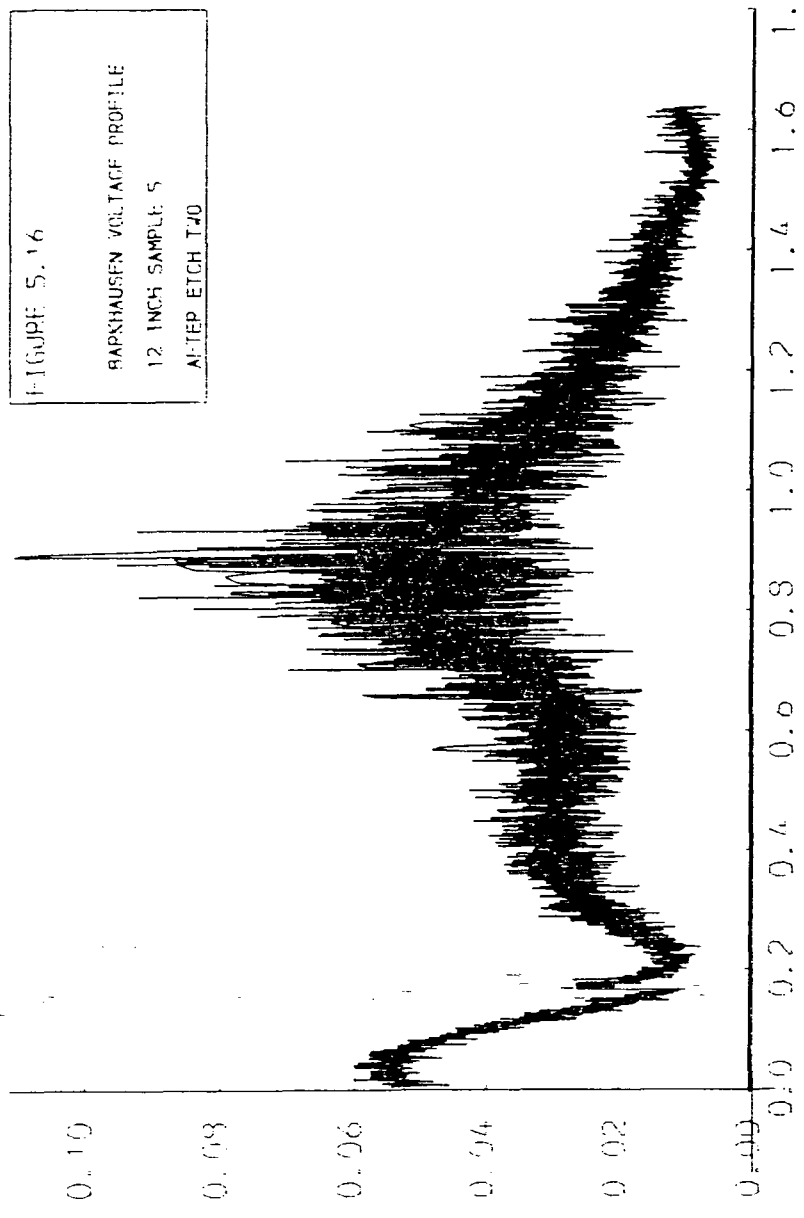
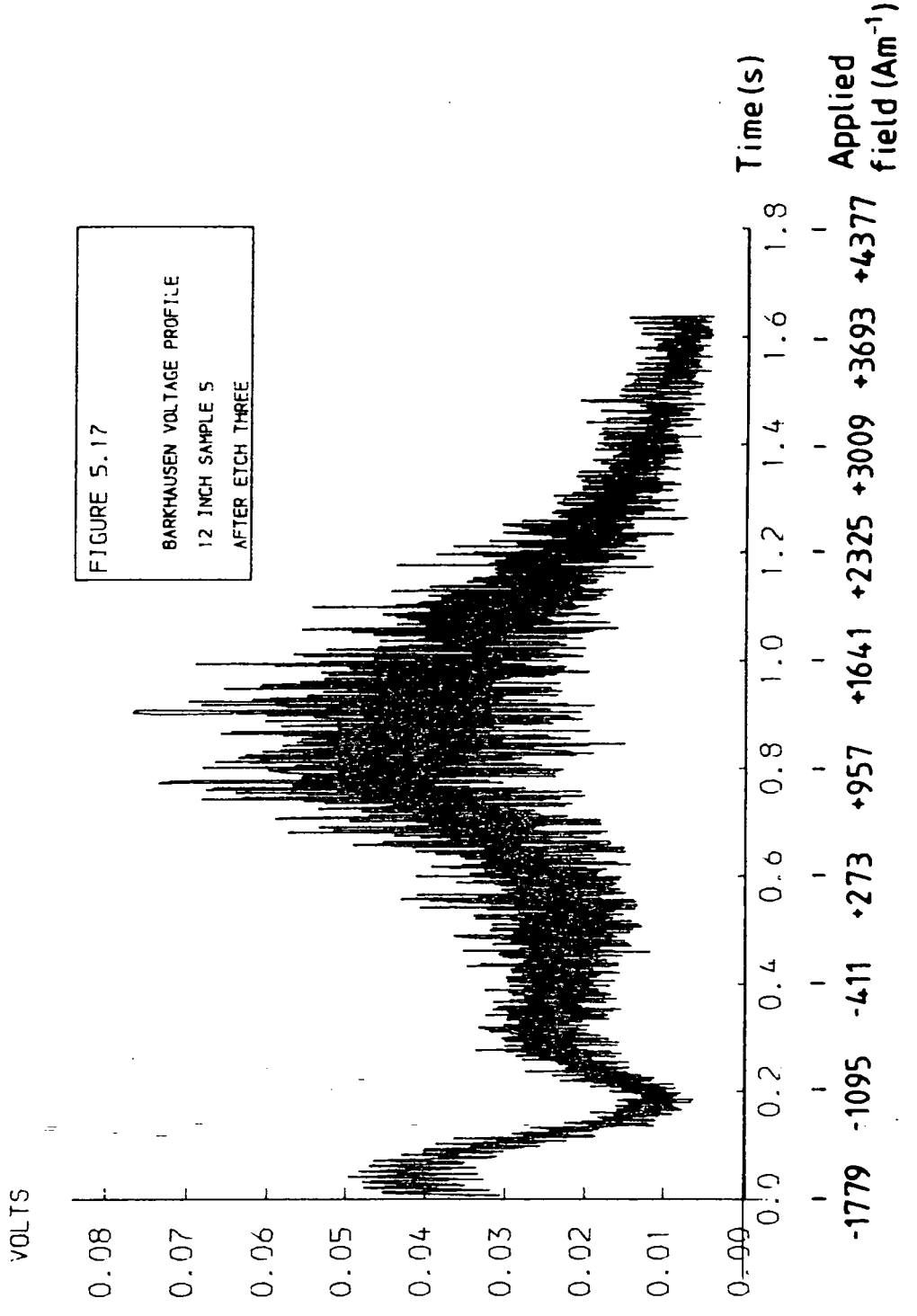


FIGURE 5.16
RAPSHAUSEN VOLTAGE PROFILE
12 INCH SAMPLE: 5
AL-TEP ETCH T20

Time (s)

Applied field (Am⁻¹)

-1779 -1095 -411 +273 +957 +1641 +2325 +3009 +3693 +4377



VOLTS

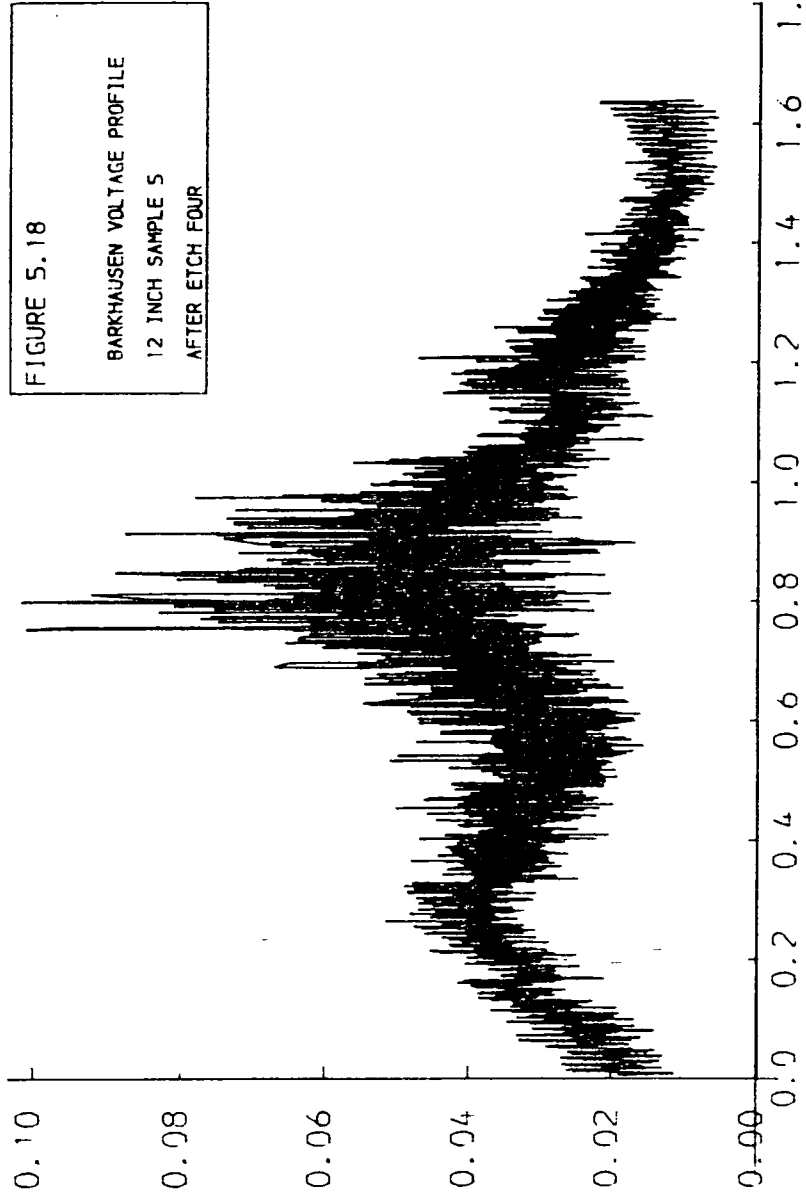


FIGURE 5.18

BARKHAUSEN VOLTAGE PROFILE
12 INCH SAMPLE 5
AFTER ETCH FOUR

Time (s)

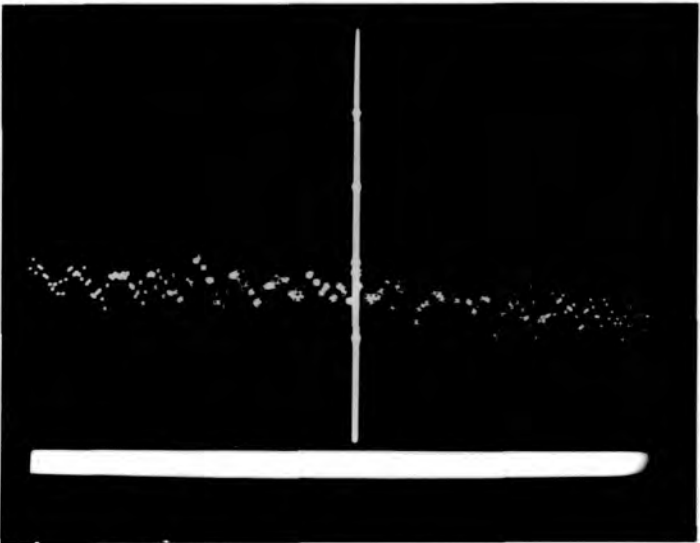
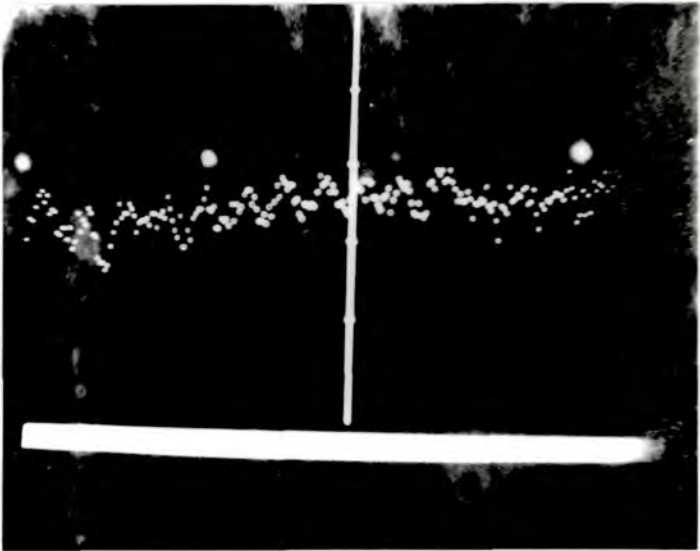
Applied
field (Am^{-1})

-1779 -1095 -411 +273 +957 +1641 +2325 +3009 +3693 +4377

It was then considered that the peak may be due to some spurious signal in the recording system. It was found, moreover, that the peak was only apparent when there was a sample in the coil system. The peak was not a function of the magnetising and recording system alone.

Steel sample 5 had its surface reground to produce a finish similar to its original surface finish. It was placed in the coil system and the signal in the second of the ten recording sections, where X was apparent, was photographed from the transient recorder screen. Photograph 5A shows the section with the sample central in the coil system. The sample was then displaced so that more material protruded from one end of the magnetising coil than the other; a photograph of the signal was taken. This was repeated with the sample displaced in the opposite direction. Photographs 5B and 5C show the effect of displacing the sample on the signal. A gradient and offset from zero are apparent in both photographs 5B and 5C.

To investigate this behaviour more fully, the waveform sampling interval on the transient recorder was changed so the whole of peak, X, could be viewed on the screen of the recorder. It was therefore possible to record the signal from the sample by photographing the screen with a polaroid camera. The signal from sample 5 was recorded in this way with the sample in a central position in the coils, offset in one direction



PHOTOGRAPHS 5A, 5B, 5C
(top to bottom)

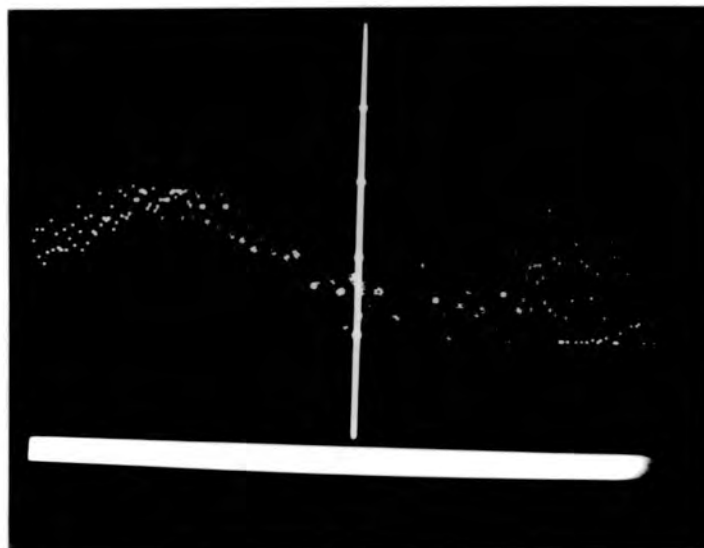
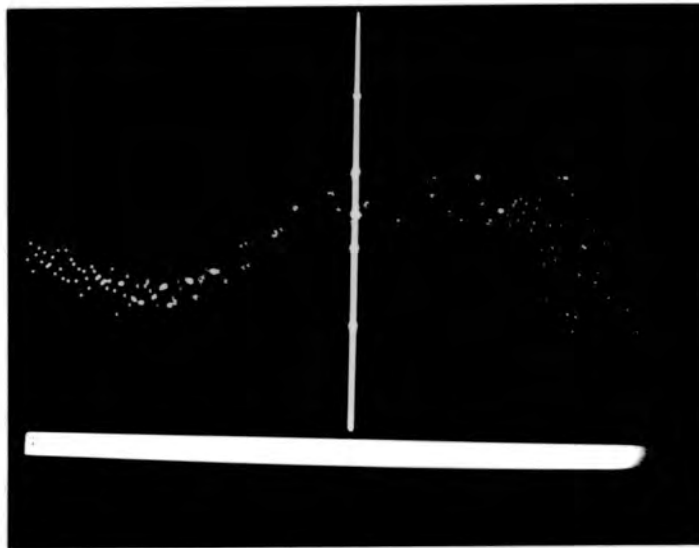
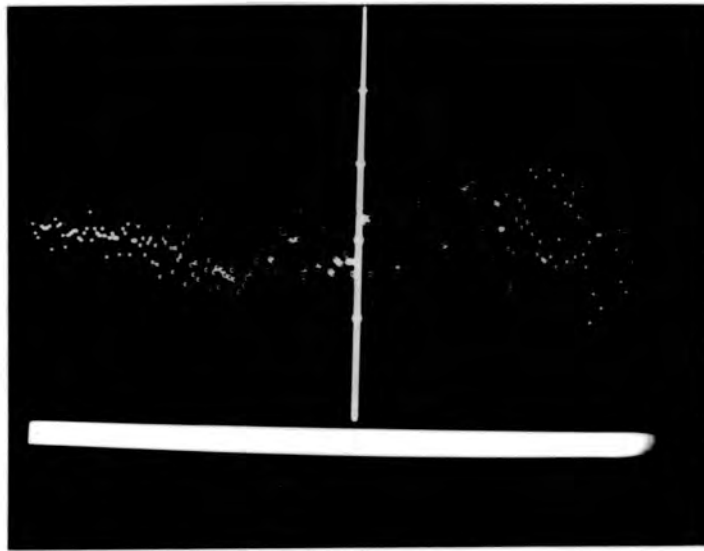
Approximate Applied Field Scale
 -1219Am^{-1} at left to -659Am^{-1} at right

and offset in the other direction (photographs 5D, 5E, 5F). The sample was rotated lengthwise, and photographs taken with the sample central and displaced in one direction (photographs 5G, 5H).

Sample 5 was replaced in the coil system by sample 33 and the signal recorded for three positions, central and offset in opposite directions (photographs 5I, 5J, 5K).

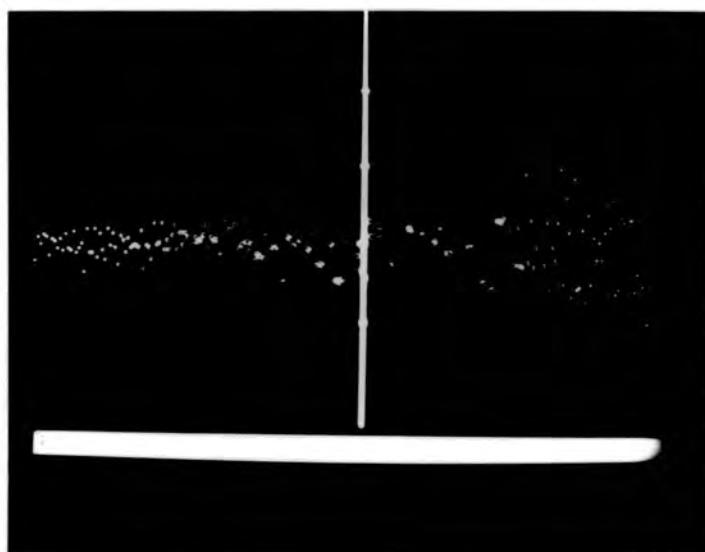
It was apparent from these photographs that an offset of the sample produced peak X. The peak could be linked either to an offset regardless of the material outside the magnetising coil or to an offset which caused more material to protrude from one end of the coil than the other.

Samples number 6 and 8, already cut shorter than the others, were used to assess which effect was causing peak X. Sample 8 was approximately the same length as the magnetising coil and was placed so that it was central in the coil with no material protruding from the ends of the coil. The signal on the transient recorder screen was photographed (photograph 5L). The sample was then displaced so that one end was outside the coil and a photograph taken (photograph 5M). It can be seen that a small peak occurs; the size is small probably because the force on the sample when not central in the coil is so strong that only a small amount of material, <1cm, could be left outside the coil without the sample moving during the experiment.



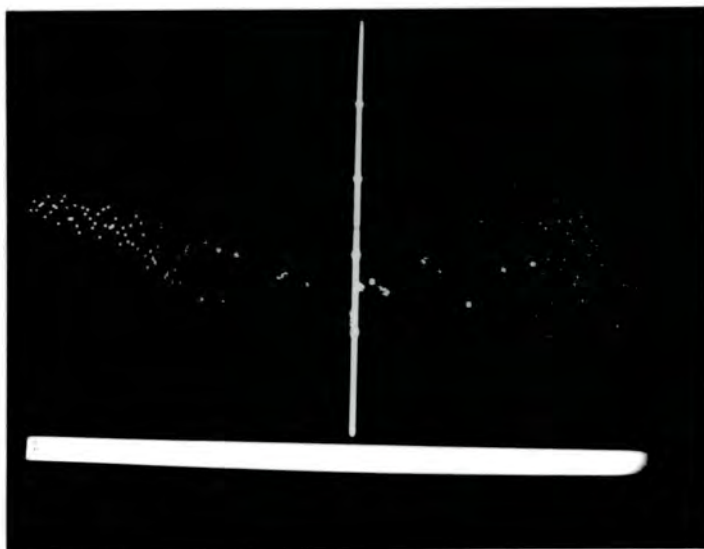
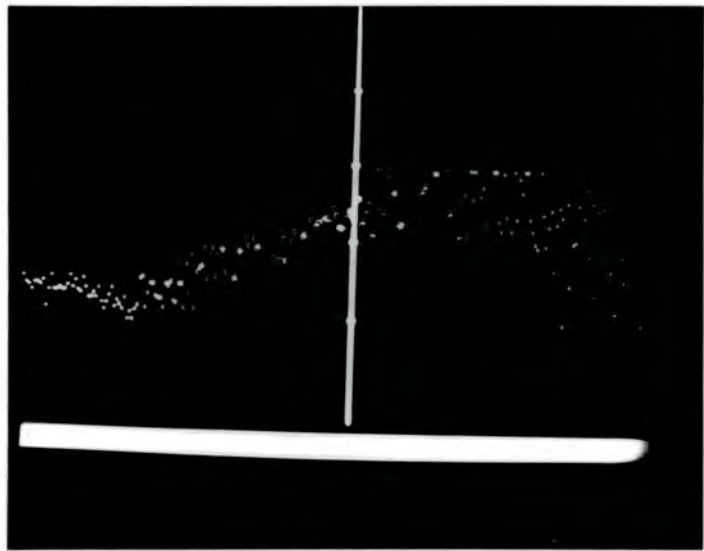
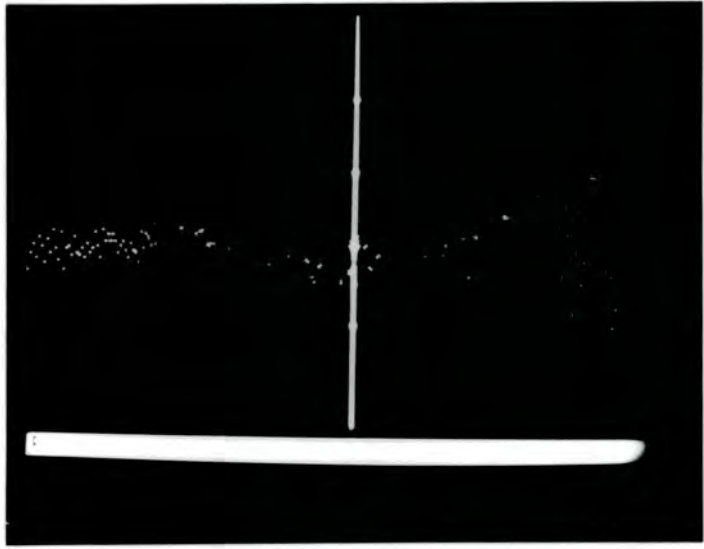
PHOTOGRAPHS 5D, 5E, 5F
(top to bottom)

Approximate Applied Field Scale
 -939Am^{-1} at left to $+181\text{Am}^{-1}$ at right



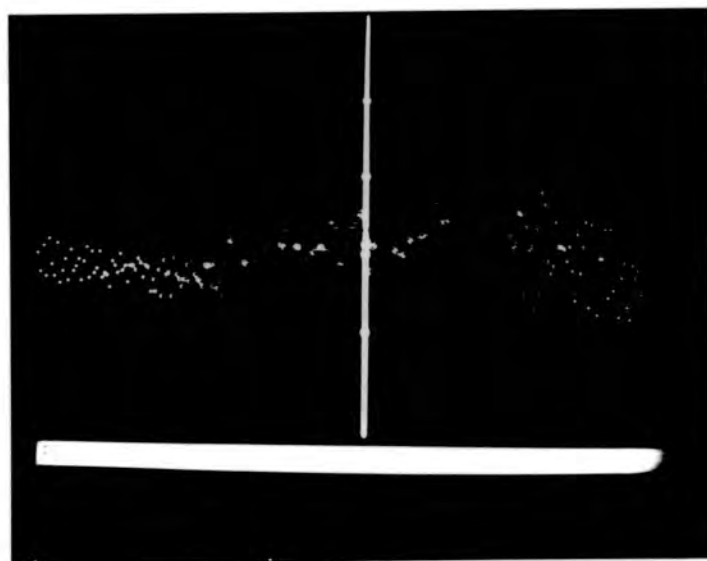
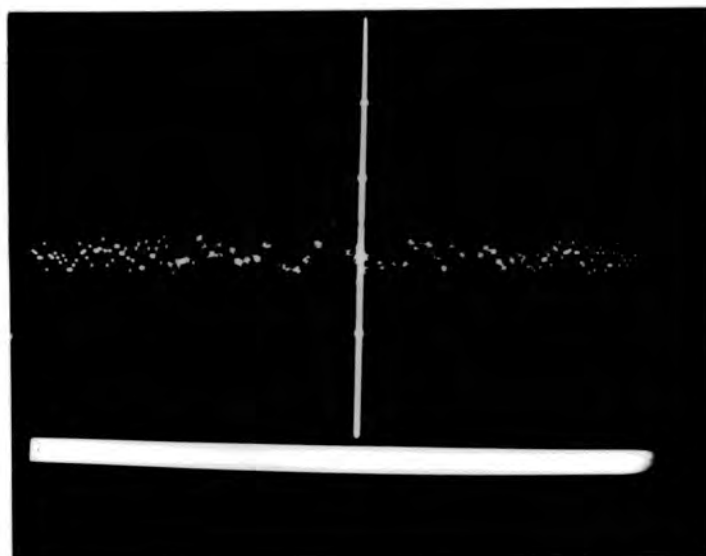
PHOTOGRAPHS 5G, 5H
(top to bottom)

Approximate Applied Field Scale
 -939Am^{-1} at left to $+181\text{Am}^{-1}$ at right



PHOTOGRAPHS 5I, 5J, 5K
(top to bottom)

Approximate Applied Field Scale
-939Am⁻¹ at left to +181Am⁻¹ at right



PHOTOGRAPHS 5L, 5M
(top to bottom)

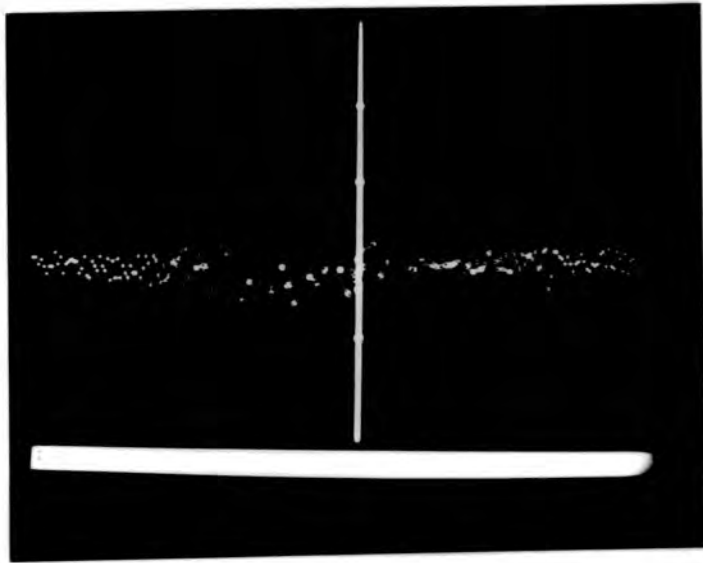
Approximate Applied Field Scale
 -939Am^{-1} at left to $+181\text{Am}^{-1}$ at right

Sample 6 was cut so that it fitted in the coil with sufficient room to offset the sample with no material outside the magnetising coil. Two photographs were taken of the signal from the sample; photograph 5N with the sample as central as possible, and photograph 5P with as large an offset as possible keeping all the steel inside the coil. It can be seen that no peak, X, occurs.

The peak, X, may therefore be attributed to the fact that the 12 inch steel samples were longer than the magnetising coil and that an offset from a central position caused more material to be outside the coil at one end than the other.

The possible explanation for the appearance of peak, X, is that the peak always occurs at a time close to the point at which the flux in the sample is zero. The difference in field gradients at either end of the sample caused by the offset may have more effect in this region. The asymmetry of the field gradient produces a vertical component of magnetisation in the sample at this point which is sensed by the pick-up coil.

The peak, X, is a function of position in the magnetising coil when the steel sample is longer than the coil. It does not occur at a position in the experimental cycle which affects the main Barkhausen activity, so it would be sensible to ignore the peak on the voltage plots.



PHOTOGRAPHS 5N, 5P
(top to bottom)

Approximate Applied Field Scale
 -939Am^{-1} at left to $+181\text{Am}^{-1}$ at right

5.3 ERROR HANDLING

It was found that the spectra plotted in the frequency domain from 1000Hz were quite well represented by straight lines. A least squares fit was performed on the spectra, with the intention to use the gradient and intercept as a means to compare the results for the different steel samples. The fitting also allowed for the repeatability of the experiments to be estimated. The way this estimate was made is illustrated by considering the FFT of three sets of data taken on the 12 inch sample number 15. The first set of data was taken with the steel sample placed along the axis of the magnetising coil, with the pick-up coil located at its centre. The second set of data was taken with the steel in a similar position but with the opposite face next to the pick-up coil. The third set was taken with the pick-up coil at a different position on the steel sample. The following values were found for the intercept and gradient of the least squares fit to the power spectra estimates from 1000Hz.

	INTERCEPT (V^2)	GRADIENT (V^2/Hz)
1.	0.04135 ± 0.00058	$-1.023 \cdot 10^{-6}$ $\pm 0.083 \cdot 10^{-6}$
2.	0.0386 ± 0.00058	$-0.809 \cdot 10^{-6}$ $\pm 0.083 \cdot 10^{-6}$
3.	0.04526 ± 0.00061	$-1.059 \cdot 10^{-6}$ $\pm 0.087 \cdot 10^{-6}$

It can be seen that the least squares fit is good for the data and the error introduced by performing this analysis is small $\approx 1\% \rightarrow 2\%$. The difference between the largest and smallest values of intercept is $0.00665V^2$. The mean of the three values of intercept is $0.04174V^2$.

This would suggest an experimental error of approximately 8% in the repeatability of the experiment. The total error for each experiment could therefore be taken as in the order of 10%.

CHAPTER 6 - CONSTRUCTIONAL STEELS - RESULTS

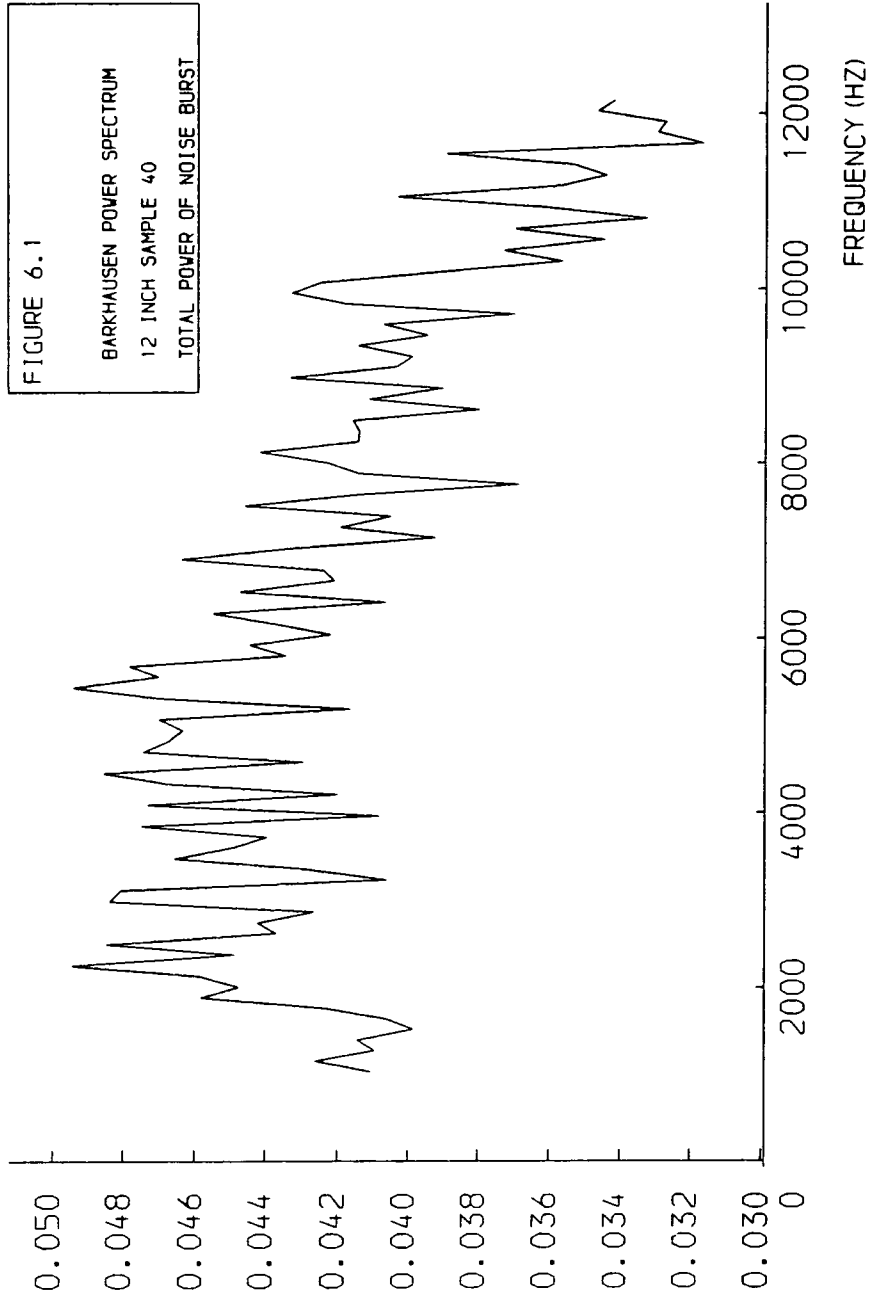
6.1 RELATIONSHIP BETWEEN POWER SPECTRA AND MAGNETIC PROPERTIES

Tests were carried out to determine whether the power spectra could be related to the bulk magnetic properties of the material forming the 12 inch samples. Information on the magnetic properties of the steel was available from the British Gas On Line Inspection Centre (OLIC), Cramlington, Northumberland.

The data for the chosen 12 inch samples was treated in the manner indicated and a value for the intercept and gradient of the least squares fit found. The most extreme values of intercept and gradient were found for samples 40 and 5; 40 giving the largest values, 5 the smallest. Figures 6.1 and 6.2 show the power spectra plotted for these two samples. The values of intercept and gradient decreased in the same order from 40 to 5. It was decided therefore that the intercept should be compared with the values of coercive field and remanence for the 12 inch samples, in order to look for some simple relationship.

The values of H_c and B_r were used and the value of B_r/H_c as an indication of the average gradient in the region in which the Barkhausen noise was measured. The value of B_r/H_c takes no account of actual differences in shape of the loops.

POWER
(V²/V)



POWER
(V \blacklozenge V)

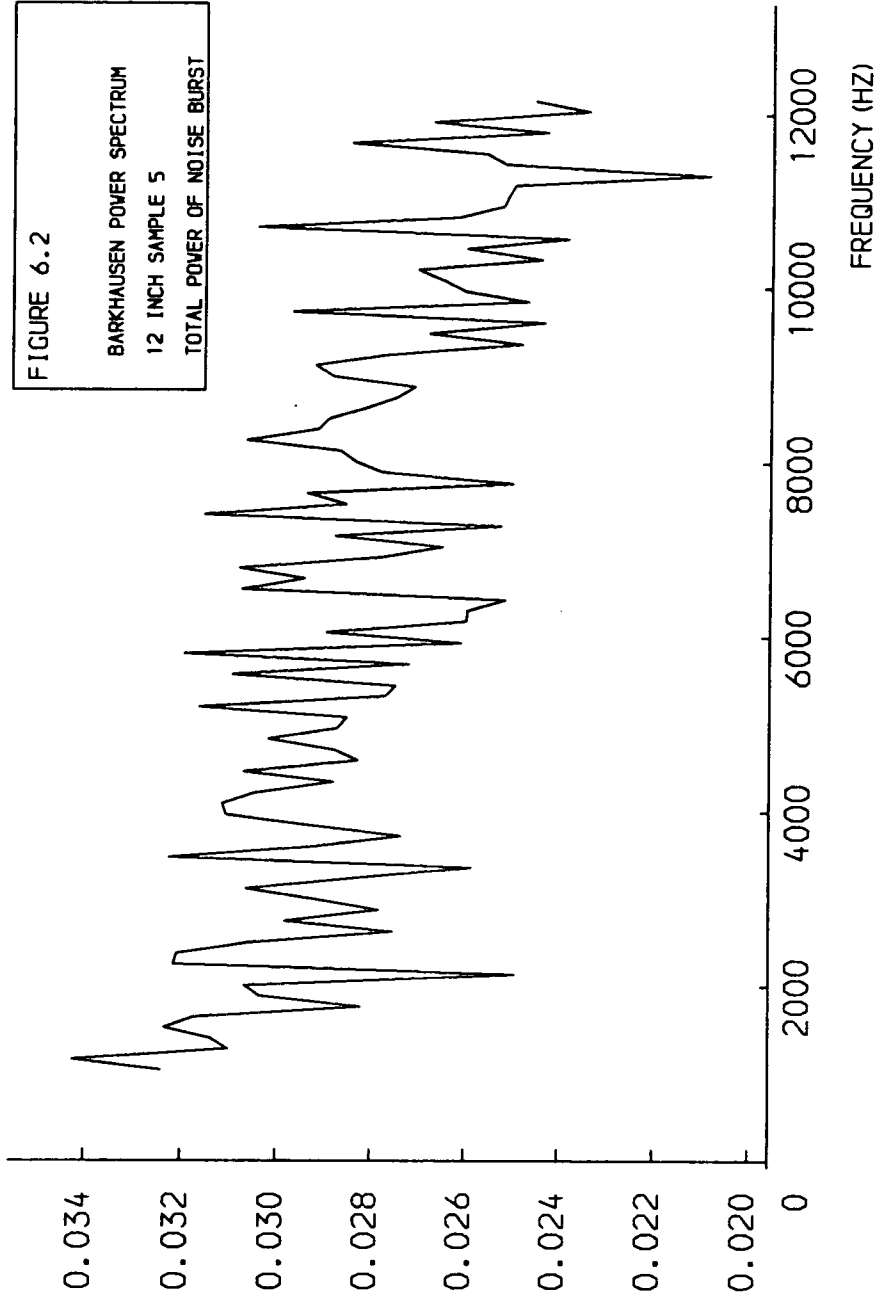


FIGURE 6.2

BARKHAUSEN POWER SPECTRUM
12 INCH SAMPLE 5
TOTAL POWER OF NOISE BURST

The following table shows the results, which are plotted in figures 6.3, 6.4 and 6.5, in order of decreasing intercept. The measurements of H_c and B_r were made by Wilcock [4].

Sample number	Intercept $\pm 10\%$ (V ²)	H_c ± 0.002 (kAm ⁻¹)	B_r ± 0.01 (T)	B_r/H_c (T/kAm ⁻¹)
40	0.050	0.342	0.94	2.75
33	0.044	0.410	0.84	2.05
2	0.044	0.330	1.05	3.18
15	0.041	0.385	0.89	2.31
39	0.040	0.365	0.93	2.55
20	0.038	0.372	0.98	2.63
34	0.036	0.385	0.91	2.36
16	0.036	0.385	0.90	2.34
11	0.034	0.345	0.93	2.70
5	0.033	0.348	0.98	2.82

It would appear at first sight that there is no simple relationship between the magnetic parameters and the power spectra intercept. The graphs do however all show a linear trend, albeit with considerable scatter, except for the sample numbers 40 and 2.

If the points for 40 and 2 are excluded the following empirical relationships may be proposed from a least squares fit to the data.

The plot of intercept (I) against H_c shows a trend of a line

$$I = -0.012 + 0.13H_c \quad \text{Equation 6.1}$$

The intercept against B_r shows a line

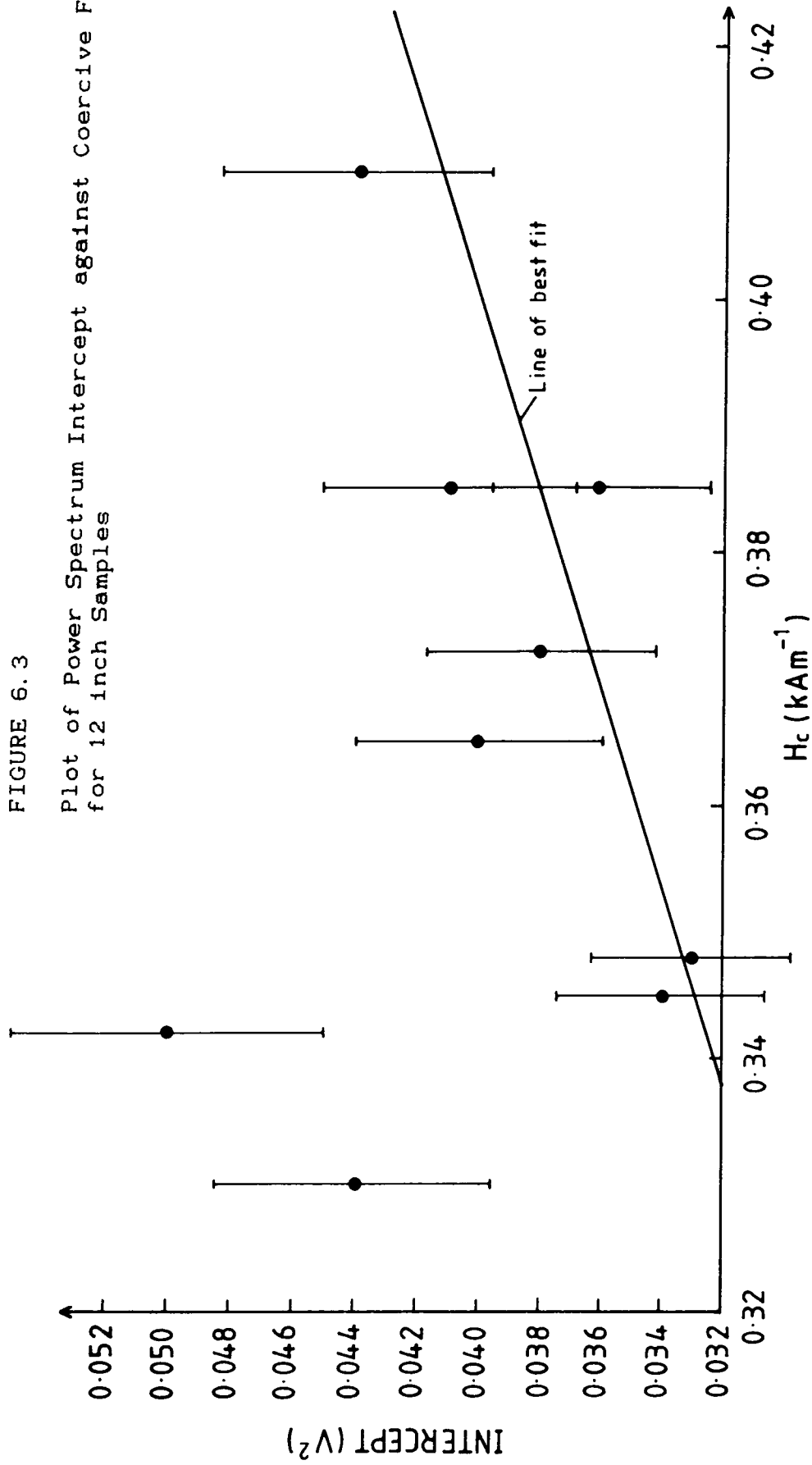
$$I = 0.088 - 0.055B_r \quad \text{Equation 6.2}$$

The intercept against gradient (G) shows

$$I = 0.066 - 0.011G \quad \text{Equation 6.3}$$

FIGURE 6.3

Plot of Power Spectrum Intercept against Coercive Field H_c
for 12 inch Samples



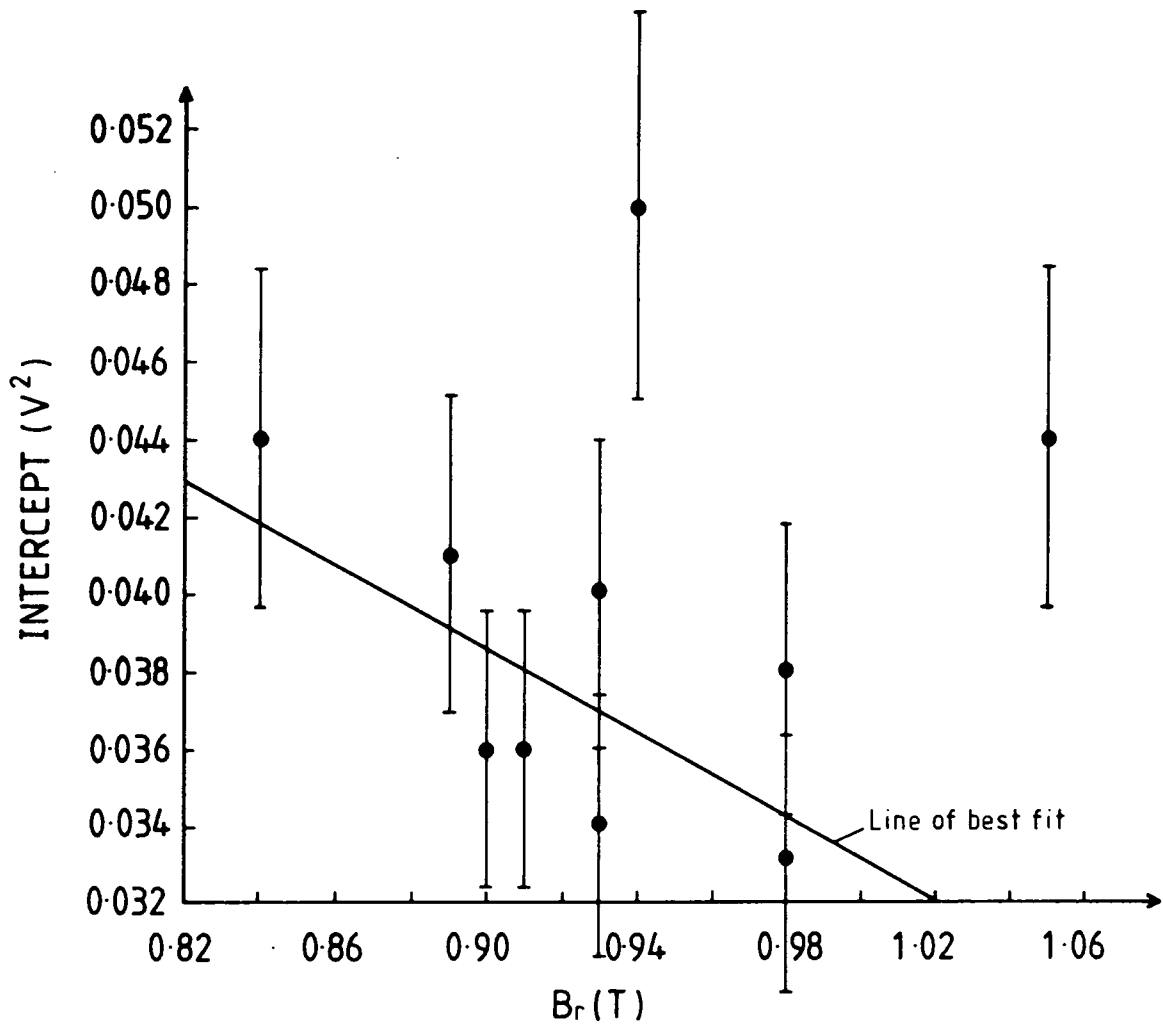


FIGURE 6.4

Plot of Power Spectrum Intercept against Remnance B_r for 12 inch Samples

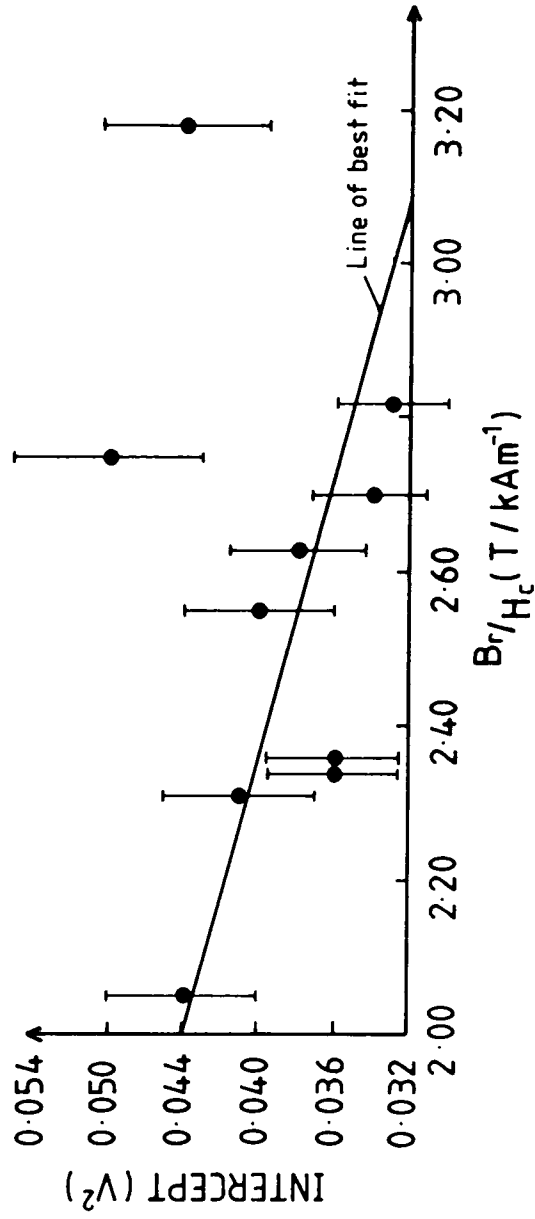


FIGURE 6.5

Plot of Power Spectrum Intercept against
Approximate Hysteresis Loop Gradient B_r / H_c
for 12 inch Samples

6.2 FURTHER POWER SPECTRA WORK

The results shown in section 6.1 suggested that there could be a simple relationship between the magnetic properties of the 12 inch pipe steel and the Barkhausen power spectra. The exception to the relationships in all three cases shown were samples 2 and 40.

As sample 40 had shown the largest intercept it was firstly considered that sample 40 had given a spurious indication either due to instrumental problems or due to surface damage in the cutting process. The instrumentation was however found to produce results that were reliable and repeatable; a visual check of the signal on the transient recorder screen showed similar signals were obtained in repeated experiments.

The 12 inch samples had all been machined in a similar manner. If surface damage were giving rise to a spurious Barkhausen signal, it would be expected that a contribution would be made in the high frequency part of the power spectrum. More small Barkhausen jumps would take place near the surface and the correlation domain would grow in smaller stages, these stages would give high frequency components in the Fourier transform. It would be expected that if the high frequency portion of the power spectrum was enhanced in this way the low frequencies would be diminished, giving a smaller intercept on the power spectrum.

The possible effect of surface damage was tackled by chemically removing the surface of sample 16 and mechanically removing the surface of sample 34. The surface of sample 34 was ground down by 1/1000 inch to give a freshly ground surface. The surface of 16 was etched in 95% ethanol and 5% nitric acid for 6½ minutes. The sample was viewed under a microscope to ensure that this was long enough to remove the grinding lines on the surface. The technique had been tested on some other pieces of pipe steel. The experiment was run in the usual way for the two samples. Sample 16 was then chemically etched again until a layer approximately 0.02mm had been removed. The depth of etching was decided by considering the damage done by grinding [1]. The experiment was again performed on sample 16.

The result of fitting a straight line to the data for the ground sample 34 was;

Intercept = 0.030V ²

Comparing the intercept with the previous result of 0.036V² shows that the two results lie within the 10% experimental limits.

The values of intercept for the two etched experimental runs of sample 16 were;

	INTERCEPT (V ²)
surface etch	0.037
deep etch	0.032
original value	0.036

Again, these agree within the 10% experimental error limits suggesting that the surface state of the samples was not contributing significantly to the Barkhausen noise.

As the exact nature of the cutting process was unknown in the 12 inch samples, several layers of material were removed from the surface of sample number 5. The layers taken off by the ethanol/nitric acid solution were at the following intervals:

	Mean thickness at centre(mm)	Amount of removal(mm)
original	5.22	—
etch 1	5.19	0.03
etch 2	5.17	0.02
etch 3	5.15	0.02
etch 4	5.13	0.02

The thickness was measured at 5 places at the centre of the sample near the position of the pick-up coil.

The following results were found for the power spectra. Figure 6.6 shows the original power spectrum.

	INTERCEPT ±10% (V ²)
original	0.033
etch 1	0.035
etch 2	0.031
etch 3	0.032
etch 4	0.038

These results show that the measurements made on the as ground material were representative of the bulk of the material within the 10% limits.

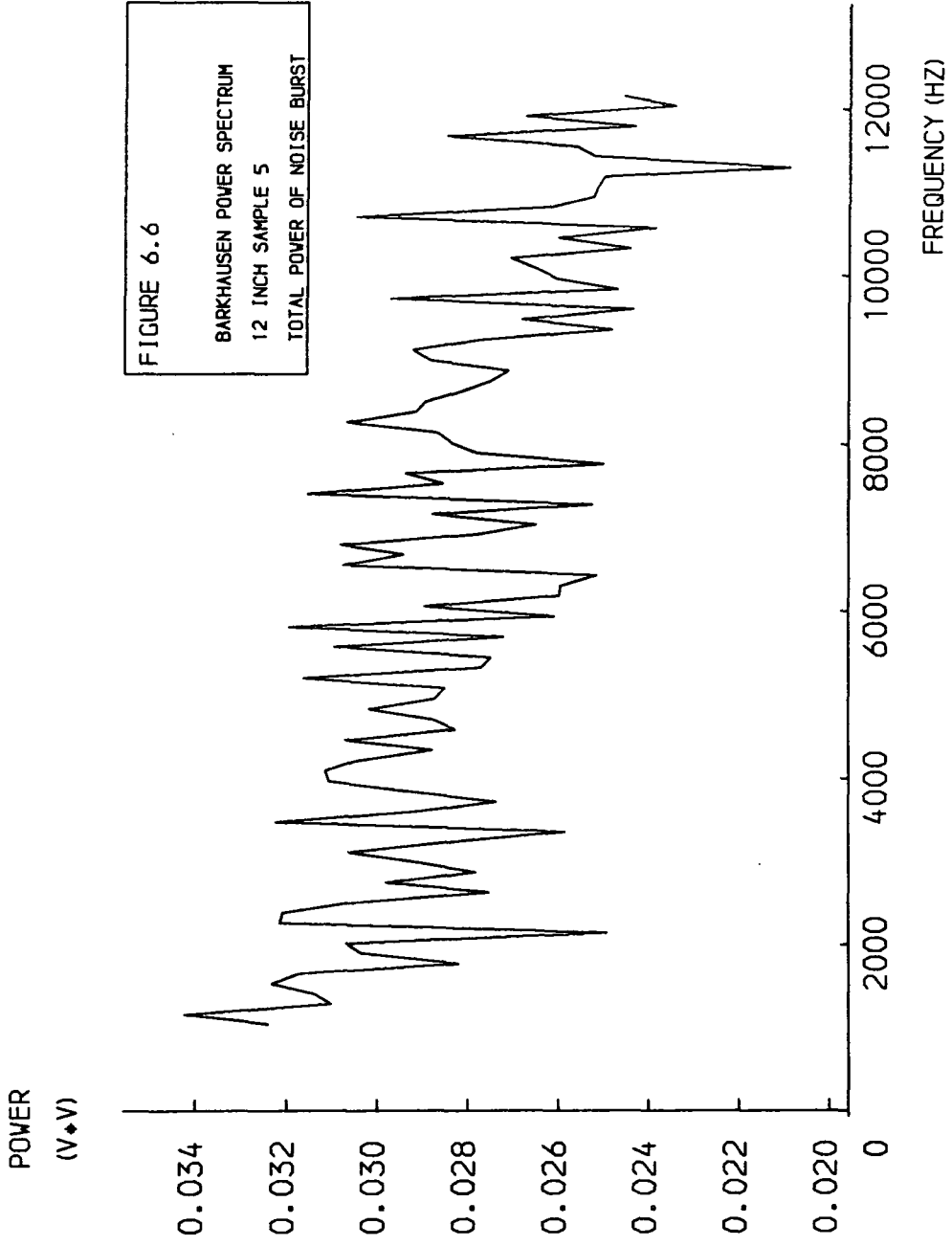


FIGURE 6.6
BARKHAUSEN POWER SPECTRUM
12 INCH SAMPLE 5
TOTAL POWER OF NOISE BURST

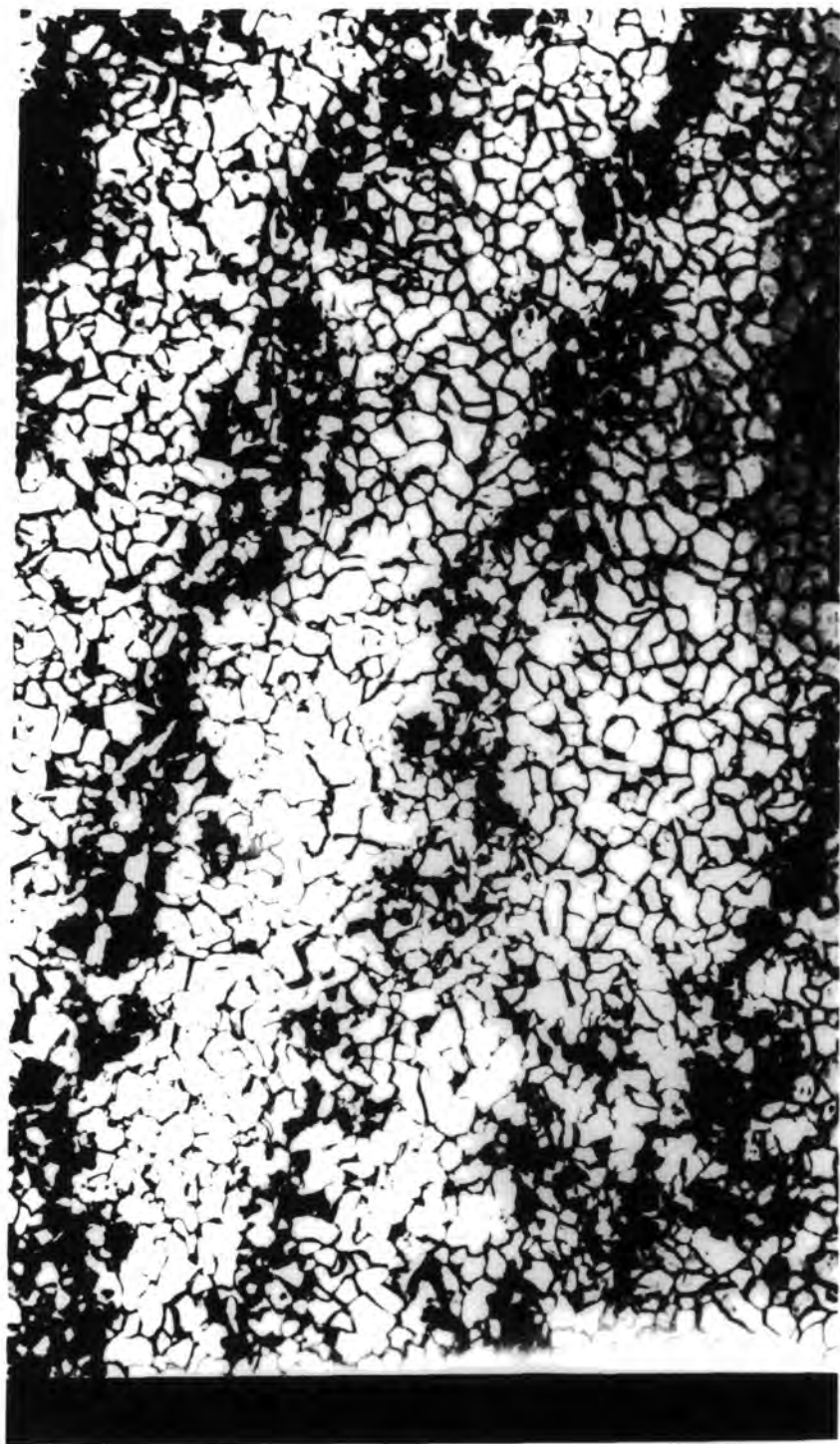
If the surface damage had been giving an anomalous high frequency portion to the power spectra, the intercepts for the etched surfaces would have risen. This was not the case so surface damage could not have caused the high intercept of sample 40.

Previous work carried out on the 12 inch pipe steel [2] indicated that there was a significant difference in pearlite fraction between samples 41 and 35. Samples 40 and 34 may be expected to show similar pearlite fractions as they are the adjacent samples. The following table summarises the information and the photographs 6A and 6B [3] show typical micrographs of the samples 41 and 35. *The dark regions are pearlite.*

SAMPLE NUMBER	% PEARLITE	INTERCEPT ±10% (V ²)
41	16.6	—————
40	—————	0.050
35	27.1	—————
34	—————	0.036

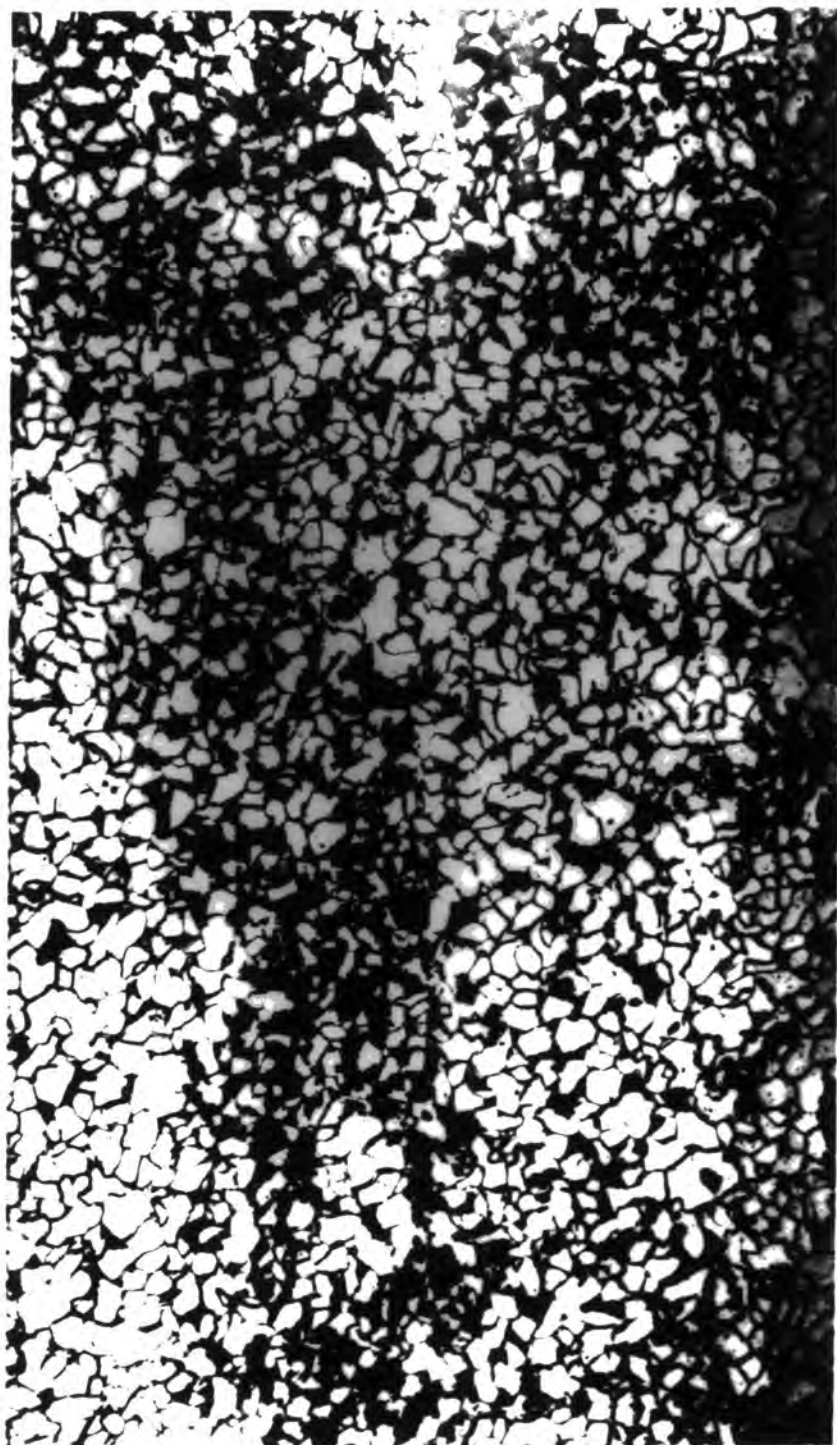
It could be suggested that the difference in pearlite content and hence the difference in the domain wall pinning at the pearlite boundaries causes the anomalously high intercept for sample 40. No mechanism has been found to account for the variation in pearlite.

The lower pearlite content may allow the correlation domain to grow in larger stages, that is taking a long time to develop the Barkhausen jump cluster, the Fourier transform of these clusters will



1mm

PHOTOGRAPH 6A Microstructure of Sample 41 (taken by Wincock [3])



1mm

PHOTOGRAPH 6B Microstructure of Sample 35
(taken by Wilcock [3])

be in the low frequency portion of the power spectrum giving rise to a higher intercept for a lower pearlite content.

6.3 COERCIVITY RANGE

The range of coercivities studied was extended by introducing the two samples DHP and DFD; DHP as its coercivity was close to that of the samples already studied and DFD as its coercivity was approximately 1.5 times larger than those of the 12 inch samples. The DHP and DFD steels were cut and finished in a similar way to the 12 inch samples. The experiment was run for DHP and DFD giving the following values for the intercept of the straight line fit:

	Intercept (V ²)	Coercivity (kAm ⁻¹)
DHP	0.056	0.396
DFD	0.056	0.538

Although both these values are higher than those of the 12 inch samples, there is little difference between the intercept values for DHP and DFD. Figure 6.7 shows the position of the results for these steels with respect to the previously predicted straight line. It can be seen that DFD is close to the straight line and DHP is not. The pearlite fraction for DFD and DHP was known from [4]; DFD has 20.5% pearlite and DHP 16.6%. This shows that the pearlite content of DHP is

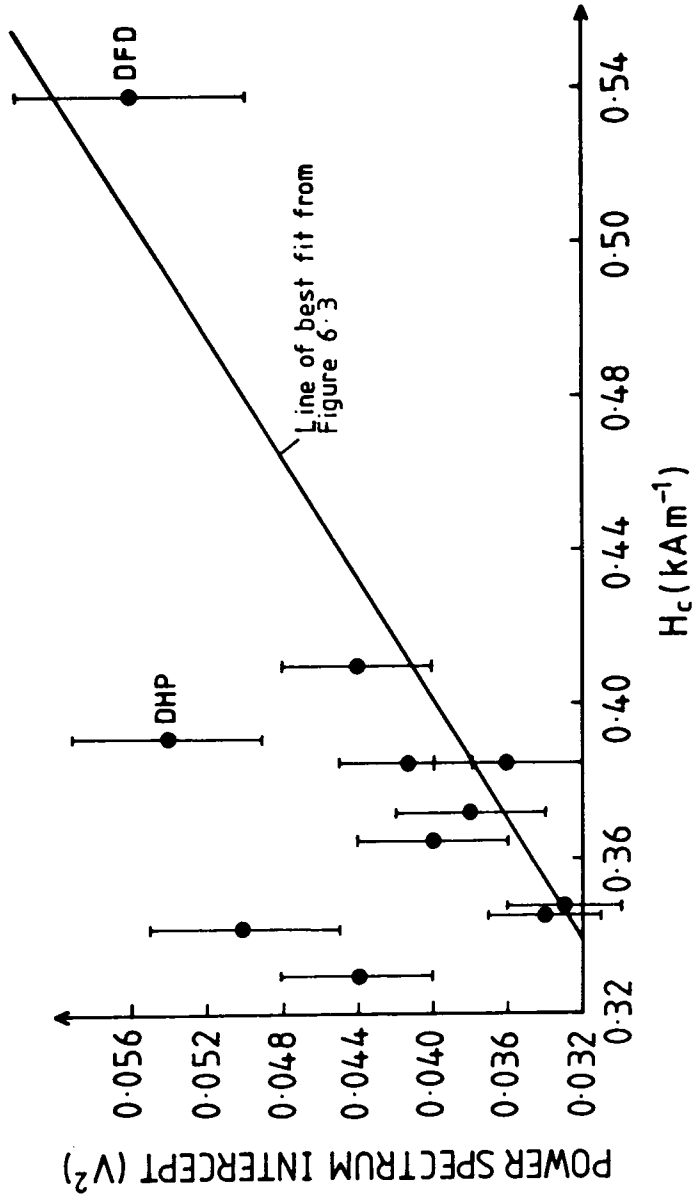


FIGURE 6.7

Graph to indicate position of DHP and DFD with respect to 12 inch Samples

similar to that of 41 (and probably 40) and this may be the reason why it does not lie along the same straight line as the other 12 inch steel samples. The pearlite content of DFD is not quite as high as that of 35 (and probably 34) but the result does appear to agree with the relationship between H_c and power spectrum intercept.

6.4 PLASTIC DEFORMATION OF SAMPLE

Sample 40 was plastically deformed at its centre using a four point bending machine. The applied load was 3.12kN and this corresponds to a point just beyond the elastic limit of the sample. Figure 6.8 shows the bending points and figure 6.9 the load curve for the bending. The experiment was carried out on both the surfaces of the sample. The intercept of the straight line fit was found. The result (A) is for the side to which the load was applied and the result (B) for the opposite face; (C) is the original value before deformation. Figure 6.10 shows the power spectrum for side B.

	INTERCEPT (V ²)
A	0.039
B	0.027
C	0.051

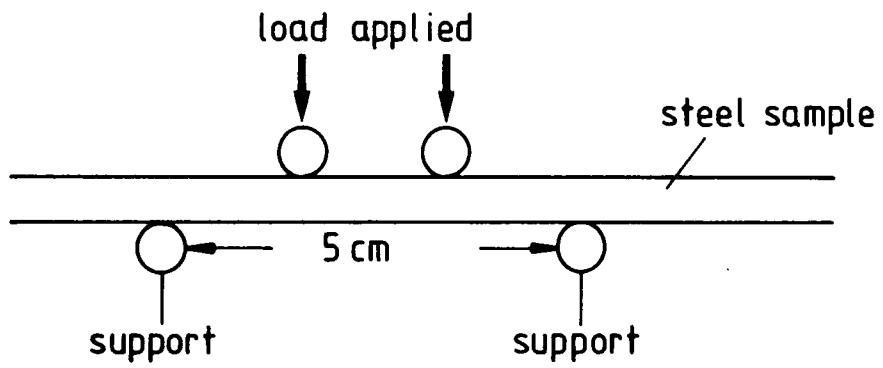


FIGURE 6.8

Diagram of Bending Points for Plastic Deformation of Sample

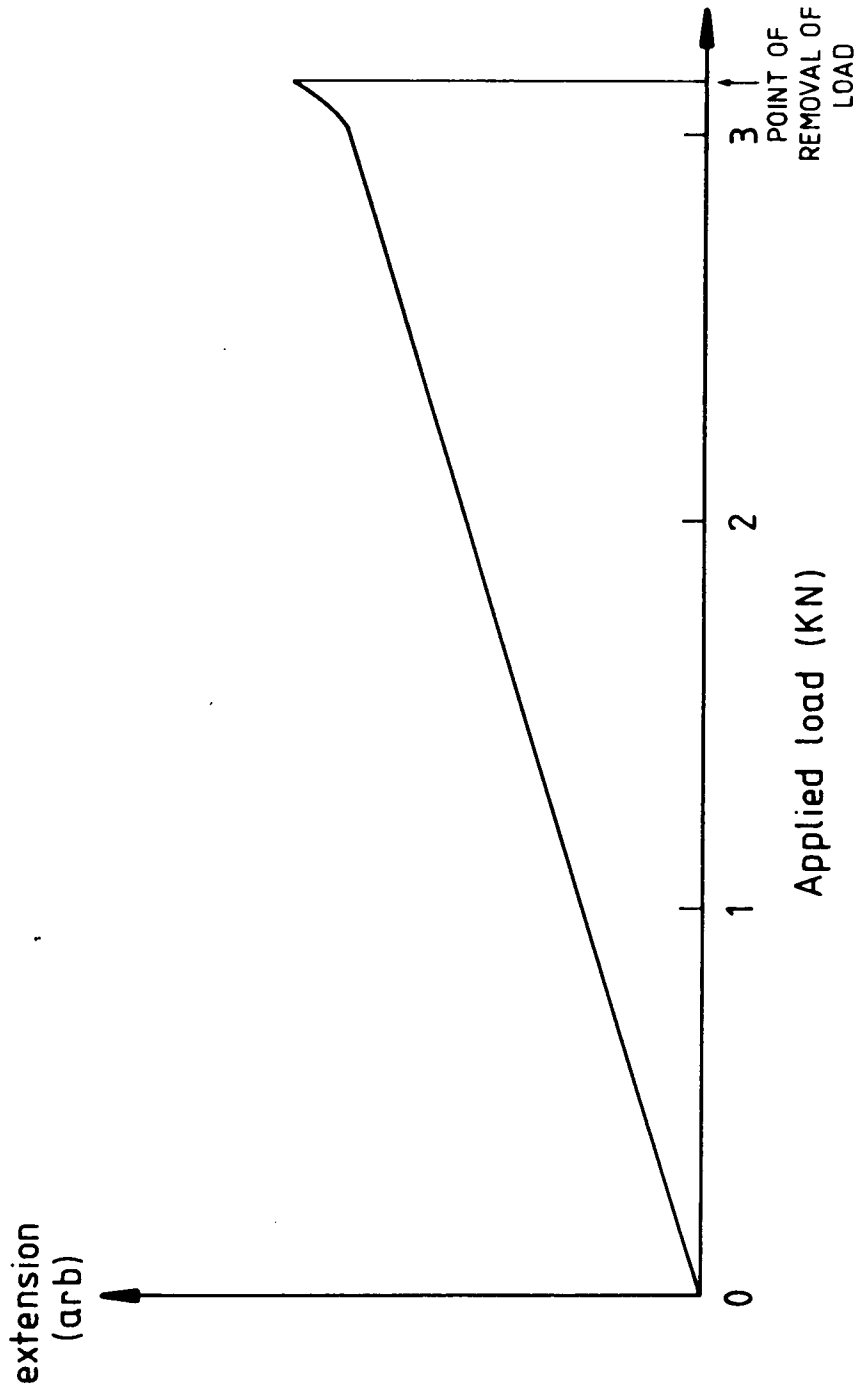
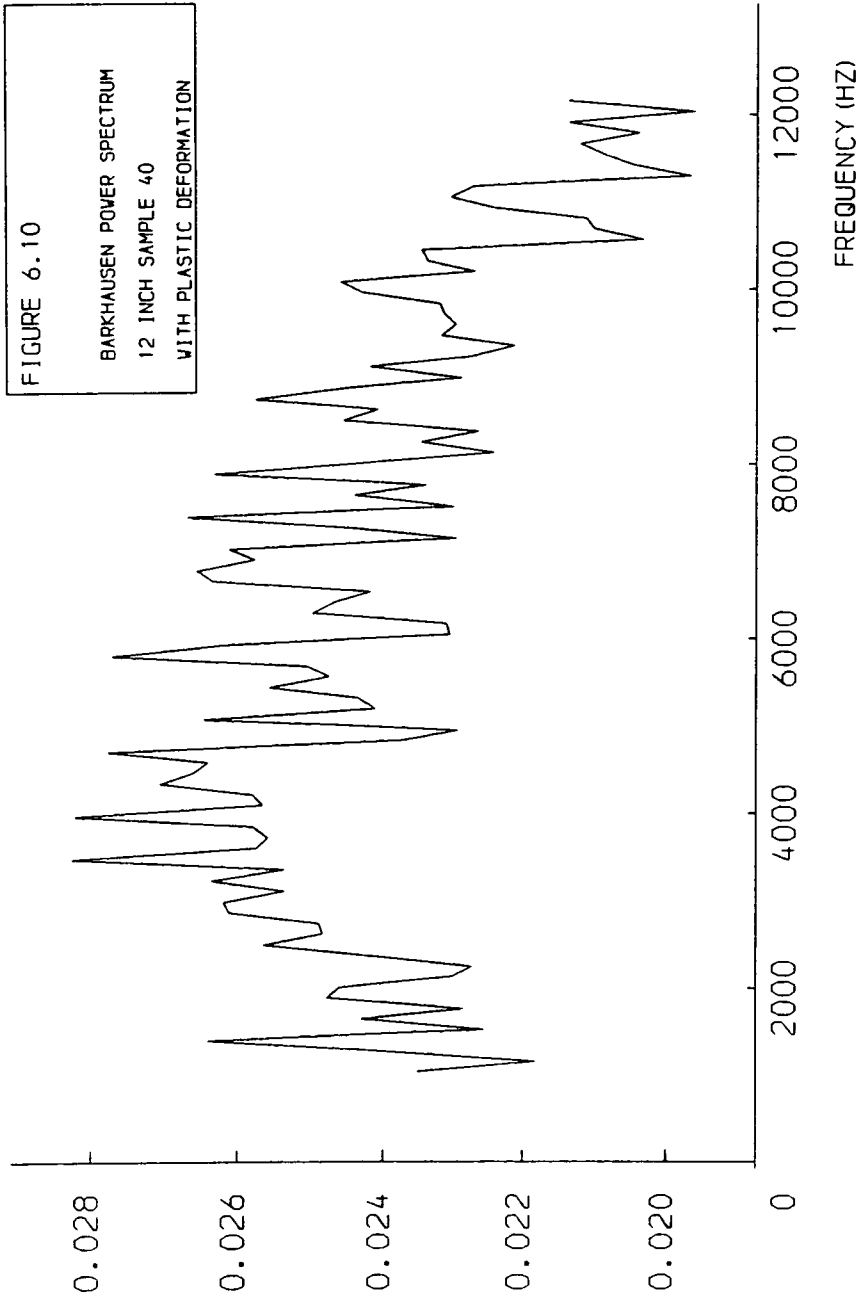


FIGURE 6.9 Load Curve for Plastic Deformation of Sample

POWER
(V \cdot V)



It can be seen that the intercept for both faces of the sample is lower than the original value. The voltage plots for the plastically deformed sample were also produced. It was noted that the plots both displayed the peak, X, discussed in paragraph 5.2b. The peak had not been visible on the original plot.

It was considered that there may be some relationship between the amount of plastic deformation, bulk magnetic properties and Barkhausen noise. The sample 40 could not have its properties adequately assessed after deformation, so a set of samples of steel type 2401 was used for further work on plastic deformation. Chapter 7 shows the results for these samples.

6.5 STRESS RELIEF OF SAMPLE

It was anticipated that each of the 12 inch samples would have a certain amount of residual stress in them. In order to investigate the effect of stress relief on the Barkhausen noise power spectrum, one sample, number 11, was heat treated in steps of 100°C up to 600°C. The temperature was held for one hour at each stage and the sample cooled in the furnace. The power spectrum intercept was plotted against temperature. The table shows the results:

Anneal Temperature	Intercept $\pm 10\%$ (V^2)
orig.	0.034
100°C	0.037
200°C	0.043
300°C	0.057
400°C	0.067
500°C	0.067
600°C	0.073

Figure 6.11 shows the results plotted. This intercept against temperature graph shows that there is a point around 400°C beyond which the intercept does not rise significantly for increased stress relief.

The power spectrum intercept gives a good indication of the amount of stress in the sample.

6.6 VOLTAGE PLOT RESULTS

The voltage profiles for all the steel samples were plotted; an example is shown in figure 6.12. Various features of the plots were measured and compared with the magnetic properties of the steels.

The most prominent feature on all the plots was the peak of Barkhausen activity. The height of the peak and the time at which the peak occurred were recorded.

Some of the voltage profiles showed a shape similar to that encountered by Buttle et al., that is that there are two distinct peaks at either side of the main peak. 40, 34, and 33 showed these peaks.

Figure 6.12 shows the voltage plot for sample 40 in

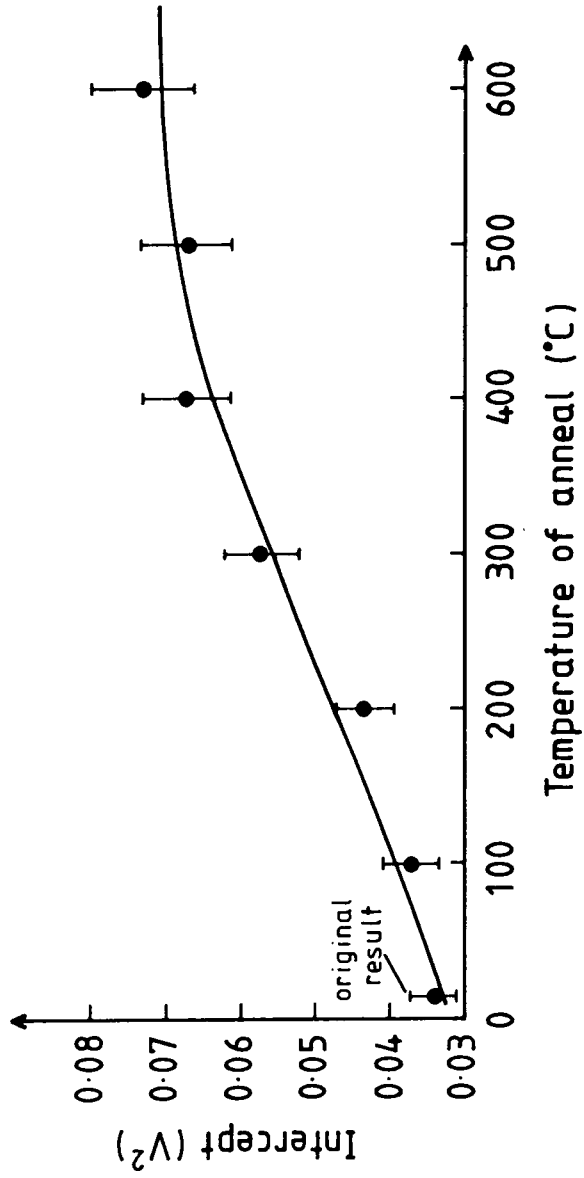
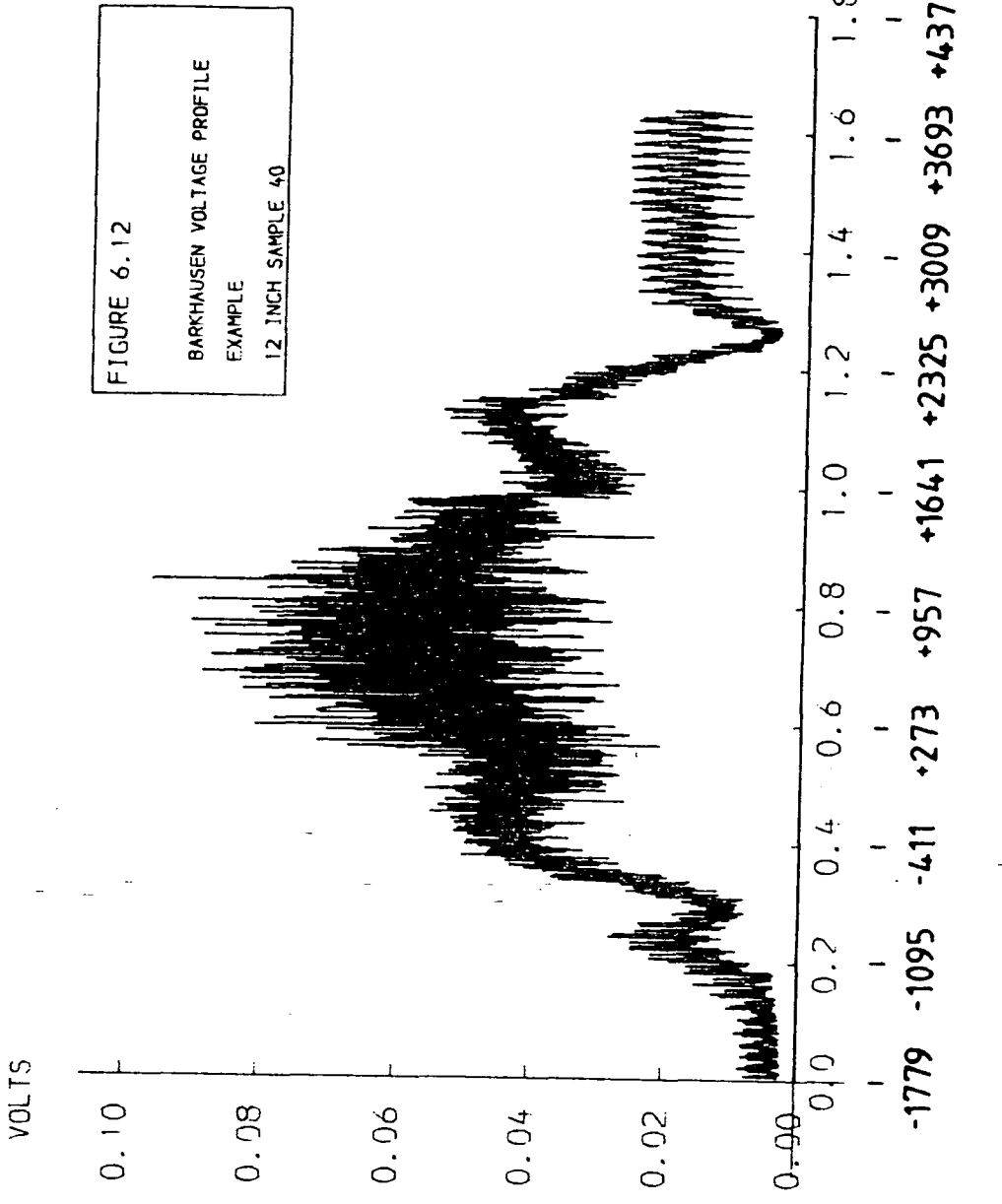


FIGURE 6.11

Plot of Power Spectrum Intercept against
Temperature of Anneal



which the peaks may be seen. More of the profiles showed just the first peak, the second being indistinguishable from the rest of the noise. 15, 39, and 11 showed just one peak. The ratio of the first peak to the main peak was found and the results put in descending order. The order was 40, 11, 15, 39, 34, 33,. Again there was no apparent relationship with H_c .

For the samples which showed both side peaks clearly, the ratio of the first to the second peak was found and ordered. The resulting order was 33, 34, 40. These do not show any particular order and the number of results is too small to form a reliable opinion.

The following table summarizes the results.

SAMPLE NUMBER	H_c ± 0.002 (kAm^{-1})	B_r/H_c (T/kAm^{-1})	PEAK HEIGHT ± 0.002 (V)	TIME OF PEAK ± 0.005 (s)
33	0.410	2.05	0.073	0.710
15	0.385	2.31	0.058	0.800
34	0.385	2.34	0.059	0.719
16	0.385	2.36	0.066	0.800
20	0.372	2.63	0.065	0.752
39	0.365	2.55	0.060	0.768
5	0.348	2.82	0.058	0.755
11	0.345	2.70	0.058	0.755
40	0.342	2.75	0.064	0.739
2	0.330	3.18	0.059	0.740

Figures 6.13, 6.14, 6.15, 6.16 show the plots of the results. It can be seen that there is no simple relationship between the plotted variables, although figures 6.15 and 6.16 do show general trends if the points for 33 and 34 are excluded. The justification for excluding these points is, however, weak. There

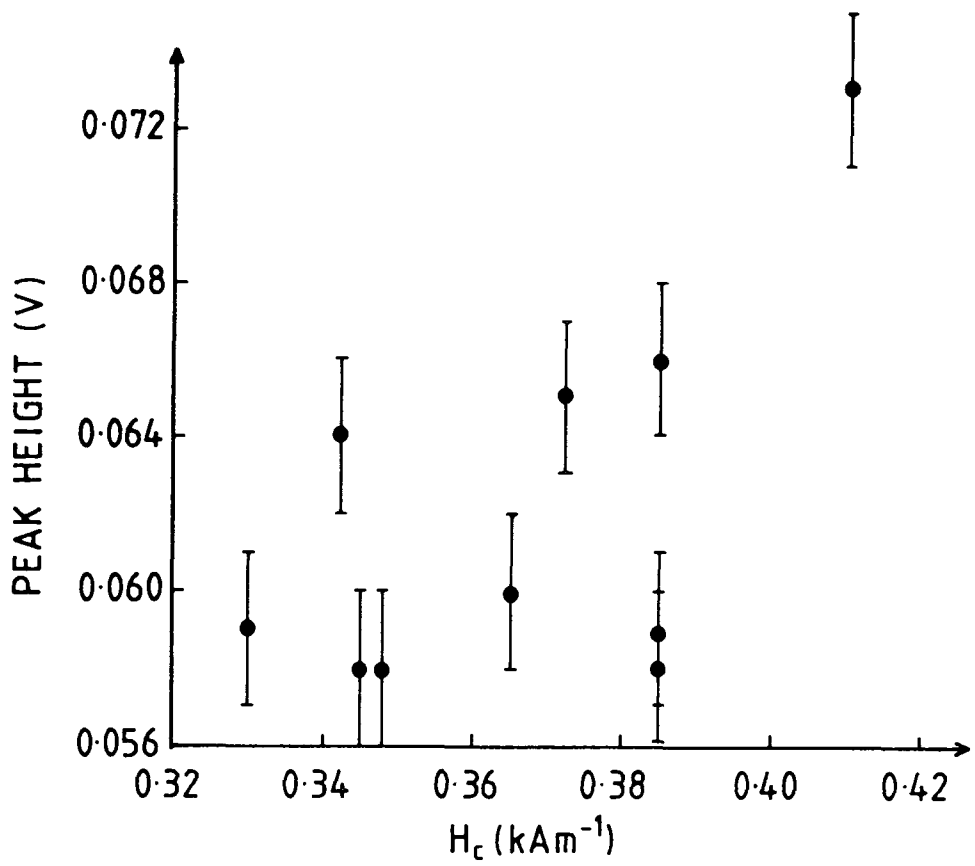


FIGURE 6.13

Plot of Barkhausen Noise Voltage Peak Height against Coercivity, H_c , for 12 inch Samples

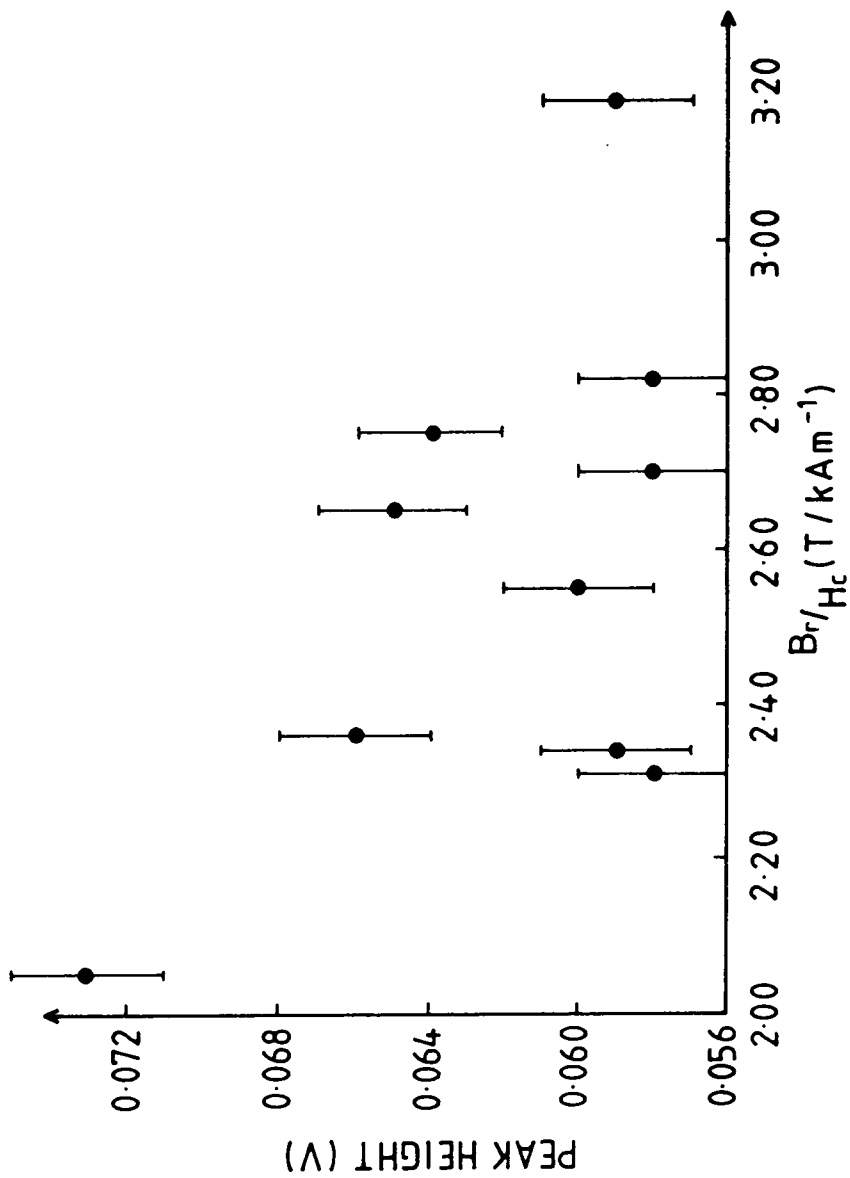


FIGURE 6. 14

Plot of Barkhausen Noise Voltage Peak Height against
Approximate Hysteresis Loop Gradient B_r / H_c
for 12 inch Samples

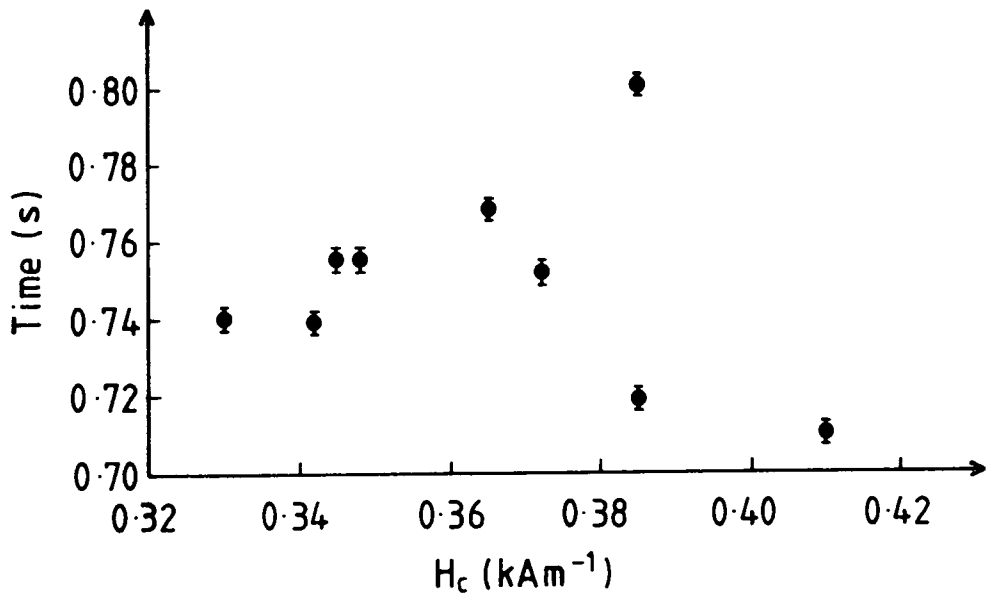


FIGURE 6.15

Plot of Time of Occurrence of Barkhausen Noise Peak from Start of Recording of Data against Coercivity, H_c , for 12 inch Samples

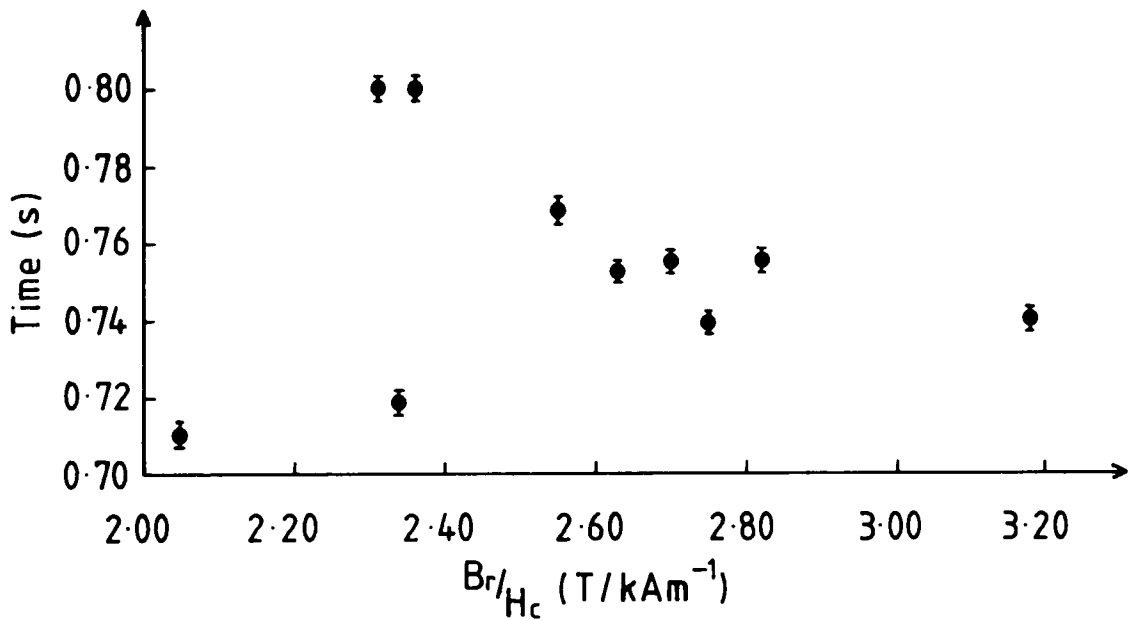


FIGURE 6.16

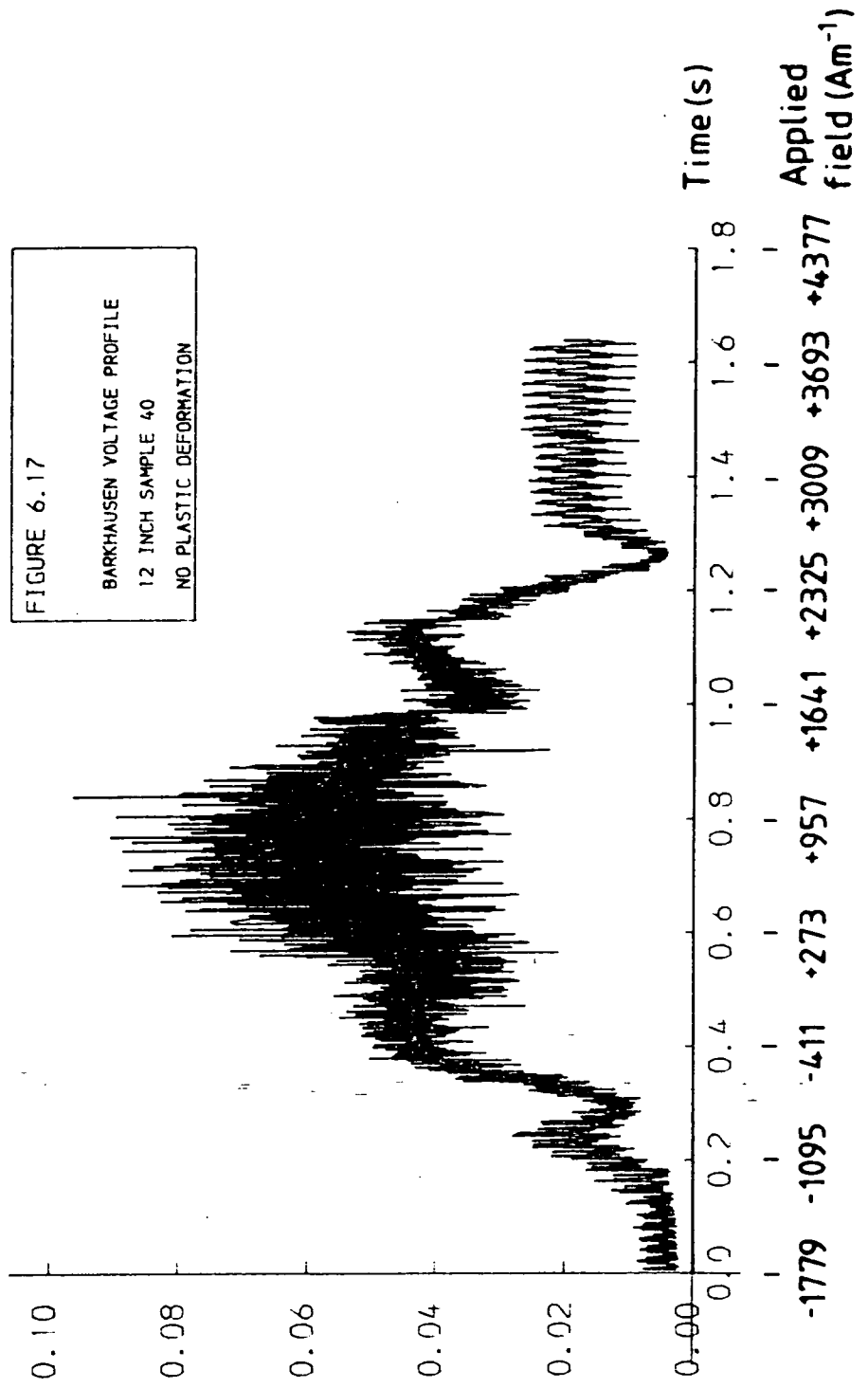
Plot of Time of Occurrence of Barkhausen Noise Peak from Start of Recording of Data against Approximate Hysteresis Loop Gradient B_r / H_c for 12 inch Samples

does not appear to be any pattern with respect to the known microstructural differences between samples.

Figures 6.17 and 6.18 show the Barkhausen noise voltage plots for sample 40 before and after plastic deformation. It can be seen that the main noise peak decreases in amplitude after deformation. The decrease in peak height is discussed in Chapter 9.

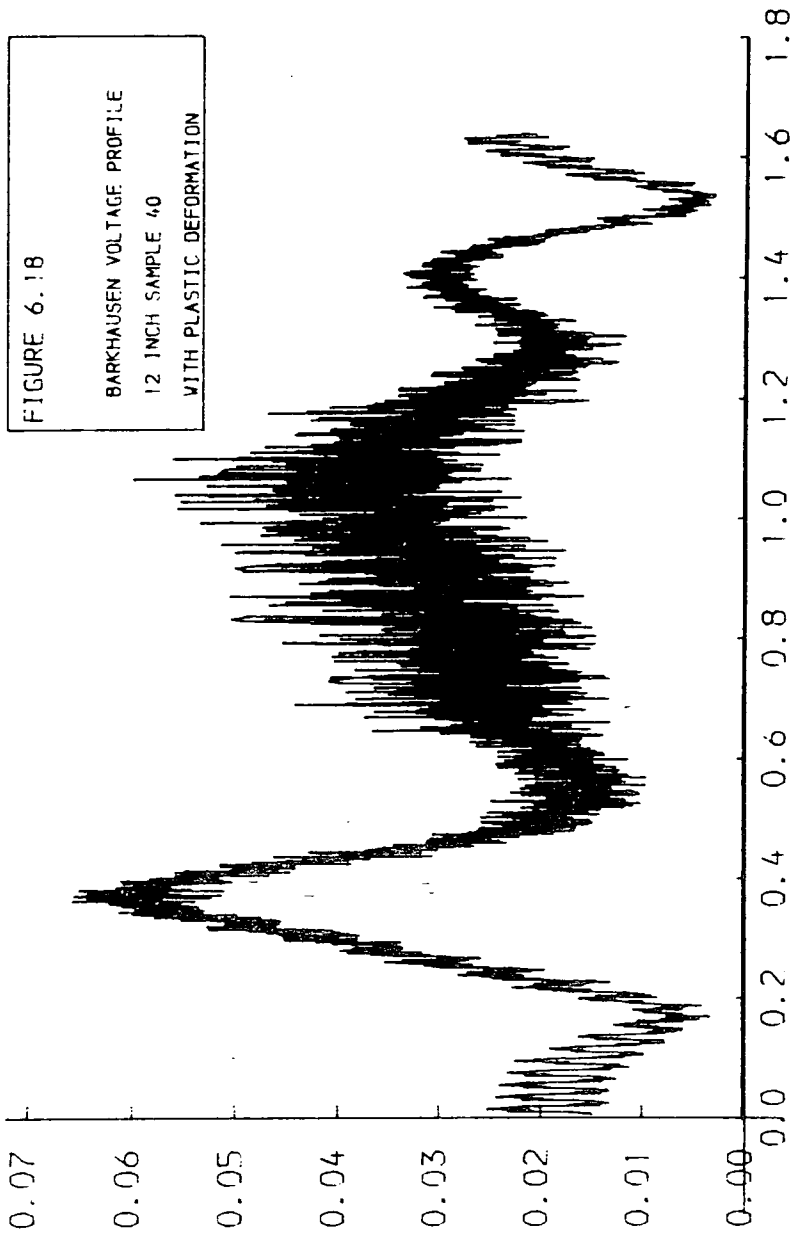
VOLTS

FIGURE 6.17
BARKHAUSEN VOLTAGE PROFILE
12 INCH SAMPLE 40
NO PLASTIC DEFORMATION



VOLTS

FIGURE 6.18
BARKHAUSEN VOLTAGE PROFILE
12 INCH SAMPLE 40
WITH PLASTIC DEFORMATION



Time (s)

Applied field ($A\cdot m^{-1}$)

- 1779
- 1095
- 411
- +273
- +957
- +1641
- +2325
- +3009
- +3693
- +4377

CHAPTER 7 - PLASTIC DEFORMATION OF STEEL TYPE 2401

7.1 SAMPLES

The samples used in this chapter were prepared by Miss. S. Thompson who also performed the plastic deformation and coercivity measurements.

A set of steel samples were cut from a piece of gas pipe, of steel type 2401. The shape of the samples is shown in figure 7.1 and the photographs 7A and 7B. The shape was chosen such that the centre of the sample could be easily deformed by applying a tensile load to the samples. The shape also had to accommodate the cutting of discs and toroids for work in coercivity measurements. Photograph 7B shows the varying degrees of deformation applied to the samples. The Barkhausen noise experiments were carried out on the samples before machining the discs and toroids for other measurements.

7.2 EXPERIMENTAL PARAMETERS

The Barkhausen noise signal from an unstressed sample was observed on the transient recorder screen. Although the samples were thicker than the 12 inch samples, there was sufficient signal for measurements to be taken with the magnetising current at the same level as for the 12 inch samples. The signal was smaller in amplitude than the signal from the 12 inch steel samples and was spread over a larger portion of the hysteresis loop. The following experimental

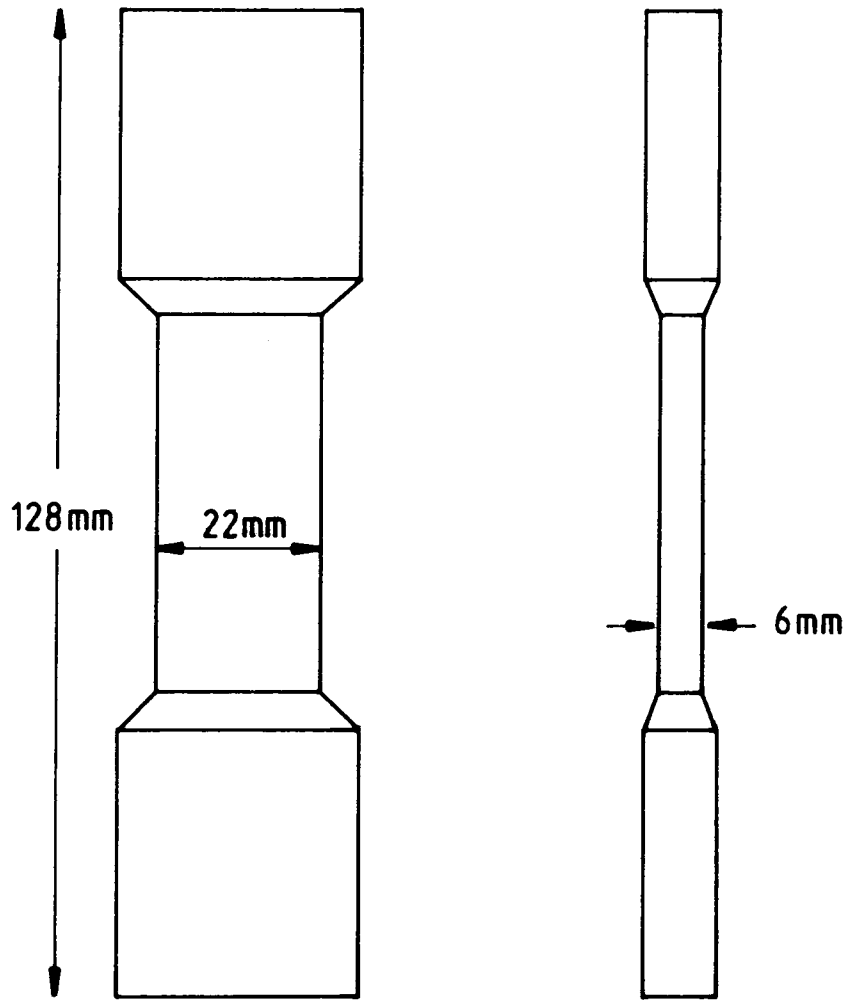
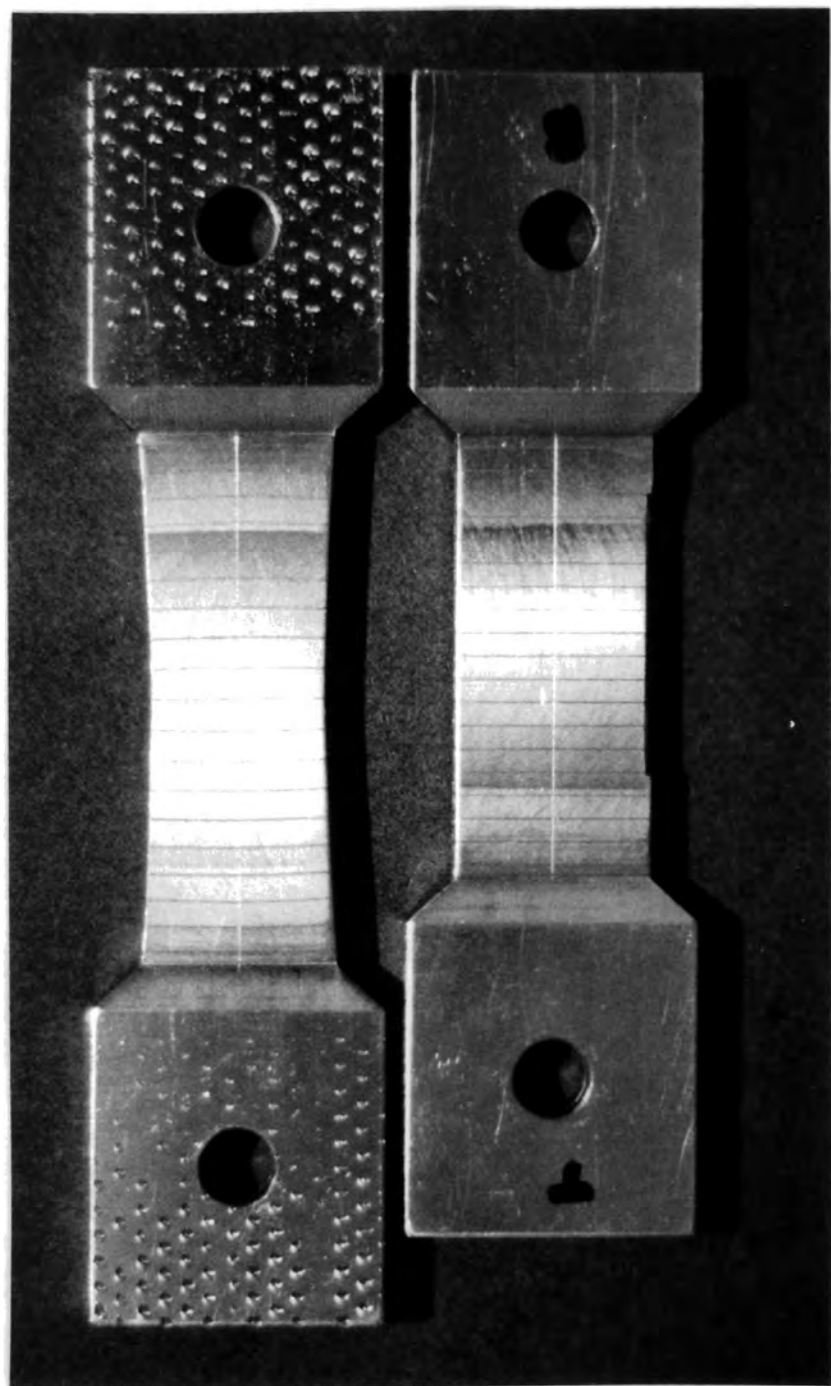
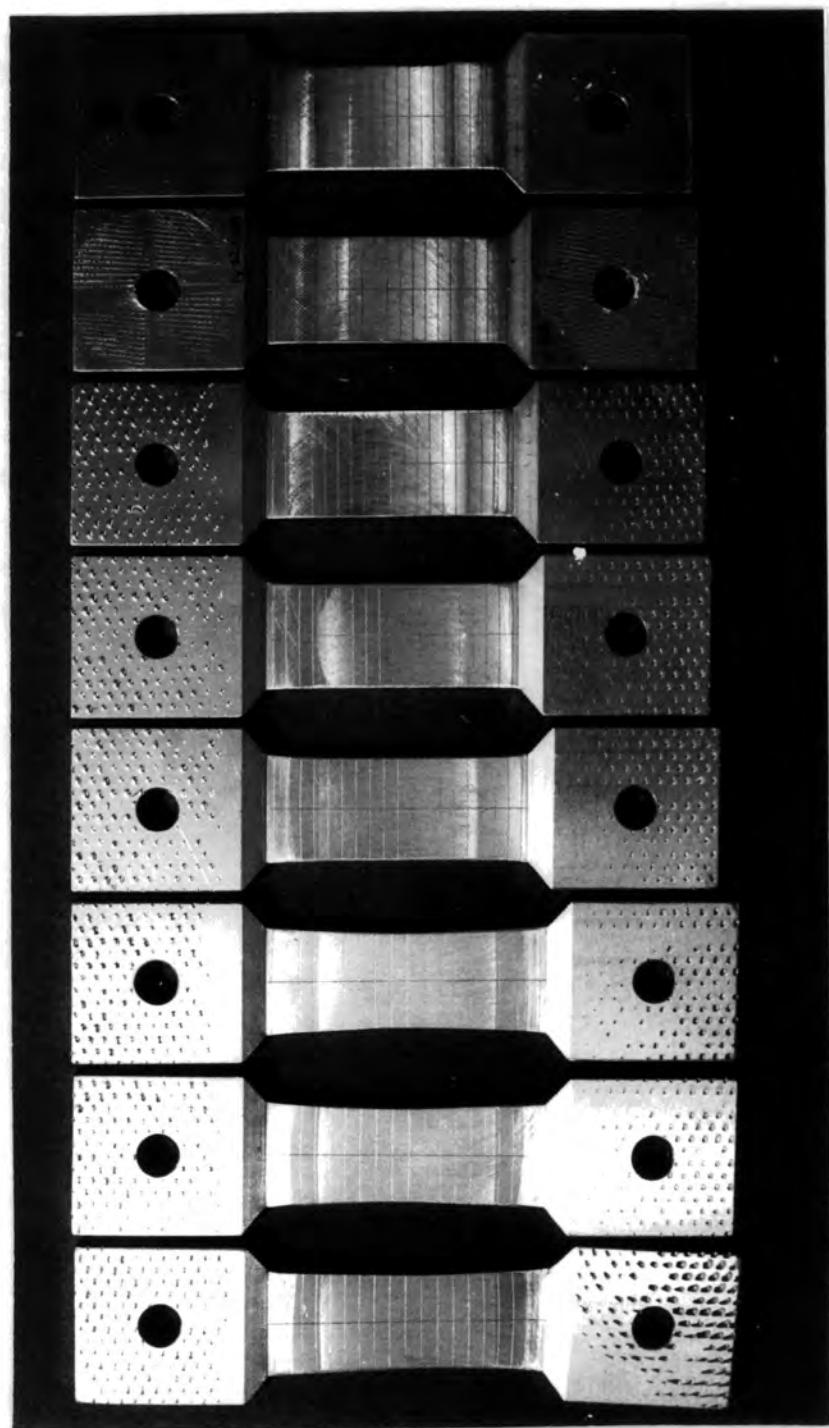


FIGURE 7.1

Shape of Samples of 2401 Steel used in Plastic Deformation Work



PHOTOGRAPH 7A Shape of Samples (Steel Type 2401)



PHOTOGRAPH 7B Shape of Samples (Steel Type 2401)

parameters were chosen for clear recording of the signal: magnetising frequency 0.1Hz; sample interval 31 μ s; filter frequency 14.5kHz. The noise burst was split into 4 sections of 1.01556 seconds and the first section of recording was started 5.5 seconds after the trigger signal was received from the waveform generator.

7.3 RESULTS

The Fourier transform routine was used to find the power spectrum of the Barkhausen noise. The power spectrum intercept was found by extrapolation of a straight line fit to the power spectrum between 400Hz and 2000Hz to 0Hz. The intercept was recorded and plotted against %plastic deformation (figure 7.2). The table below shows the results.

% DEFORMATION	INTERCEPT (V ²) ±10%
0	0.0048
2.4	0.0039
6.1	0.0034
7.6	0.0033
7.8	0.0032
11.5	0.0016
11.9	0.0011
20.3	0.0014
20.4	0.0012

The value of coercive field was found by use of a vibrating sample magnetometer [1]. The samples had small discs machined from them for this purpose. The

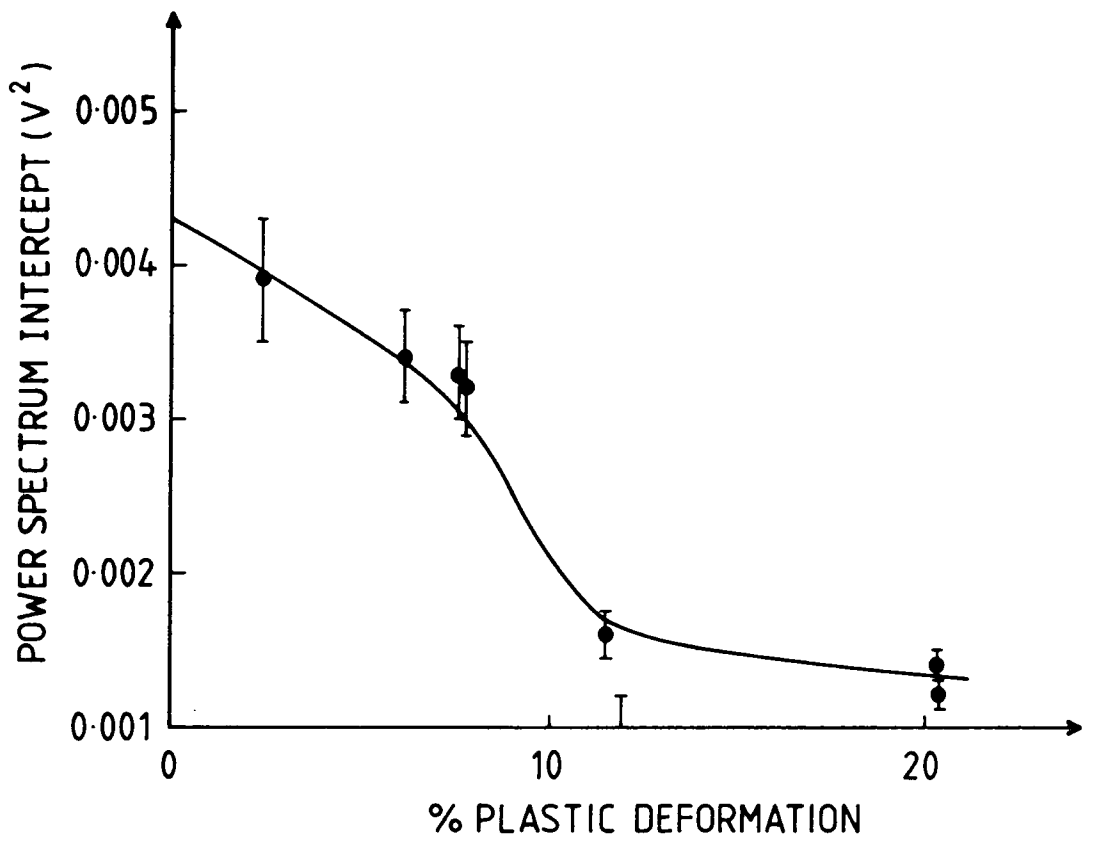


FIGURE 7.2

Plot of Power Spectrum Intercept against Plastic Deformation for Steel Type 2401

following values were given for H_c for the samples [2].

% DEFORMATION	H_c (kAm^{-1}) $\pm 3.5\%$
0	0.331
2.4	0.382
6.1	0.438
7.6	0.444
7.8	0.525
11.5	0.468
11.9	0.476
20.3	0.498
20.4	0.597

The following table shows the value of power spectrum intercept and H_c for each of the samples and figure 7.3 shows the plot of these results and figure 7.4 the value of H_c against plastic deformation.

H_c (kAm^{-1}) $\pm 3.5\%$	INTERCEPT $\pm 10\%$
0.331	0.0048
0.382	0.0039
0.438	0.0034
0.444	0.0033
0.525	0.0032
0.468	0.0016
0.476	0.0011
0.498	0.0014
0.597	0.0012

It can be seen from the graphs plotted that the power spectrum intercept decreases for increasing plastic deformation up to approximately 10% where the value of power spectrum intercept drops sharply to a reasonably constant level. The intercept also decreases for increasing H_c , the opposite effect to that displayed by most of the 12 inch samples.

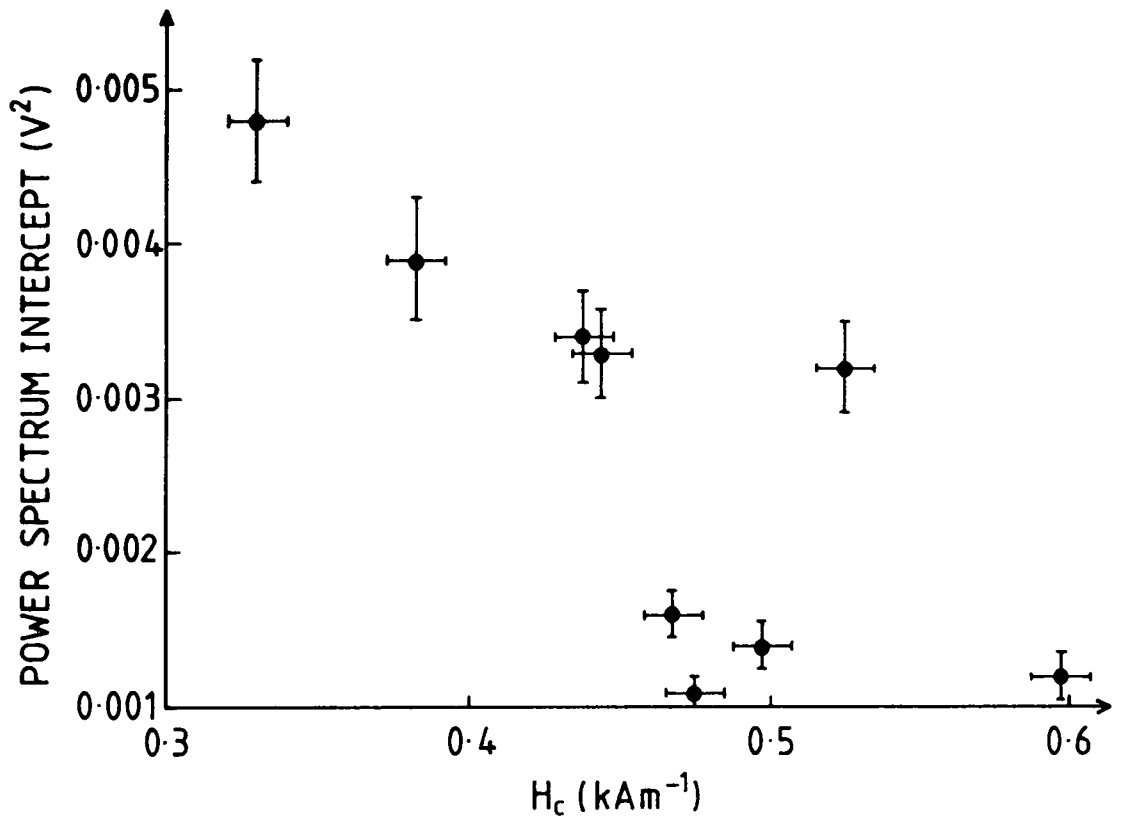


FIGURE 7.3

Plot of Power Spectrum Intercept against Coercive Field, H_c , for Steel Type 2401

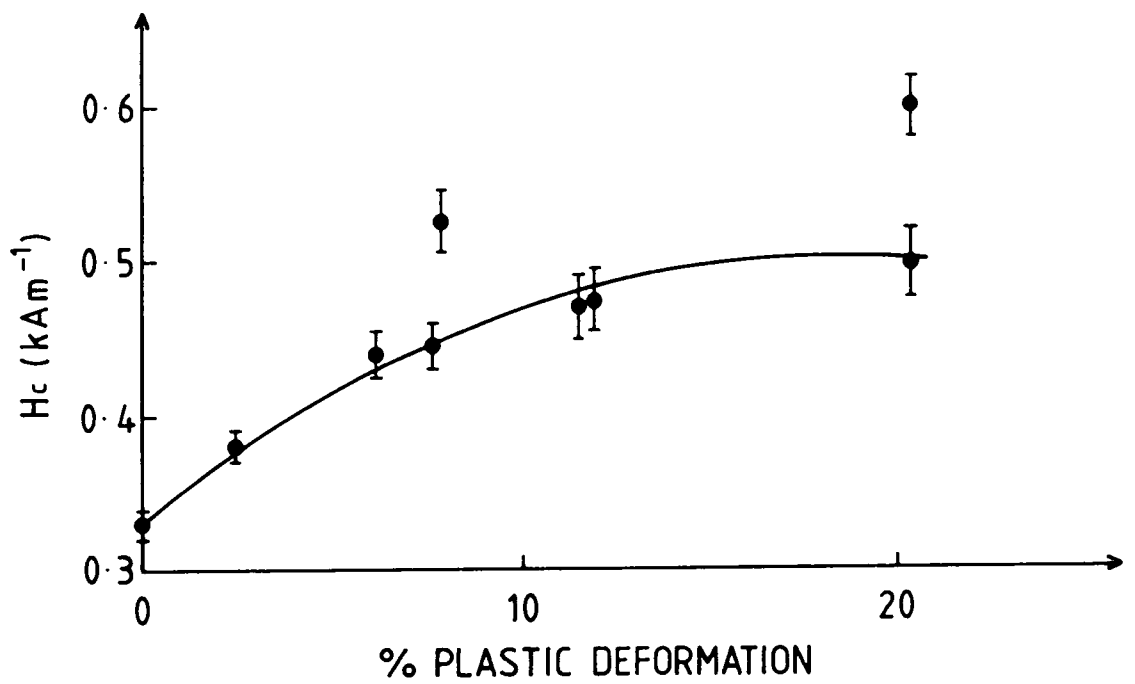


FIGURE 7.4

Plot of Coercive Field, H_c , against
Plastic Deformation for Steel Type 2401

There are two points which do not appear to be in agreement with the other points on the H_c against Plastic Deformation graph. These points were checked carefully. The same two samples do not appear to be anomalous on the Power Spectrum Intercept against Plastic Deformation plot. An explanation for this may be that the coercivity measurements were made on machined discs and the machining influenced the results for that sample. There is also a possibility that the assessment of the amount of plastic deformation was not accurate for the samples.

CHAPTER 8 - INDUSTRIAL APPLICATION OF BARKHAUSEN NOISE

8.1 EQUIPMENT AND SAMPLES

Barkhausen noise analysis has been developed into a commercially available unit, Rollscan 100, which is marketed by American Stress Technologies. The Barkhausen noise is analyzed in terms of the median amplitude of the pulse height distribution of the noise burst. A figure called the 'magnetic parameter' is displayed on the instrument and with appropriate calibration the number may be related to residual stress or microstructure depending on the application.

The Rollscan equipment was used on site at Eaton Limited (Axle Division), Newton Aycliffe. The product of Eaton is heavy duty axles and gear sets for the truck market. The components investigated with the Rollscan equipment were the crownwheels of the driving axle (figure 8.1). These ring gears vary in size between approximately 16 and 23 inches in diameter and the number of teeth per gear varies according to application and mechanical noise characteristics. The gears are manufactured from a case hardening class of steel, AISI 8822.

There are two methods of cutting the teeth of the gear into the machined blank, Oerlikon and Gleason, each named after the developing company. The Oerlikon method is a single cutting operation in which the

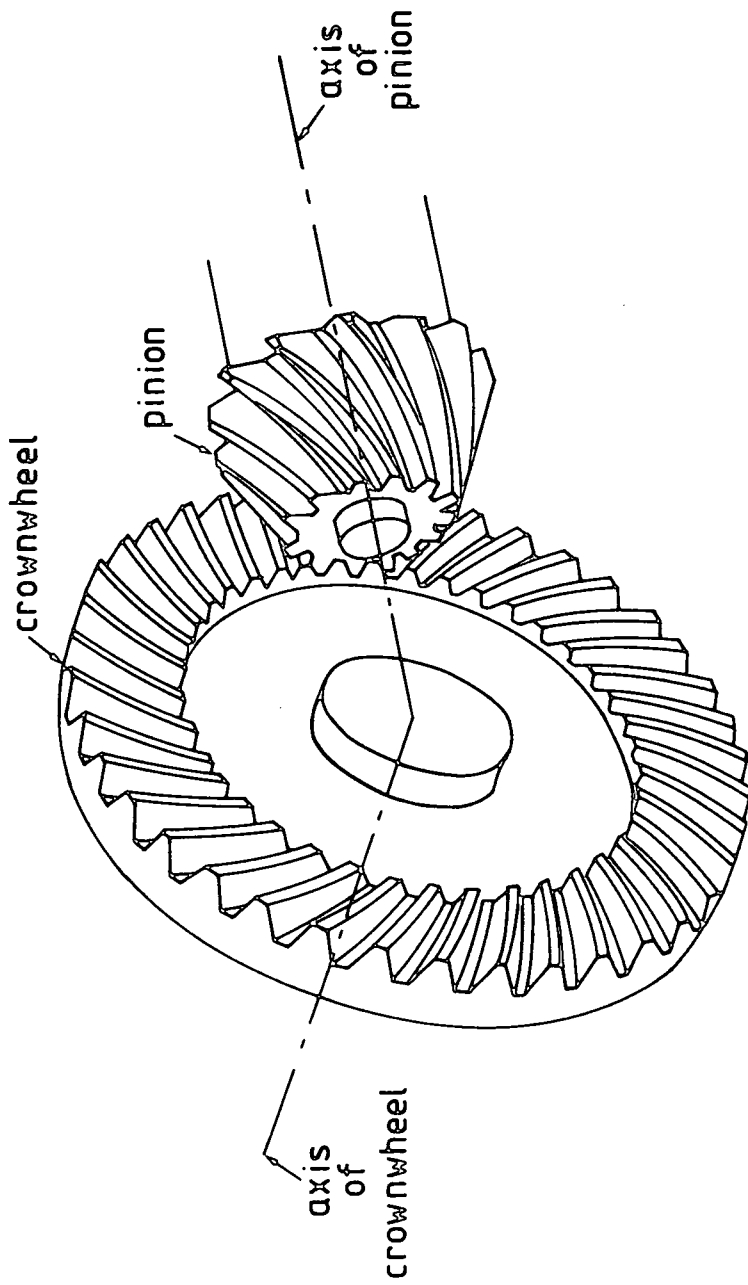


FIGURE 8.1 Gear Set of Driving Axle, Crownwheel and Pinion

cutters plunge into the blank removing the necessary stock. The cutters are arranged such that all the teeth are cut at the same time. The Gleason method consists of two different operations; a roughing operation in which the teeth are cut almost to size and a finishing operation in which the teeth have a small amount of stock removed on a separate machine. The teeth in this process are cut individually, the blank indexing before each cut.

The main purpose of the investigation at Eaton was to establish whether the Rollscan equipment could be used to assess the residual stresses left by the cutting procedure in the gear teeth and whether the two cutting methods showed different levels of stress in the teeth. A secondary consideration in the work was to establish if the shot cleaning of crownwheels was even across the surface of the wheel.

A measurement procedure was established which involved taking three readings of magnetic parameter on each tooth. The measurements were taken at approximately half tooth height, near the 'pitch line', at the toe, centre and heel of the tooth (figure 8.2). The probe used was not a custom made probe so positioning was approximate. The readings obtained, however, were still repeatable to a good degree of accuracy.

The probe used should be accurately calibrated for each material used, as the time period for use of the

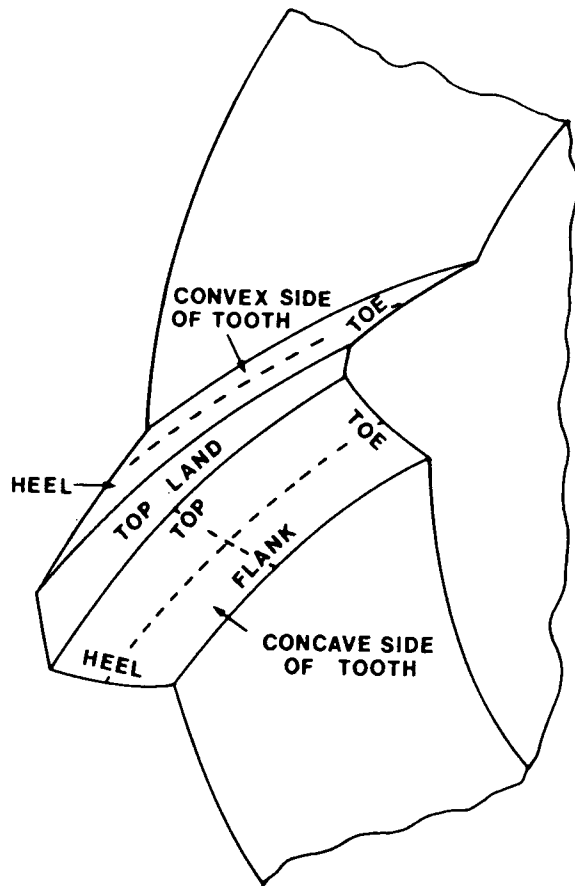


FIGURE 8.2 Crownwheel Tooth

equipment was limited it was decided to use an approximate method of calibration. Two pieces of crownwheel material were cut to be stress relieved in a muffle furnace. The first was in the pre-heat treated condition, that is the soft, as received material, the second was in the case carburized condition and was coated with a compound which prevents loss of carbon from the surface. The two were heated to a suitable temperature for stress relief under the guidance of the Eaton metallurgist. Rollscan measurements were then taken on the surfaces of these samples to give a value of magnetic parameter for the stress free condition. The value of magnetic parameter found in the gear teeth could then be associated with either a tensile or compressive residual stress; a value of magnetic parameter higher than the stress free value indicating a tensile stress and one lower than the stress free value a compressive stress.

All the measurements in the work were taken to a nominal depth of 0.02mm as indicated on the Rollscan equipment. There are two nominal depths of measurement, 0.02mm and 0.2mm; the difference between the two is that the frequency range considered in the electronics of the system is greater for the deeper measurement so that damped signals from deeper in the material may be assessed. The exact depth of measurement depends on the material under investigation.

8.2 RESULTS

It was found that for both cutting methods there was a considerable difference between the value of magnetic parameter on either side of a tooth. The coast (concave) side of the tooth showed a much lower value than the drive (convex) side. Typical values are shown below.

	OERLIKON			GLEASON		
	Heel	Centre	Toe	Heel	Centre	Toe
COAST	114	99	93	97	101	105
DRIVE	183	178	169	166	161	152

The following values were found for the mean and standard deviation for the 39 teeth of a Gleason cut crownwheel on the coast side of the tooth.

	MEAN MP	STANDARD DEVIATION
HEEL	92	5
CENTRE	98	4
TOE	105	4

Similar spreads of values were found for the Oerlikon cut wheels.

The stress relieved piece of 'soft' steel gave a mean magnetic parameter of 116 so it can be seen that for both cutting methods the levels of residual stress are of different types on either side of the tooth. The coast side of the tooth apparently being in compression and the drive side in tension. It can be seen, however, that the level of stress on the coast

side of the tooth is not considerably different for the two cutting methods but the Oerlikon cut shows a higher level on the drive side. It was also noted that there was a change in magnetic parameter along the tooth on both sides, the change being in the opposite direction on the coast side of the tooth for the two cutting methods. The difference is thought to occur because the direction of cut is opposite on the coast side for the two methods, although further work would be required to establish the relationship more fully.

A number of Gleason cut crownwheels were inspected with the Rollscan equipment immediately after heat treatment and before the shot clean operation. The value of magnetic parameter was found to be very low and even around the wheels. The value of magnetic parameter found for the stress relieved piece of hardened crownwheel material was off scale (higher than 199) using the value of magnetising current used in the rest of the work; an approximation was made by using half the magnetising current and the doubling the magnetic parameter found, the instrument manufacturer having recommended this procedure. The mean value of magnetic parameter found was 154, so the value of magnetic parameter approximated for the stress free condition was 308. The table shows typical values obtained from the teeth of the hardened crownwheels after heat treatment.

	HEEL	CENTRE	TOE
COAST	12	10	11
DRIVE	32	28	30

The same crownwheels were inspected again after the shot clean operation and there was found to be a considerable difference in the Rollscan readings. The difference was, however, only found on the drive side of the tooth where the value of magnetic parameter had changed by at least 30% after shot clean. The most significant change was that on certain teeth the magnetic parameter was between 4 and 5 times the value before shot clean. Some typical sections of the results for the drive side are shown below.

	HEEL	CENTRE	TOE
Drive 1	62	84	58
Drive 2	76	127	94
Drive 3	111	73	78

The shot clean operation is not performed to change the stress on the surface of the gear teeth, but simply to remove any burnt oil or scale that may be left after heat treatment. However, it is clear that there is a significant change in the stress after shot clean. As a comparison with these readings, the Rollscan equipment was used on a gear which had been shot peened. Shot peening is a controlled operation where shot of a particular hardness is fired at the root of a gear tooth in a particular direction at a particular speed. The purpose of the process is to

increase the compressive stress at the root of the tooth which improves fatigue life and prevents the development of cracks. The level of the measurements in the shot peened gears was similar to that of certain teeth in the shot cleaned gears, the shot peened gears gave values of magnetic parameter between 120 and 160 along the tooth.

It is unclear how a gear surface would be affected by the variations caused by shot cleaning in an inconsistent manner. It has been suggested that the long term effect may be to produce uneven wear on the teeth of a gear as it runs in service and that the ultimate result would be a noisy gear set. To establish this relationship would obviously take a number of years of service or a severe laboratory test.

CHAPTER 9 - DISCUSSION

9.1 POWER SPECTRA CONSTRUCTIONAL STEELS

The power spectra plotted showed no unusual features and use of a modified Fourier Transform routine, employing data windowing, revealed no further information about the spectra. The data were all treated in the same manner.

The plots in Chapter 6 show no simple relationship between the known magnetic properties of the 12 inch pipe steel and the Barkhausen noise spectra, although some empirical relationships may be found by excluding certain results.

It was hoped that steel samples having similar H_c values would display similar Barkhausen noise extrapolated intercept values, although this parameter has not previously been used to characterise spectra.

Samples 15, 16 and 34 have the same H_c value and, within the 10% experimental error limits, the results for these samples are acceptable. Samples 5, 11 and 40 have similar H_c values, but sample 40 displays a very much greater value of noise power spectrum intercept.

The possibility of obtaining a spurious reading owing to surface damage was explored in section 6.2 and the results show that, although there will be some damage due to surface grinding the samples, there is no significant contribution to the power spectrum. It may

therefore be concluded that the spectra represent phenomena taking place in the interior of the sample and not purely surface phenomena. The contributions to the power spectrum must therefore be considered in more detail.

The hysteresis loops for the 12 inch samples were examined and an approximate gradient calculated for each loop. It was found that the loop for sample 40 had a steeper gradient than the other samples, and that of 34 a shallower gradient. Figures 9.1 and 9.2 show the part loops for these samples.

In the power spectrum equation shown in Chapter 2;

$$\Phi(\omega) = \phi(\omega) \left(1 + \frac{2\rho(1-v\tau_0)^2}{1+\omega^2\rho^2\tau_0^2(1-v\tau_0)^2} \right)$$

the value of τ_0 , the time between single Barkhausen events, will depend on the rate of change of magnetisation in the sample. Celasco et al. [1] showed that at low magnetising frequency the quantity $v\tau_0 \ll 1$ (v is the average number of single Barkhausen events/unit time) and that for frequency analysis between 1 Hz and 20 kHz;

$$\Phi(\omega) = \phi(\omega) \left(\frac{2\rho}{1+\omega^2\rho^2\tau_0^2} \right)$$

is a valid approximation to the power spectrum. The

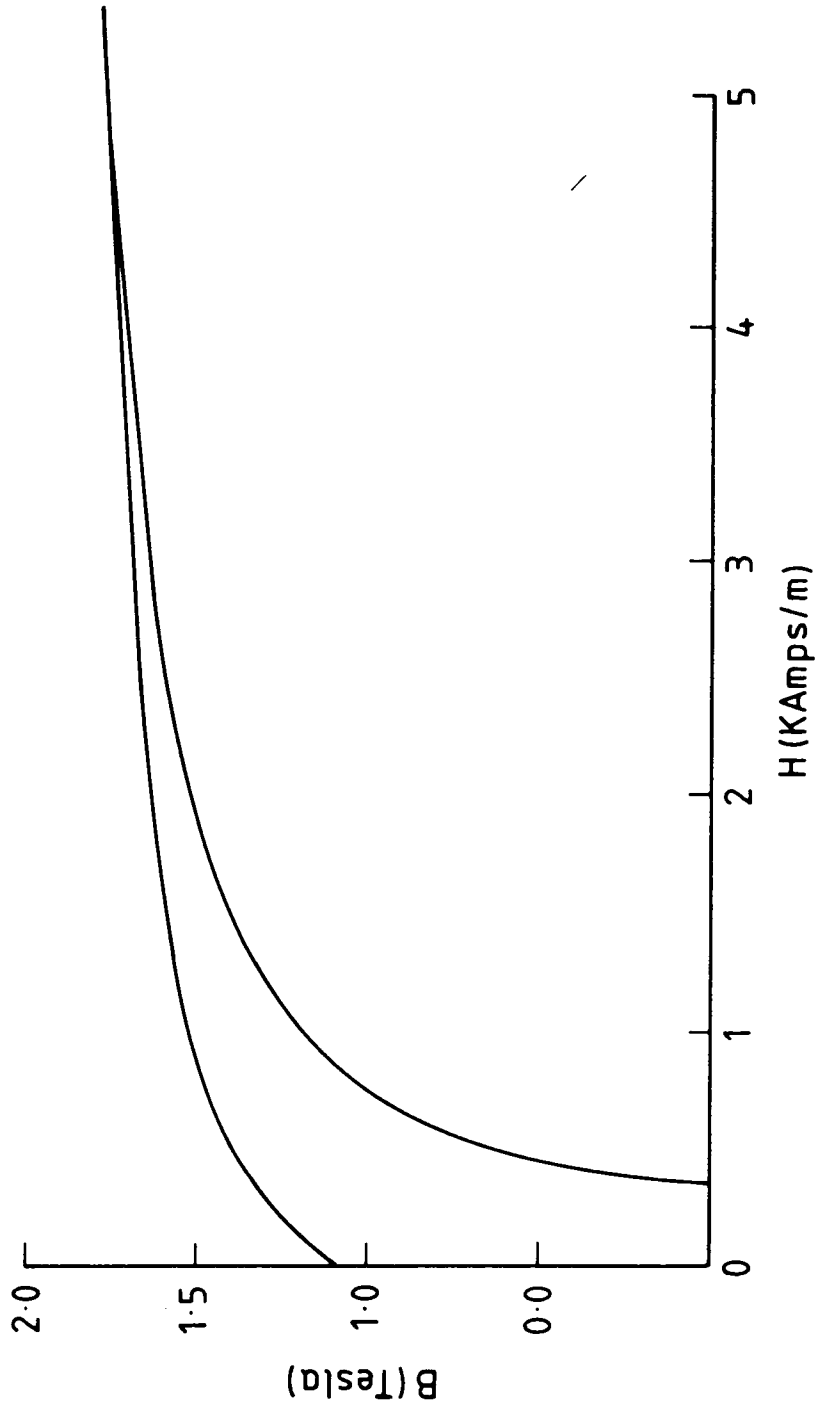


FIGURE 9.1 Part Hysteresis Loop for 12 inch Sample 40 (provided by British Gas)

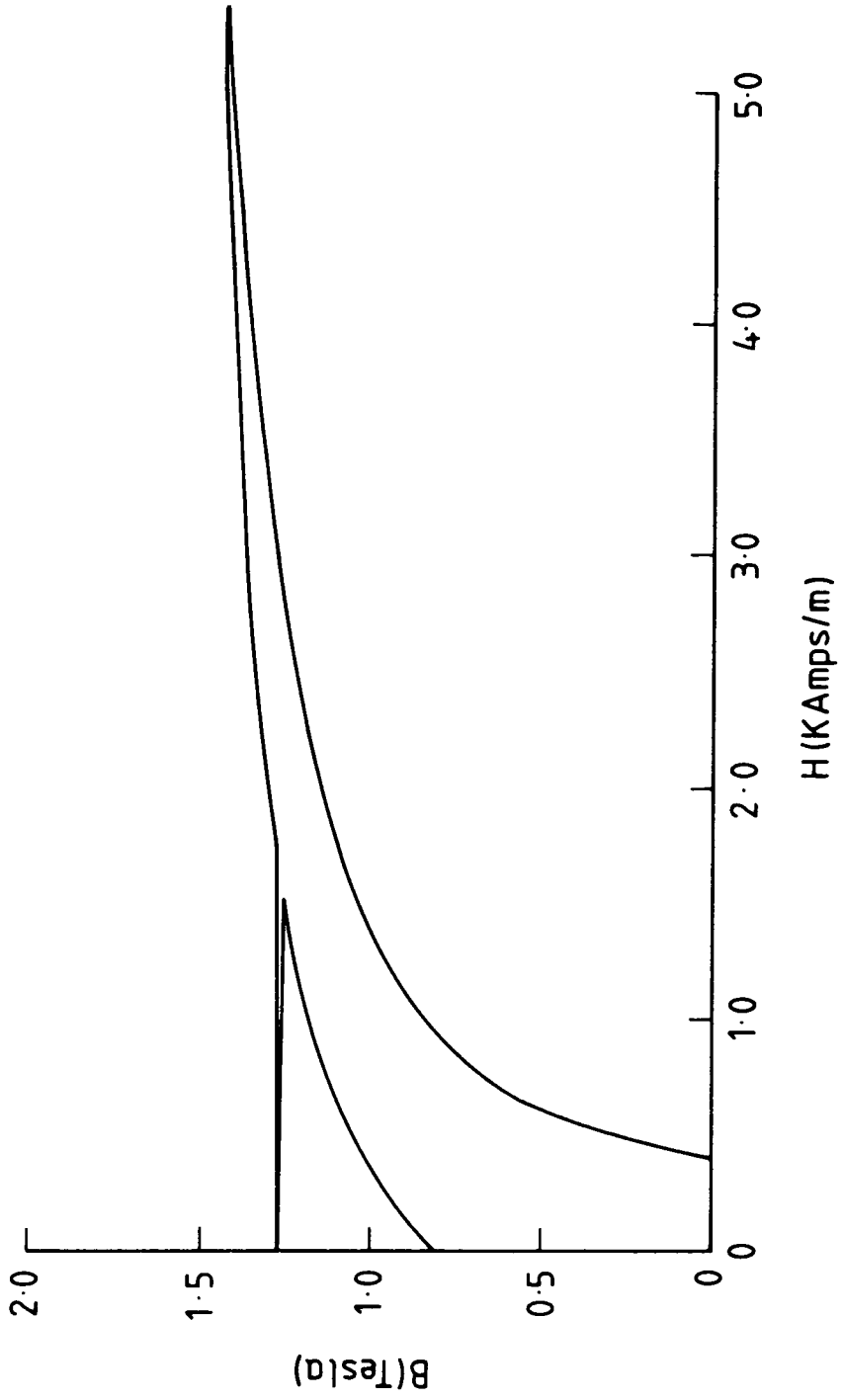


FIGURE 9.2 Part Hysteresis Loop for 12 inch Sample 34 (provided by British Gas)

factor $\phi(\omega)\rho$ may be considered to be proportional to magnetising frequency [1] and constant for all the experiments.

It may be seen that $(\rho\tau_0)^2$ is the important parameter in the equation, ρ is the number of single events in a cluster and τ_0 the time between single events. The gradient of the hysteresis loop will affect the value of τ_0 and it would be expected that τ_0 would be smaller for a steeper gradient. If the gradient of the hysteresis loop were the only influencing parameter on the presented spectra, 40 would be expected to have the largest intercept and 34 the smallest. This is not the case, which implies that ρ , the number of single events in a cluster, must change from sample to sample also.

The value of ρ will depend on the growth of the correlation domain discussed in section 2.6. The correlation domain growth will depend upon the grain size of the material and the strength of pinning of domain walls at various sites in the material.

Samples 35 and 41 have been examined for their grain size and microstructure [2] and it may be assumed that the samples 34 and 40 should display similar microstructure to those samples respectively. The mean grain size of 35 was $11.0\mu\text{m}$ for pearlite and $13.0\mu\text{m}$ for ferrite, that of 41 was $9.6\mu\text{m}$ for pearlite and $15.3\mu\text{m}$ for ferrite. There was a significant difference in the pearlite content in the two samples; 35 having 27.1%

pearlite and 41 having 16.6% pearlite. It was also noted that there was a significant difference in the distribution of the pearlite, in that 41 showed a banded structure and 35 a more evenly distributed structure. The photographs 6A and 6B (Chapter 6) show typical micrographs for samples 35 and 41.

The grain sizes do not show a significant difference between the samples, so it was considered that the variation in pearlite content could be the factor which affects the power spectrum by varying the value of ρ . It is known that pearlite pins domain boundaries strongly, a higher pearlite content would therefore be expected to cause the correlation domain to grow in small connected stages. Each section of growth, a Barkhausen jump cluster, will be made up of many small Barkhausen jumps. A lower pearlite content would be expected to give fewer Barkhausen jumps in each stage of growth in the correlation domain and hence a lower value of ρ . In the power spectrum equation it would be anticipated that the lower the value of ρ the higher the value of power spectrum intercept. The behaviour of sample 40 could be partly explained in this way.

The results presented show, however, that for the set of 12 inch samples the power spectrum intercept may be expressed in an empirical way with the properties H_c , B_r and B_r/H_c . The points for samples 40 and 2 do not follow these relationships.

9.2 PLASTIC DEFORMATION OF SAMPLE 40

The plastic deformation of sample 40 gave a smaller extrapolated intercept on the power spectrum plot than the original sample (figures 9.5, 9.6). The plastic deformation of the sample will increase the dislocation density and introduce a new residual stress pattern. In general, it would be considered that there would be a significant number of individual Barkhausen jumps due to the increased number of pinning sites. It has been shown [5] that in silicon iron under plastic strain the median value of clusters of Barkhausen noise in the amplitude domain increases with plastic strain, at small strain values, when the sample is magnetised parallel to the strain direction. This means that the clusters of individual Barkhausen jumps tend to be larger in amplitude for plastic strain. This would seem sensible as, on average, more domain walls will be moving at a given time as a result of the increase in the number of pinning sites. The movements may be considered as pulses being added together and the resultant of adding together more jumps will give a larger amplitude. The increase in the median value of the Barkhausen jump clusters for plastic strain implies that there will be more single events packed into each cluster. In the equation for the power spectrum;

POWER
(V \cdot V)

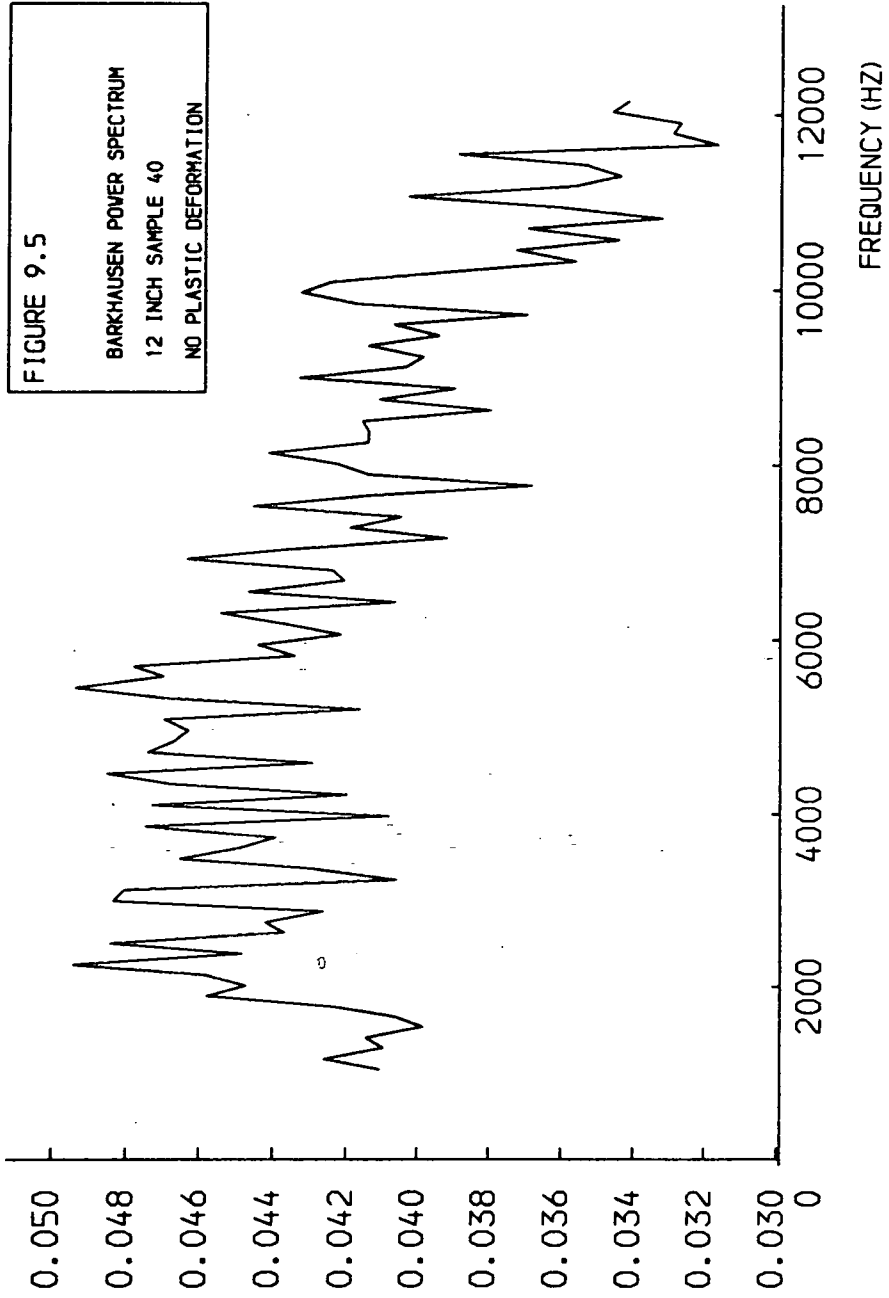


FIGURE 9.5

BARKHAUSEN POWER SPECTRUM
12 INCH SAMPLE 40
NO PLASTIC DEFORMATION

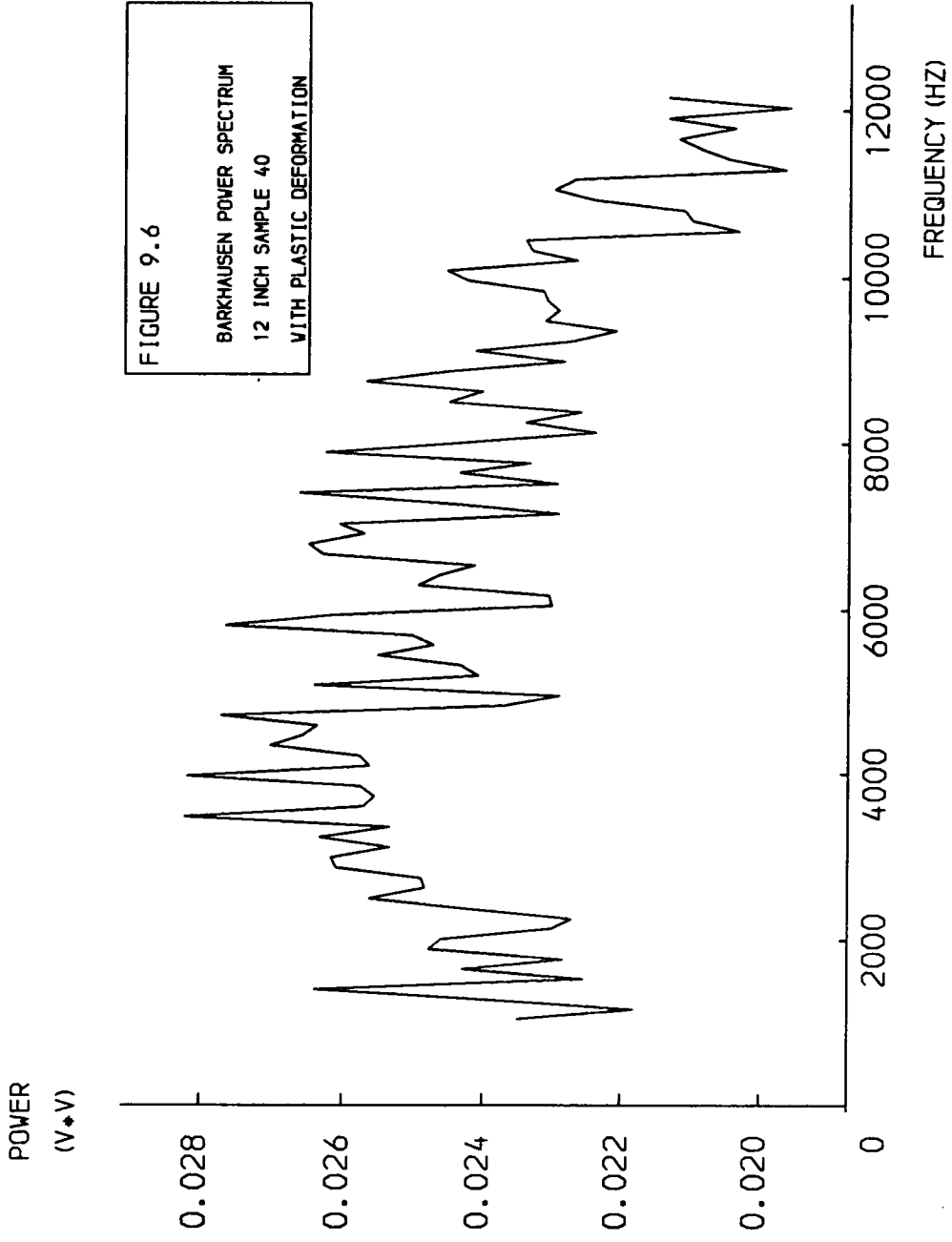


FIGURE 9.6
BARKHAUSEN POWER SPECTRUM
12 INCH SAMPLE 40
WITH PLASTIC DEFORMATION

$$\Phi(\omega) = \varphi(\omega) \left(1 + \frac{2\rho(1-v\tau_0)^2}{1+\omega^2\rho^2\tau_0^2(1-v\tau_0)^2} \right)$$

the value of ρ , the average number of single Barkhausen events in a cluster will be increased.

In the material the value of τ_0 will depend on the rate of change of magnetisation. Plastic deformation of a small amount tends to shear the hysteresis loop [6], giving a smaller change of magnetisation in the sample for a certain change in applied field. The value of τ_0 will therefore be increased in the plastically deformed material.

It is therefore possible to imply that $\rho\tau_0$, the duration of a cluster, will be increased for plastic deformation.

In the reduced equation for the power spectrum

$$\Phi(\omega) = \varphi(\omega) \left(\frac{2\rho}{1+\omega^2\rho^2\tau_0^2} \right)$$

as the magnetising frequency is constant over the experiments, the value of $\{\rho\varphi(\omega)\}$ will be similar for all cases. It can therefore be seen that the value of $\Phi(\omega)$ will be smaller for the plastically deformed sample where $(\rho\tau_0)$ is larger.

The extrapolated intercept of the Barkhausen noise power spectrum for sample 40 drops by approximately

half in the plastically deformed cases suggesting that the value of $(\rho\tau_0)^2$ is twice its original value, i. e. $\rho\tau_0$ is $\sqrt{2}$ of its original value.

Lieneweg [7] suggests that the value of the noise power at zero frequency is proportional to the mean volume of material experiencing flux reversal associated with a Barkhausen jump. This would suggest that the effect of the plastic strain introduced to sample 40 has approximately halved the mean volume of material changing in a Barkhausen jump.

9.3 BARKHAUSEN NOISE VOLTAGE PROFILE PLOTS OF CONSTRUCTIONAL STEELS

It is apparent from the voltage profiles plotted that the peak heights observed and the position on the hysteresis loop of the peaks are not simply related to the bulk magnetic properties of the steel samples.

There is evidence for an inverse relationship between the principal peak height and the time from the start of the experiment at which the peak occurs. The product of these two quantities is shown below.

SAMPLE NUMBER	PEAK HT. * PEAK TIME (Vs)
33	0.052
15	0.046
34	0.042
16	0.053
39	0.046
5	0.044
11	0.044
40	0.047
2	0.044
20	0.049

The estimated error in the peak height is $\pm 0.002V$ and that in the time of the peak is $\pm 0.005s$. The error in the product values is therefore in the order of $\pm 0.003Vs$, so the product is approximately constant with the exception of 16 and 33. The relationship shows that the longer the peak takes to develop the smaller the peak height achieved.

Three interesting points were raised by the voltage plots generally, they are; the anomalous peak, X, the effect of plastic deformation in sample 40 and the effect of surface removal.

All the voltage plots for these samples were made by the same averaging process so they can be compared directly. Taking the modulus of, and averaging the voltage data will have enhanced regions of the plot where the noise signal was not varying considerably, such as the regions at the extreme times of the plots. The regions at the extreme times show little Barkhausen noise but mostly experimental noise in the form of pick-up from the magnetising field and 50Hz.

The time axis of the plots is proportional to applied field. It can be seen from the Barkhausen noise voltage plots that the majority of the Barkhausen noise occurs after the crossing point at H_c . This would be expected as the field in the sample is changing rapidly in this region causing domain walls to move from one pinning site to another. The motion of the walls may be impeded by the formation of domains of

reverse magnetisation in the form of spikes or by the simple 'trapping' of a domain wall at the impediment [8].

9.3a Peak X

The peak, X, has been shown to be related to the position of the steel sample in the coil system, the asymmetry of the fields in the sample causing a spurious signal. The peak is actually exaggerated on the plots by the averaging procedure.

A similar large peak to the peak, X, at the start of the Barkhausen noise has been observed by Barton and Kusenberger [9] in the testing of bearings under a radial load. The peak was observed after the bearings had been tested both in the laboratory and in service for up to 983 hours. The Barkhausen noise characteristics of the bearings which had been in service were compared with those from bearings tested in the laboratory. The peak was apparent in both sets of data. The explanation offered for the peak is the decrease in surface compressive stress over the time period tested; equally it could be argued that an increase in tensile stress would produce a similar effect. The tests on bearings from service showed the pronounced peak occurred in 60% of the bearings tested.

The method of measurement here was with a small 'stand-on' transducer. The peak observed may have been caused by a similar asymmetry in the field as the

transducer is smaller than the sample. There are no other reports of this type of anomalous signal, although the plotting of the direct voltage output of the pick-up coil has not been reported by many workers.

9.3b Plastic Deformation of Sample 40

The voltage plots for sample 40 show that there is a decrease in the main Barkhausen noise peak after deformation. This decrease is difficult to explain in terms of the clustering of Barkhausen jumps as the median value of the clusters would be expected to increase with plastic strain. A possible explanation may be that, although the amplitude of the clusters is larger, there is a greater time between clusters [1] so at each sample time there will not be as many clusters superimposed on each other and the peak height is reduced. This interpretation would only be valid for the coil system and recording parameters in this work.

A different explanation for the decrease in peak height may be that, as shown in figure 9.7 [10], there is a net compressive stress at the surface of a plastically deformed rod. It has been shown by Rautioaho and Karjalainen [11] that a compressive stress, elastically induced, will cause a drop in the true RMS voltage of the Barkhausen noise if the sample is magnetised in the direction of the stress. It could be supposed that a plastically induced compressive stress would have a similar effect, the decrease in RMS

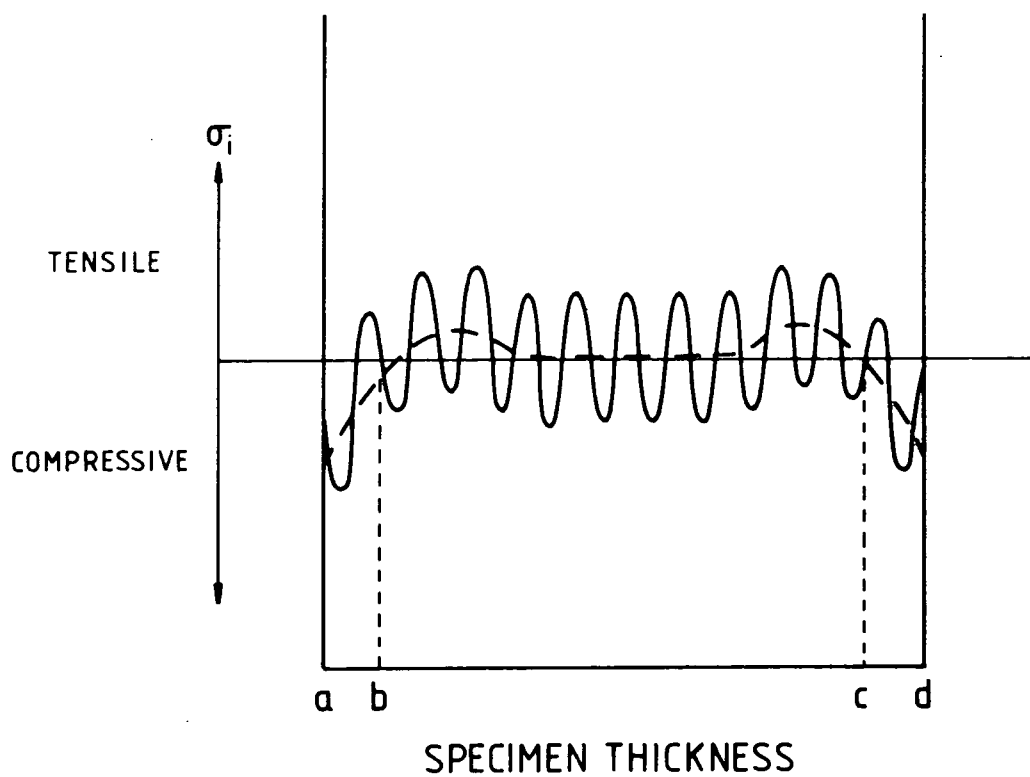


FIGURE 9.7

Expected Distribution of Microstresses (full line)
 after Uniaxial Plastic Deformation
 Superimposed on Macrostress Distribution
 (dashed line) (after James and Buck) [10]

voltage being reflected in the lower peak height of the voltage plot of the plastically deformed sample 40.

9.3c Surface Removal

The results of surface removal show that the Barkhausen noise pick-up from the material was not significantly affected by the damage in the surface caused by sample preparation. This result shows that the results for the samples should be reliable and that they are representative of the bulk material.

The voltage profiles for the etched samples show that the 90° domain wall peak is not always apparent on the voltage plot. The reason for this is not clear but it may be anticipated that the peak would be discernible for a slower magnetising frequency and a different waveform sampling rate.

9.4 PLASTIC DEFORMATION OF STEEL TYPE 2401

The results for the steel type 2401 showed that for increasing plastic deformation and for increasing H_c the value of power spectrum intercept decreases. The decrease with plastic deformation is explained in a similar manner to the decrease observed in power spectrum intercept for sample number 40 of the 12 inch samples. The apparent saturation of the value of power spectrum at plastic deformation higher than 10% indicates that the increase in the number of

dislocations does not cause the correlation domain to grow in any smaller stages.

The decrease in power spectrum intercept with H_c may be explained by considering the contributions to the value of bulk coercivity in a similar manner to the considerations for the 12 inch samples. The value of coercivity may be estimated in terms of the following equation:

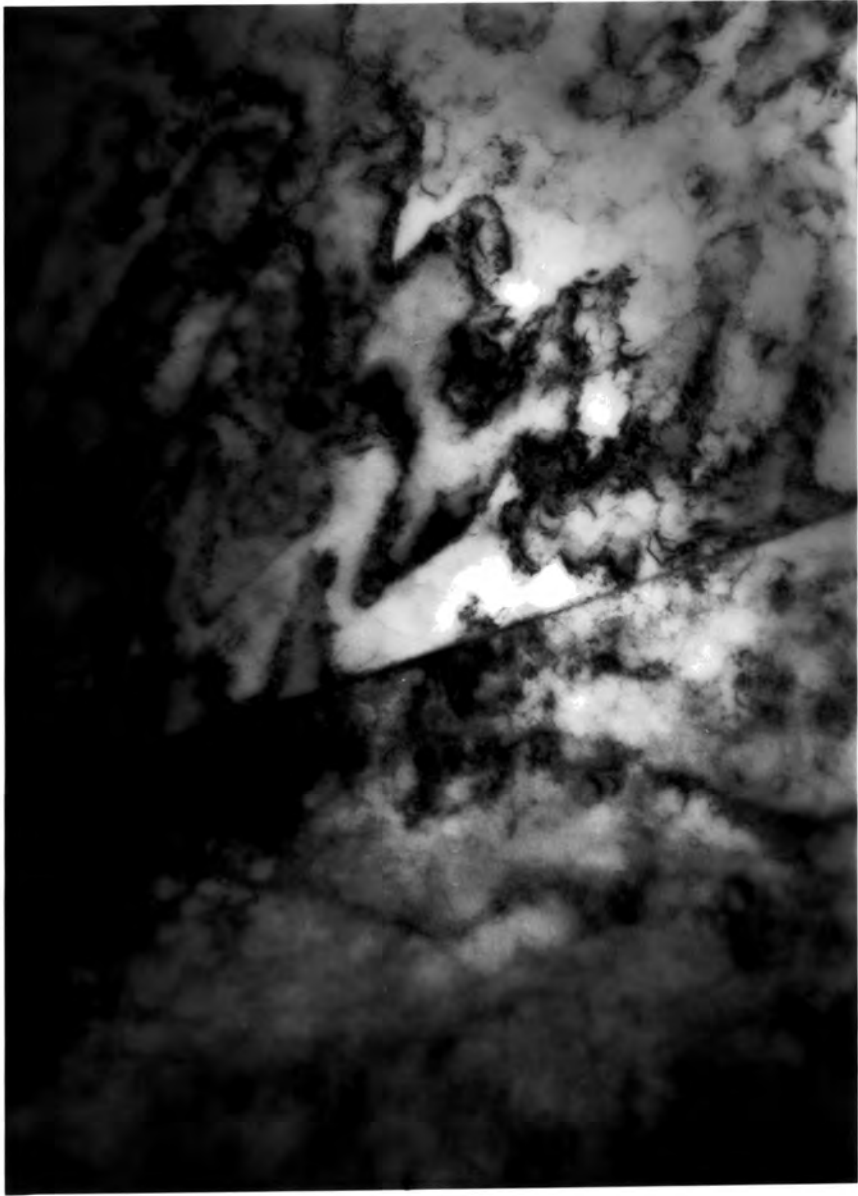
$$H_c = H_1 (\text{incl}) + H_2 (\omega^*) + H_3 (\omega_1^*) + H_4 (\sigma) + H_5 (\text{disloc})$$

The 12 inch samples had variations in H_c due to changes in the value of H_2 , H_3 and H_4 , the value of H_5 was assumed to be constant. For the samples of 2401 steel the value of H_5 has been changed by the plastic deformation of the samples so this must be taken into consideration.

The plastic deformation will increase the number of pinning sites in the material. The increase will cause the correlation domain to grow in smaller stages giving an increase in the high frequency portion of the power spectrum and a subsequent decrease in the lower frequencies. The number of pinning sites, however, reaches a point where any further increase does not alter the size of the stages of growth of the correlation domain. The value of H_c will increase as the value of H_5 is proportional to the number of dislocations in the material.

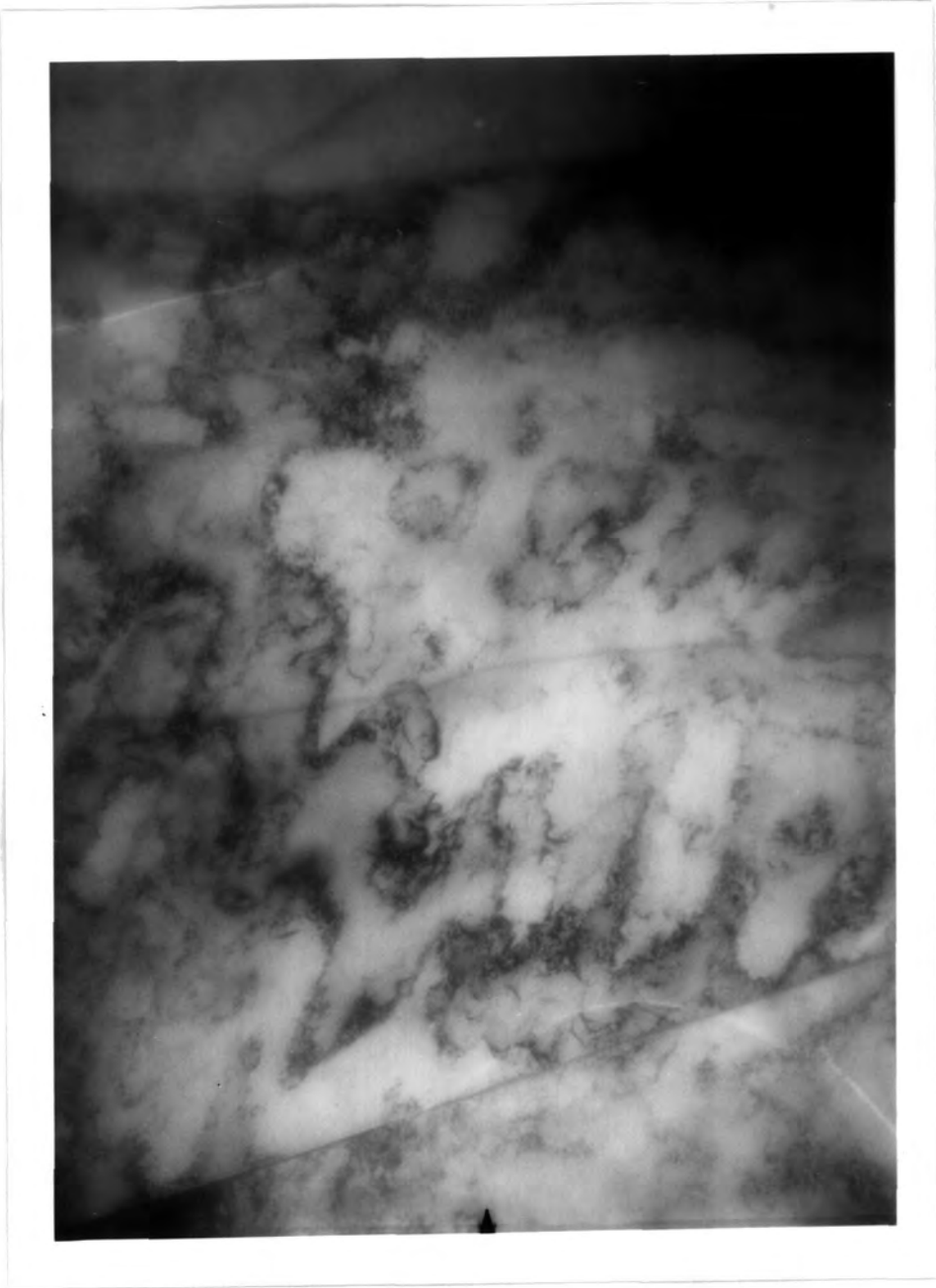
Photographs 9A, 9B, 9C and 9D, 9E show some electron micrographs of the structure of the samples. **The micrographs were obtained by Sarah Thompson.** [12]. [^] 9A, 9B and 9C show three views of the same sample, the deformation in the sample being approximately 20%. The dark undulating lines on all the photographs are dislocations in the steel. 9A is the in-focus view with a grain boundary running from left to right across the photograph. 9B and 9C show the same grain boundary running from the bottom left corner across the view, the grain boundary appears to be the same colour in each photograph. A domain wall is shown on 9B and 9C; the position of the wall being almost central in the photographs and the contrast of the wall changing between the under-focus 9B and over-focus 9C views. It can be seen that the domain wall is not straight, suggesting that it is pinned by the dislocations in the steel. In the bottom right hand corner of the over-focus view it is also possible to see a domain wall being pinned by the grain boundary.

Photographs 9D and 9E show two views of a 7.8% deformed sample, with a field of 8.27kAm^{-1} applied parallel to the domain wall on 9E. The in-focus view, 9D, shows a grain boundary across the photograph. The same grain boundary is shown in a slightly lower position on 9E. The light line on 9E is a domain wall clearly showing pinning along its length. The applied field causes the wall to 'bow' between pinning sites,



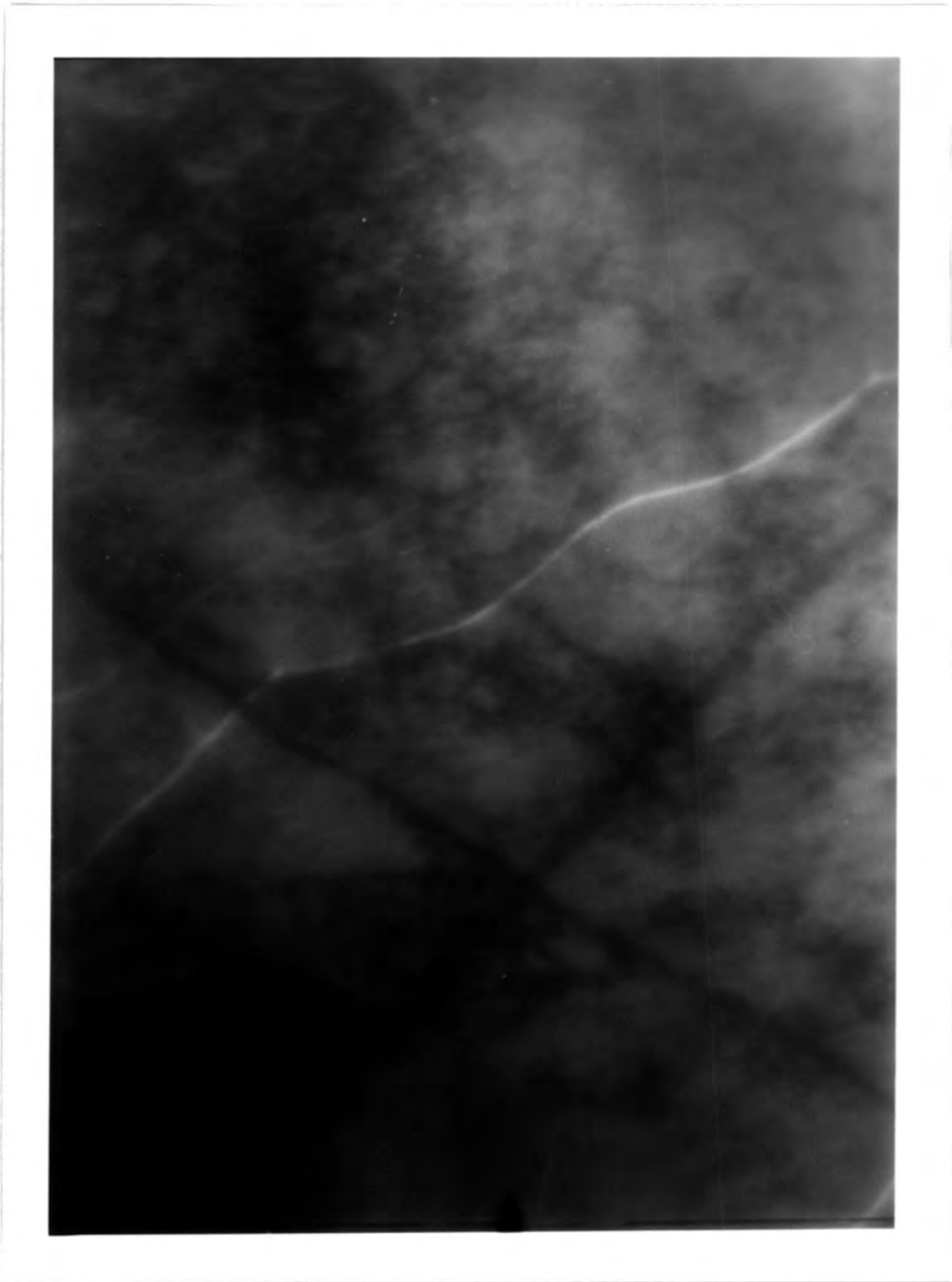
PHOTOGRAPH 9A In-Focus View, 20% Deformation (approx.) [12]
(taken by Thompson)

1.6 μ m



PHOTOGRAPH 9B Under-Focus View, 20% Deformation (approx.) [12]
(taken by Thompson)

1.6 μ m



PHOTOGRAPH 9E 7.8% Deformation, Applied Field [12]
(taken by Thompson)

0.8 μ m

so the pinning is more easily discernible than with no applied field.

9.5 INDUSTRIAL APPLICATION OF BARKHAUSEN NOISE

It has been shown that it is possible to evaluate residual stress from cutting with a commercially available unit. The unit makes use of the change in median value of Barkhausen jump cluster for its evaluation. It has also been shown that the power spectrum intercept, extrapolated from a suitable value which avoids the noisy part of the signal, is sensitive to plastic deformation. It would therefore be possible to develop a sensor and electronics system which would show the amount of deformation in terms of the power spectrum intercept. The advantage of this type of sensor may be that with suitable calibration it would be possible in certain instances to imply something about the magnetic properties of the steel under examination.

CHAPTER 10 - CONCLUSIONS AND SUGGESTIONS

The work presented here has shown that Barkhausen noise power spectra show no simple general relationships to the bulk magnetic properties of constructional steels, but certain relationships may hold under particular conditions. The complex processes which form the individual Barkhausen jumps into clusters of related jumps are associated with the microstructure of the steel and the shape of the hysteresis loop.

The power spectra could be used to determine the state of stress in a material as they are sensitive to both elastic and plastic strain. It is shown here that if there is a suitable reference in an unstrained material a qualitative conclusion can be made as to the stress state of the material. Further investigation may reveal a suitable measurement from the power spectra to be linked quantitatively to residual stress.

The NDT systems already developed with Barkhausen noise analysis do not use power spectra as their analysis medium but rely on amplitude measurements. The amplitude measurements are very sensitive to grain size and can be related to magnetic parameters in a rather qualitative manner. It would be appropriate, therefore, to follow up these qualitative measurements and to attempt to relate the noise and magnetic parameters quantitatively. The equipment used for the

measurements made here could be modified for amplitude measurements by the use of gating and a multi-channel analyzer instead of the transient recorder.

It has been indicated by Rautioaho and Karjalainen [1] that it is possible to qualitatively relate the true RMS value of Barkhausen noise in the hysteresis loop to the residual stresses in a material; this was tested by stress relief of welded samples. There is, as yet, no quantitative analysis. It is shown here that the power spectrum intercept is sensitive to stress relief and plastic deformation, so it should be possible to undertake a similar analysis involving power spectra.

The equipment used for this work has been proved to be of a reasonable quality for making measurements of Barkhausen noise in the laboratory. Future developments for the equipment would be to make it more efficient; the method of dividing the loop and being limited by the computer and transient recorder available meant that one sample took at least 5 hours to transfer to PET disc, 20 minutes to transfer to BBC disc and 1 hour 40 minutes to transfer to NUMAC, a total of 7 hours without any analysis being done. A spectrum analyzer would be much quicker and easier, although expensive.

Further work on Barkhausen noise would have to include the development of a magnetic transducer and its electronics. A crude transducer was made during

the course of this work but its use was limited to observations on an oscilloscope screen. It would appear that the transducers are reasonably easy to make in this crude form, but for effective noise analysis the characteristics would have to be well developed.

The future development of NDT techniques based on Barkhausen noise is likely to involve the relationship between the magnetic Barkhausen noise and the ultrasonic (acoustic) noise also generated in the material. It has been shown by Buttle et al. [2] that the acoustic noise is sensitive to dislocation density as is Barkhausen noise. There may be a method by which the two could be combined to give a quantitative analysis of dislocation density.

The bulk magnetic properties of a material have not been related to acoustic noise, an examination of materials with an acoustic transducer may provide information about these properties which Barkhausen noise alone cannot.

APPENDIX A

The following program was used to find the FFT of the Barkhausen noise data. The program is written in FORTRAN and is for use on an MTS (Michigan Terminal System) such as NUMAC. The program shown is that used for the constructional steels; certain parameters were changed for the silicon iron work.

```
C      DECLARATION OF VARIABLES
C
C          INTEGER I, IFAIL, J, JM1, N2, NJ, M(8, 4096), L
C          INTEGER K, LL, MM, NBIN, NBP
C          DOUBLE PRECISION A(32768), B(32768), SUB(32768)
C          DOUBLE PRECISION TOTAL(32768), X(32768)
C          DOUBLE PRECISION Z, YMAX
C          REAL T
C
C      THE VARIABLES DECLARED HAVE THE FOLLOWING MEANINGS
C      M the values from the transient recorder
C      YMAX the transient recorder maximum used
C      L the number of lines of data to be read
C      X the voltage equivalent of the data
C      A, B the real and imaginary parts of the FFT
C      SUB the sum of A**2 and B**2
C      TOTAL the square root of SUB
C      T the total time of the data recording
C      NBIN the number of points per bin
C      NBP the number of bins plotted on the graphs
C      Z the mean value of FFT in a bin
C      K, LL, MM are introduced for arithmetic
C      I, IFAIL, J, NJ, JM1, N2 are all necessary for the
C      external library routine
C
C      SET UP FFT PARAMETERS
C
C          N=32760
C          T=0.1638
C          L=4095
C
C      INPUT THE TRANSIENT RECORDER MAXIMUM
C      The division by 1000 is to allow for amplification
C
C          WRITE (6, 4)
C          4      FORMAT (' ', 'MAX/1000?')
C          READ (5, *) YMAX
C
C      READ THE DATA FROM THE DATA FILE
C
C          IF (N. LE. 1) STOP
C          DO 10 I=1, L
C          10      READ (7, *) (M(K, I), K=1, 8)
```

```

C
C   CALCULATE THE VOLTAGE EQUIVALENT SQUARED
C
      J=0
      DO 20 I=1, L
      DO 30 K=1, 8
      J=J+1
      X(J)=(M(K, I)-522)*YMAX)**2
30    CONTINUE
20    CONTINUE
C
C   CALL THE NAG FFT ROUTINE
C
      IFAIL=0
      CALL COGEAF (X, N, IFAIL)
      A(1)=X(1)
      B(1)=0.0DO
      N2=(N+1)/2
      DO 40 J=2, N2
      NJ=N-J+2
      A(J)=X(J)
      B(NJ)=X(NJ)
      B(NJ)=-X(NJ)
40    CONTINUE
      IF (MOD(N, 2).NE.0) GOTO 50
      A(N2+1)=X(N2+1)
      B(N2+1)=0.0DO
C
C   CALCULATE THE MODULUS OF THE FFT
C
      DO 60 J=1, N2
      SUB(J)=(A(J)**2+B(J)**2)
      TOTAL(J)=DSQRT(SUB(J))
60    CONTINUE
C
C   SET NBIN AND NBP AND FIND THE MEAN OF EACH BIN
C
      NBIN=20
      NBP=100
      LL=1
      MM=1
      K=NBIN*NBP
      I=NBIN
200   TT=0.0
      Z=0.0
      DO 100 J=LL, NBIN
      TT=TT+TOTAL(J)
100   CONTINUE
      Z=TT/I

```

```
C
C   WRITE MEAN TO OUTPUT FILE
C
      WRITE (10,22) Z
22   FORMAT (F15.10)
      LL=LL+1
      MM=MM+1
      NBIN=I*MM
      IF (NBIN. LE. K) GOTO 200
      STOP
      END
```

The following program was used for plotting the Power Spectra. The calls are made to the GHOST library held at NUMAC. The program was modified for the voltage profile plots.

```

C     DECLARATION OF VARIABLES
C
C           REAL Y(16384),X(16384),T,Z
C           INTEGER J, N, NBIN, M, NBP, N2
C
C     THE VARIABLES DECLARED HAVE THE FOLLOWING MEANINGS
C     X, Y the co-ordinates to be plotted
C     T the total recording time
C     NBIN the number of points per bin
C     N the total number of points
C     M the number of points plotted
C     Z, N2 are for arithmetic
C
C     SET THE PARAMETERS
C
C           T=0.1638
C           NBIN=20
C           NBP=100
C           M=NBP
C
C     FIND THE VALUES TO BE PLOTTED
C
C           DO 20 J=1, M
C           Z=NBIN*(2*J-1)/(2*T)
C           X(J)=Z
20      CONTINUE
C           DO 10 J=1, M
C           READ (10,*) Y(J)
10      CONTINUE
C
C     DO THE PLOTTING
C
C           CALL PAPER (1)
C           CALL PSPACE (0.2, 0.8, 0.2, 0.6)
C           CALL CTRSET (4)
C           CALL CTRMAG (5)
C           CALL MASK (0.6, 0.8, 0.5, 0.6)
C           CALL CURVEO (X, Y, 9, M)
C           CALL AXES
C           CALL UNMASK (0)
C           CALL PSPACE (0.6, 0.8, 0.5, 0.6)
C           CALL BORDER
C           CALL CTRSET (1)
C           CALL CTRMAG (9)
C           CALL MAP (0., 100., 0., 100.)
C           CALL PLOTCS (4., 85., '... 25 CHARACTERS...', 25)
C           CALL CTRMAG (7)
C           CALL PLOTCS (10., 65., '... 16 CHARACTERS...', 16)
C           CALL PLOTCS (10., 45., '... 26 CHARACTERS...', 26)
C           CALL PLOTCS (10., 25., '... 26 CHARACTERS...', 26)
C           CALL PLOTCS (10., 5., '... 26 CHARACTERS...', 26)
C           CALL PSPACE (0.1, 0.9, 0.05, 0.9)

```

```
CALL MAP (0., 100., 0., 100.)  
CALL CTRSET (1)  
CALL CTRMAG (10)  
CALL PCSEND (85., 12., '13 CHARACTERS', 13)  
CALL PCSEND (15., 71., '5CHRS', 5)  
CALL PCSEND (15., 68., '5CHRS', 5)  
CALL GREND  
STOP  
END
```

CHAPTER 1

- [1] Weiss, P., L'hypothèse du Champ Moléculaire et la Propriété Ferromagnétique, J. Phys. 6, 661, 1907
- [2] Brailsford, F., Physical Principles of Magnetism, Van Nostrand, 1966

CHAPTER 2

- [1] Barkhausen, H., Zwei mit Hilfe der neuen Verstärker entdeckte Erscheinungen, Phys. Z., 20, 401, 1919
- [2] Tiitto, S., Säynäjäkangas, S., and Rulka, R., High Frequency Investigations of Magnetic Noise Characteristics, IEEE Trans., Mag., Vol. MAG 12, No. 4, 406, 1976
- [3] Säynäjäkangas, S., A New Surface Transducer for Generating and Detecting Magnetic Field Transients in Ferromagnetics, IEEE Trans. Mag., Vol. MAG 10, No. 1, 44, 1974
- [4] Säynäjäkangas, S., Practical Realization of a Signal Processor for the Non-destructive Electromagnetic Testing Method, Sähkö Electricity in Finland, Vol. 46, No. 11, 513, 1973
- [5] British Steel Corporation, Basic Properties of Grain Oriented Electrotechnical Steels, Draft Final Report, 1981
- [6] Biorci, G., and Pescetti, D., Frequency Spectrum of Barkhausen Noise, J. Appl. Phys., 28, 777, 1957
- [7] Gründl, A., Deimel, P., Röde, B., and Daniel, H., Three Dimensional Measurement of the Barkhausen Effect, Physica, 86-88B, 1379, 1977
- [8] Tebble, R. S., Skidmore, I. C., and Corner, W. D., The Barkhausen Effect, Proc. Phys. Soc. London, Section A, A63, 739, 1950
- [9] Heiden, Chr. and Storm, L., Grundsätzliches zur Bestimmung der Grössenverteilung der Barkhausen Volumina in Ferromagnetika, Z. Angew. Phys., 21(4), 349, 1966
- [10] McClure, J. C. (Jr), and Schröder, K., The Magnetic Barkhausen Effect, CRC Critical Reviews in Solid State Sciences, 45, 1976
- [11] Säynäjäkangas, S., Statistical Properties of Magnetization Discontinuities in Technical Steels, IEEE Trans. Mag., Vol. MAG 10, No. 1, 1974
- [12] Säynäjäkangas, S., A Non-destructive Electromagnetic Method for Structural Studies of Ferrous Alloys, Acta Pol. Scand. E Series 33, 1973

- [13] Mazzetti, P. and Montalenti, G., Power Spectrum of the Barkhausen Noise of Various Magnetic Materials, J. Appl. Phys., Vol. 34, No. 11, 3223, 1963
- [14] Celasco, M., Fiorillo, F., and Mazzetti, P., Time Amplitude Correlation Effect between Large Barkhausen Discontinuities (in the Magnetization Noise), Il Nuovo Cimento, Vol., 23B, N2, 376, 1974
- [15] Tiitto, S. and Säynäjäkangas, S., Spectral Damping in Barkhausen Noise, IEEE Trans. Mag., Vol. MAG 11, No. 6, 1666, 1975
- [16] Celasco, M., and Fiorillo, F., The Effect of Surface on the Power Spectrum of the Barkhausen Noise in Ferromagnetic Materials, IEEE Trans. Mag., Vol. MAG 10, No. 2, 115, 1974
- [17] Storm, L., Heiden, C., and Grosse-Nobis, W., The Power Spectrum of the Barkhausen Noise of Grain Oriented Three Percent Silicon Iron, IEEE Trans. Mag., Vol. MAG 2, No. 3, 434, 1966
- [18] Mazzetti, P. and Montalenti, G., Proceedings of the International Conference on Magnetism (Nottingham), 701, 1964
- [19] Tiitto, S., On the Mechanism of Magnetization Transitions in Steel, IEEE Trans. Mag., Vol. MAG 14, No. 5, 527, 1978
- [20] Manson, G., and Hoffmann de Visme, G., The Frequency Spectrum of Barkhausen Noise, J. Phys. D: Appl. Phys., Vol. 5, 1389, 1972
- [21] Gardner, C.G., and Barton, J.R., Recent Advances in Magnetic Field Methods of Non-destructive Evaluation for Aerospace Applications, Propulsion and Energetics Panel Meeting, London, 1970
- [22] Lomaev, G.V., Magnetic Noise Method in Non Destructive Inspection of Ferromagnetics, Soviet J. Nondest. Test. 13, No. 4, 425, 1978
- [23] Rautioaho, R.H. and Karjalainen, L.P., Application of Barkhausen Noise Measurements to Residual Stress Analysis in Structural Steels, Acta Univ. Oul. C26, Metallurg 4, 1983
- [24] Karjalainen, L.P. and Moilanen, M., Detection of Plastic Deformation During Fatigue of Mild Steel by the Measurement of Barkhausen Noise, NDT International, 51, 1979



- [25] Lomaev, G. V., Malyshev, V. S., and Degterev, A. P., Review of the Application of the Barkhausen Effect in Non-destructive Inspection, Soviet J. Nondest. Test., No. 3, 54, 1984
- [26] Lieneweg, U., Barkhausen Noise of 3% Si-Fe Strips After Plastic Deformation, IEEE Trans. Mag., Vol. MAG 10, No. 2, 118, 1974
- [27] Rautioaho, R. H., Karjalainen, L. P., and Moilanen, M., Coercivity and Power Spectrum of Barkhausen Noise in Structural Steels, Journal of Magnetism and Magnetic Materials 61, 183, 1986
- [28] Lord, A. E. Jr. in Physical Acoustics (ed. W. P. Mason and R. N. Thurston), Academic Press, New York, Vol. XI, 290
- [29] Buttle, D. J., Briggs, G. A. D., Jakubovics, J. P., Little, E. A., and Scruby, C. B., Magneto-acoustic and Barkhausen Emission in Ferromagnetic Materials, Phil. Trans. R. Soc. London A (GB) Vol. 320, No. 1554, 367, 1986
- [30] Burkhardt, G. L., Beissner, R. E., Matzkanin, G. A. and King, J. D., Acoustic Methods for Obtaining Barkhausen Noise Stress Measurements, Mat. Eval. 40, 669, 1982
- [31] Eadie, G. C., Basic Properties of Grain-Oriented Electrotechnical Steels, British Steel Corporation, Draft Final Report, Vol. 1, 1979
- [32] Bertotti, G., Fiorillo, F., and Sassi, M. P., Barkhausen Noise and Domain Structure Dynamics in Si-Fe at Different Points of the Magnetisation Curve, Journal of Magnetism and Magnetic Materials, 23, 136, 1981
- [33] Tiitto, S., On the Influence of Microstructure on Magnetization Transitions in Steel, Acta Polytechnica Scandinavica, Applied Physics Series no. 119, 1977

CHAPTER 3

- [11] Tebble, R. S., Skidmore, I. C., and Corner, W. D., The Barkhausen Effect, Proc. Phys. Soc. London, Sect. A, A63, 739, 1950
- [22] Rulka, R., A New Laboratory Apparatus for Investigating the Magnetic Properties of Magnetic Materials, University of Oulu, Rep. T29, 1975
- [33] Tiitto, S., On the Influence of Microstructure on Magnetization Transitions in Steel, Acta Polytechnica Scandinavica, Applied Physics Series No. 119, 1977
- [44] Ott, H. W., Noise Reduction Techniques in Electronic Systems, Wiley - Interscience, 1976
- [55] Wohlfarth, E. P., (Ed.), Selected Topics in Solid State Physics, Vol. IX, Zijlstra, H., Experimental Methods in Magnetism I, Generation and Computation of Magnetic Fields, North Holland Pub. Co., 1967
- [66] Tiitto, S. and Säynäjäkangas, S., Spectral Damping in Barkhausen Noise, IEEE Trans. Mag., Vol. MAG 11, 1666 - 1672, 1975
- [77] Bertotti, G., Fiorillo, F., and Sassi, M. P., Barkhausen Noise and Domain Structure Dynamics in Si-Fe at Different Points of the Magnetization Curve, Journal of Magnetism and Magnetic Materials 23, 136 - 148, 1981
- [88] De Sa, A., Principles of Electronic Instrumentation, Arnold, 1981
- [99] Williams, A. B., Electronic Filter Design Handbook, McGraw - Hill Book Company, 2 - 54, 1980
- [100] Osborn, J. A., Demagnetizing Factors of the General Ellipsoid, Physical Review Vol. 67, Nos. 11 and 12, 351, 1945
- [111] British Steel Corporation, Basic Properties of Grain Oriented Electrotechnical Steels, Technical Report No. 2, 1979
- [122] Willcock, S. N. M., An Investigation of the Magnetic Properties of High Tensile Steels, PhD Thesis, University of Durham, 1985

CHAPTER 4

- [1] British Steel Corporation, Basic Properties of Grain Oriented Electrotechnical Steels, Draft Final Report, 1981
- [2] Eadie, G.C., Basic Properties of Grain-Oriented Electrotechnical Steels, British Steel Corporation, Draft Final Report, Vol. 1, 1979

CHAPTER 5

- [1] Petzow, G., Metallographic Etching: Metallographic and Ceramographic Methods for Revealing Microstructure: translated from German, R. Koch and J. A. Nelson, Metals Park, A. S. M., 1978

CHAPTER 6

- [1] Petzow, G., Metallographic Etching: Metallographic and Ceramographic Methods for Revealing Microstructure: translated from German, R. Koch and J. A. Nelson, Metals Park, A. S. M., 1978
and Kundell, P. A.
- [2] Willcock, S. N. M. and Tanner, B. K., The Magnetic Properties of Seamless Steel Pipe, Journal of Magnetism and Magnetic Materials 66, 153, 1987
- [3] Willcock, S. N. M., Private Communication, 1988
- [4] Willcock, S. N. M., An Investigation of the Magnetic Properties of High Tensile Steels, PhD Thesis, University of Durham, 1985

CHAPTER 7

- [1] Willcock, S.N.M., An Investigation of the Magnetic Properties of High Tensile Steels, PhD Thesis, University of Durham, 1985
- [2] Thompson, S., Private Communication, 1988

CHAPTER 9

- [11] Celasco, M., Fiorillo, F., and Mazzetti, P., Time Amplitude Correlation Effect between Large Barkhausen Discontinuities (in the Magnetization Noise), *Il Nuovo Cimento*, Vol., 23B, N2, 376, 1974
and Mundell, P.A.
- [2] Willcock, S.N.M. and Tanner, B.K., The Magnetic Properties of Seamless Steel Pipe, *Journal of Magnetism and Magnetic Materials* 66, 153, 1987
- [3] Rautioaho, R.H., Karjalainen, L.P. and Moilanen, M., Coercivity and Power Spectrum of Barkhausen Noise in Structural Steels, *Journal of Magnetism and Magnetic Materials* 61, 183, 1986
- [4] Goodenough, J.B., A Theory of Domain Creation and Coercive Force in Polycrystalline Ferromagnetics, *Physical Review* 95, 4, 917, 1954
- [5] Tiitto, S., On the Influence of Microstructure on Magnetization Transitions in Steel, *Acta Polytechnica Scandinavica, Applied Physics Series no. 119*, 1977
- [6] Storm, L., Heiden, C., and Grosse-Nobis, W., The Power Spectrum of the Barkhausen Noise of Grain Oriented Three Percent Silicon Iron, *IEEE Trans. Mag.*, Vol. MAG 2, No. 3, 434, 1966
- [7] Lieneweg, U., Barkhausen Noise of 3% Si-Fe Strips After Plastic Deformation, *IEEE Trans. Mag.*, Vol. MAG 10, No. 2, 118, 1974
- [8] Tebble, R.S. and Craik, D.J., *Magnetic Materials*, Wiley-Interscience, 1969
- [9] Barton, J.R. and Kusenberger, F.N., Residual Stresses in Gas Turbine Engine Components from Barkhausen Noise Analysis, *J. of Engineering for Power* p. 349, 1974
- [10] James, M.R. and Buck, O., Quantitative Nondestructive Measurements of Residual Stresses, *CRC Critical Reviews in Solid State and Materials Sciences*, 61, August 1980
- [11] Rautioaho, R.H. and Karjalainen, L.P., Application of Barkhausen Noise Measurements to Residual Stress Analysis in Structural Steels, *Acta Univ. Oul. C26, Metallurg* 4, 1983
- [12] Thompson, S., **Private Communication**, 1988

CHAPTER 10

- [1] Rautioaho, R.H. and Karjalainen, L.P., Application of Barkhausen Noise Measurements to Residual Stress Analysis in Structural Steels, Acta Univ. Oul. C26, Metallurg 4, 1983
- [2] Buttle, D.J., Briggs, G.A.D., Jakubovics, J.P., Little, E.A., and Scruby, C.B., Magneto-acoustic and Barkhausen Emission in Ferromagnetic Materials, Phil. Trans. R. Soc. London A (GB) Vol. 320, No. 1554, 367, 1986

